COMMONWEALTH OF PENNSYLVANIA
DEPARTMENT OF TRANSPORTATION

PENNDOT RESEARCH

PENNDOT

BRIDGE DECK PATCHING MATERIALS

Final Report

PennDOT/MAUTC Partnership, Work Order No. 10
Research Agreement No. 510401

June 2008

By N. M. Cervo and A. J. Schokker

PENNSTATE

1855

The Thomas D. Larson
Pennsylvania Transportation Institute

The Pennsylvania State University
Transportation Research Building
University Park, PA 16802-4710
(814) 865-1891 www.pti.psu.edu

Technical Report Documentation Page

1. Report No. FHWA-PA-2007-023-510401-10	**2. Government Accession No.**	**3. Recipient's Catalog No.**
4. Title and Subtitle Bridge Deck Patching Materials		**5. Report Date** June 2008 **6. Performing Organization Code**
7. Author(s) Nicholas M. Cervo and Andrea J. Schokker, Ph.D.		**8. Performing Organization Report No.** PTI 2008-13
9. Performing Organization Name and Address The Thomas D. Larson Pennsylvania Transportation Institute The Pennsylvania State University 201 Transportation Research Building University Park, PA 16802		**10. Work Unit No. (TRAIS)** **11. Contract or Grant No.** 510401, Work Order No. 10
12. Sponsoring Agency Name and Address The Pennsylvania Department of Transportation Bureau of Planning and Research Commonwealth Keystone Building 400 North Street, 6th Floor Harrisburg, PA 17120-0064		**13. Type of Report and Period Covered** Final Report 1/3/2007 – 7/2/2008 **14. Sponsoring Agency Code**
15. Supplementary Notes		

16. Abstract

With the aging of bridges in Pennsylvania, an increasing concern is the deterioration of concrete bridge decks over time, and subsequently, the best way to repair them. Complete deck replacement, although often the best for the bridge, is far from the most economical solution. Therefore, a number of rapid-setting concrete patching materials have been used by PennDOT to repair areas of deterioration along the deck. Unfortunately, some of these materials have proven to be ineffective in the long term due to durability issues from vibration and heavy traffic volume. Therefore, there is a need to research, test, and evaluate the various patching materials on the market to determine their effectiveness in variable conditions. The variables include the area of the patch, depth of the patch, and environment (corrosive agents and traffic load). The objectives of this project were to determine the most suitable quick-setting patching material for patches of varying area and depth; determine the corrosion protection provided by the patch to the underlying reinforcement and verify that the patch does not increase corrosion rates in bars contained in the base material; and develop a recommended testing protocol for evaluation of patching materials.

17. Key Words Concrete bridge deck, deterioration, patching materials, corrosion, durability		**18. Distribution Statement** No restrictions. This document is available from the National Technical Information Service, Springfield, VA 22161	
19. Security Classif. (of this report) Unclassified	**20. Security Classif. (of this page)** Unclassified	**21. No. of Pages** 143	**22. Price**

Form DOT F 1700.7 (8-72) Reproduction of completed page authorized

BRIDGE DECK PATCHING MATERIALS

Final Report

PennDOT/MAUTC Partnership, Work Order No. 10
Research Agreement No. 510401

Prepared for

Bureau of Planning and Research
Commonwealth of Pennsylvania
Department of Transportation

By

Nicholas M. Cervo and Andrea J. Schokker

The Thomas D. Larson
Pennsylvania Transportation Institute
The Pennsylvania State University
Transportation Research Building
University Park, PA 16802-4710

June 2008

PTI 2008-13

This work was sponsored by the Pennsylvania Department of Transportation and the U.S. Department of Transportation, Federal Highway Administration. The contents of this report reflect the views of the authors, who are responsible for the facts and the accuracy of the data presented herein. The contents do not necessarily reflect the official views or policies of the Federal Highway Administration, U.S. Department of Transportation, or the Commonwealth of Pennsylvania at the time of publication. This report does not constitute a standard, specification, or regulation.

TABLE OF CONTENTS

LIST OF TABLES

LIST OF FIGURES

LIST OF FIGURES (cont.)

Chapter 1

Introduction and Literature Review

1.1 Problem Statement

With the aging of bridges in Pennsylvania, an increasing concern is the deterioration of concrete bridge decks over time, and subsequently, the best way to repair them. Complete deck replacement, although often the best for the bridge, is far from the most economical solution. Therefore, a number of rapid-setting concrete patching materials have been used by PennDOT to repair areas of deterioration along the deck. Unfortunately, some of these materials have proven to be ineffective in the long-term due to durability issues from vibration and heavy traffic volume. Therefore, there is a need to research, test, and evaluate the various patching materials on the market to determine their effectiveness in variable conditions. The variables include the area of the patch, depth of the patch, and environment (corrosive agents and traffic load).

1.2 Objectives

1. Determine the most suitable quick-setting patching material for patches of varying area and depth.
2. Determine the corrosion protection provided by the patch to the underlying reinforcement and verify that the patch does not increase corrosion rates in bars contained in the base material.

3. Develop a recommended testing protocol for evaluation of patching materials.

1.3 Scope

To determine the most suitable patching material for various conditions dependent on a variety of variables, such as environment, patching depth, and patching area, the following tasks were performed:

1. A literature review was conducted to determine the top six patching material candidates to test, incorporating materials from each of the major groups of patch type/material.
2. Standard ASTM tests were performed, as recommended by the National Transportation Product Evaluation Program (NTPEP) (National Transportation Product Evaluation Program 2005), on these six materials to determine the top two materials.
3. Specialized tests were developed and conducted for these two patching materials to address issues not covered by standard ASTM tests.
4. Based on ASTM and specialized testing, the most appropriate patching material was identified for the various conditions described above.

1.4 Literature Review

The following sections review the various types of deterioration that can occur in bridge decks, both in the reinforcement and in the concrete. Also, the various types of

PennDOT patching materials are discussed, along with the ASTM tests that determine basic material properties of the chosen patch materials.

1.4.1 Bridge Deck Deterioration

To determine the best way to repair deterioration in bridge decks, one must first understand the various mechanisms by which deterioration can take place. The following is a description of the major mechanisms that lead to deterioration.

1.4.1.1 Deterioration of Reinforcement

1.4.1.1.1 Corrosion Due to De-icing Salts

Corrosion is defined as the deterioration of a metal by way of an electrochemical process, in which the metal reacts with its environment (i.e., oxygen and water). When steel is subjected to oxygen within a moist environment, the metal tends to break down, wishing to revert to its ore form (Richardson 2002).

To fully understand how steel corrodes within concrete, it is first important to understand how steel does *not* corrode inside concrete. After all, it is a common observation that a piece of steel left exposed to the environment deteriorates as a result of the corrosion process. So what is different about the steel within reinforced concrete? The answer is in the environment that the concrete creates for the steel. As stated above, the corrosion of steel requires both oxygen and water. If enough concrete cover is provided for the reinforcement, and this concrete is impermeable, the steel is protected since two major ingredients of corrosion are missing. Unfortunately for the steel, though, concrete is not a completely impermeable material. Although concrete may appear to be completely solid, it actually is not, due to a system of voids that naturally occur when the concrete is cast. These voids allow for the diffusion of oxygen and water toward the reinforcement. Therefore, the concrete cover shields the rebar somewhat, but does not completely prevent interaction between the steel and the outside environment (Richardson 2002). The amount of cover may be able to slow down the rate of corrosion, but the true protection against corrosion lies in the alkalinity of the concrete. Concrete is a basic material with a pH between 12 and 13. At this pH level, an oxide film, known as a passive film, forms around the reinforcement. This passive film, which is primarily composed of hydrated iron oxides, is only a few nanometers thick (Bertolini 2004). The film is dense and impenetrable, and can even regenerate when it is damaged, as long as the environment remains alkaline. When in place, it is far better than any man-made protection, such as galvanizing or epoxy coating, and can safeguard the integrity of the reinforcement for as long as it exists (Broomfield 2007).

Unfortunately, the passive film is not completely invulnerable to the environment. Two main culprits lead to the depassivation of the steel in concrete: carbon dioxide and chlorides. Carbon dioxide that is present in the atmosphere can eventually diffuse through the concrete cover and reach the passive film. Once this occurs, the pH drops to about 9 and the stability of the passive film is lost (Bertolini 2004). Chloride ions, which are found in deicing salts commonly used in winter weather, also can penetrate the concrete. Once enough ions reach the reinforcement, local damage to the passive film can occur (Poulsen 2006).

When the passive film is destroyed by carbonation or chloride ions, the steel is vulnerable to the corrosion process. This process begins by the iron giving up its electrons in an anodic reaction, as denoted by Reaction 1 below (American Concrete Institute 1987):

Reaction 1: $Fe \rightarrow Fe^{2+} + 2e^{-}$.

This reaction must be accompanied by a cathodic reaction where the electrons are consumed, in order to keep charge neutrality. This is where the oxygen and water come into play, as shown in Reaction 2 (American Concrete Institute 1987):

Reaction 2: $2e^{-} + H_2O + ½O_2 \rightarrow 2OH^{-}$.

Refer to Figure **1-1** to see the entire electrochemical reaction.

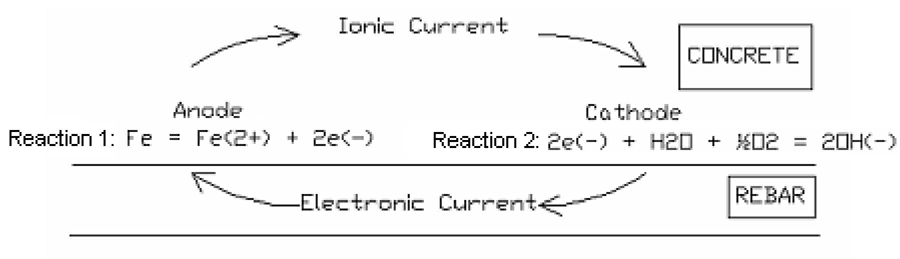

Figure **1-1**: Corrosion Current (Broomfield 2007)

The entire process is not complete at this point, though, since the iron has only broken down into the ferrous ion. As is often observed, when steel corrodes, rust is the final product. This occurs through a series of reactions. First, the ferrous ions react with the hydroxyl ions to produce ferrous hydroxide, as shown in Reaction 3 (Broomfield 2007):

Reaction 3: $Fe^{2+} + 2OH^{-} \rightarrow Fe(OH)_2$.

Then, the ferrous hydroxide reacts with oxygen and water to produce ferric hydroxide, as shown in Reaction 4 (Broomfield 2007):

Reaction 4: $4Fe(OH)_2 + O_2 + 2H_2O \rightarrow 4Fe(OH)_3$.

And finally, the ferric hydroxide breaks down into the hydrated ferric oxide, commonly known as rust, as shown in Reaction 5 (Broomfield 2007):

Reaction 5: $2Fe(OH)_3 \rightarrow Fe_2O_3 \cdot H_2O + 2H_2O$.

The problem with rust is that it has seven times the volume of steel with none of its excellent mechanical properties. So not only is the rust incapable of holding the tensile load that the steel was designed to take, but it also expands within the concrete, causing a buildup of stresses that leads to cracking and spalling of the concrete, which can allow even more chlorides to penetrate to the reinforcement. Therefore, the integrity of both the steel and the surrounding concrete has been compromised, leading to possible failure of the entire system (Broomfield 2007).

A phenomenon of corrosion known as the “halo effect” is of particular concern for bridge deck patching. When corrosion causes a need for repair, the spalling concrete is removed from the area of deterioration, and repaired material is put in its place. Unfortunately, in the area surrounding the replaced concrete, there is a buildup of chloride ions. This abrupt difference in chloride content between new and old concrete can create large corrosion potentials, leading to rapid corrosion in the area around the repair, thus causing a “halo” of deterioration around the repair material (Whitmore 2005).

1.4.1.1.2 Other De-Icing Products

In addition to standard de-icing salt (NaCl), other products are also used as de-icing products. These include magnesium chloride ($MgCl_2$), potassium chloride (KCl), calcium chloride ($CaCl_2$), and urea (CON_2H_4). The chloride compounds all contribute to the corrosion process described above (Kirchner 2001). Urea, a non-chloride deicer, has been tested and was found to cause even greater deterioration in the concrete while also being harmful to the environment. This greater deterioration is the result of adverse freeze-thaw effects that the urea has on the concrete, reducing the concrete's strength and elasticity (Farha 2002).

1.4.1.2 Deterioration of Concrete

1.4.1.2.1 Freezing and Thawing

Moisture from precipitation and other sources can saturate the voids found in concrete. It is this water that is the source of the problem with respect to freezing and thawing. In climates where the temperature can fluctuate above and below the freezing point, such as the climate that covers all of Pennsylvania, water in the voids of the concrete will freeze and expand when the freezing point is reached, thus increasing the pressure within the concrete. When temperatures increase, the ice will melt and the system will again be at the starting point. This ongoing cycle of freezing and thawing that accompanies temperature changes repeatedly stresses the concrete and leads to deterioration. A common deterioration associated with freezing and thawing is scaling, which is a crumbling of the surface mortar over a large area (Cordon 1966).

1.4.1.2.2 Traffic Loading

Deterioration from vehicular loads is due to abrasion damage caused by the contact between the wheel and the road. In particular, studded tires, chained tires and blades of snowplows can scrape at the surface of the bridge deck, thus causing damage through years of repeated abuse (Russell 2004).

1.4.1.2.3 Chemical Attacks

A number of mechanisms of concrete deterioration exist due to the reaction of the concrete with various chemicals. Most notable are sulfates that react with components of the cement and cause the concrete to expand and the cement paste to soften and disintegrate (Mindess 2003). This occurs as a result of three reactions: The sulfate ions react with the calcium ions, hydrated calcium aluminate, and carbon dioxide to form gypsum, calcium sulfoaluminate (ettringite), and thaumasite, respectively. These products have larger volumes than the reactants, thus causing a buildup of internal pressure that leads to cracking and eventual deterioration (Walker 2000).

1.4.2 Patching Materials

A wide variety of patching and patch-related materials are listed in the PennDOT publication, "Bulletin 15," which is a list of all materials that are allowed to be used in PennDOT projects (Pennsylvania Department of Transportation 2006). Table 1-1 breaks them down by category.

Table 1-1: PennDOT-approved patching and patch-related materials (PennDOT 2006).

Packaged Dry Cement		
	Rapid Set Concrete Mix	
Rapid Set Concrete Patching Materials – Cementitious, Non-Metallic, Non-Staining		
	BC Quick Patch #2	Euco-Speed
	Swift Set 120	Speed Crete 2028
	IFSCEM 110	Speed Crete Green Line
	Bonsal F-77 Construction Grout	Express repair
	Power Set 120	5 Star Highway patch
	Power Set 120A	5 Star Structural Concrete
	IFSCEM 115	5 Star Structural Concrete V/O
	Tyberpatch HS	Gill 33B & P Superbond
	Pavemend 15.0	Durapatch Hiway
	CGM Highway Patch	Crystex
	Chemspeed 65	Rapid Road Repair
	Pave Patch 3000	FastSet™ Non-Shrink Grout
	Perma Patch	FastSet™ Dot Mix
	HD-50	CG FastSet™ Concrete Mix
	Thoroc 10-60 Rapid Mortar	Sikatop III
	Road Patch II	Sika Set Road Patch
	Thorite	SikaQuick 2500
	Set Instant Concrete	SikaQuick 1000
	Emaco T415 Repair Mortar	
Rapid Set Concrete Patching Materials – Magnesium Phosphate Cement-based Materials		
	Duracal	Set 45 Hot weather
	Duracal-S	Euco-Speed M.P.
	Magna 100	Darex 240
	Set 45 regular	

Table 1-1: PennDOT-approved patching and patch-related materials (continued).

Rapid Set Concrete Patching Materials – Polymer Mortar and Concrete	
Emaco 2020	Dural 317
RM 698 Epoxy Patch	Flexolith
Duracryl	T17 Polymer Concrete
Polymer Modified and Special Cements, Mortars and Concrete	
BC Non-shrink grouting & Aggregate	HiCap Light Patching Compound
Speed Patch	HiCap Patching Compound
ThoRoc HB2 Repair Mortar	Flexkrete Technologies 102
Thorogrip Anchoring Cement	PipeWipe
Emaco T415 Mortar	Type IP Blended
Emaco R320 CI	T-SF Blended
Emaco S88-CI	Permacrete
Emaco R320	Blend Crete
Emaco R310	Shotcrete MS
Emaco S66-CI	FastSet^{TM} Cement
Rapid Set Cement	FastSet^{TM} Repair Mortar
Rapid Set Concrete Mix	FastSet^{TM} Non-Shrink Grout
Chem Comp III	FastSet^{TM} Dot Mix
CTS Type K	Speedcrete Red Line
Day Chem Ad Bond (J-40)	Sikatop Plus 111
HD-25	Sikatop Plus 121
Type S Cement	Sikatop Plus 122
Type M Cement	Sikatop Plus 123
Type N Cement	Sikadur 42 Grout Pak
Eurocrete Thin Top Supreme	Sika Cem 133
FastSet^{TM} Commercial Grade Concrete Mix	High Power DOT Grade Repair Mortar
Concrete Top Supreme	High Power Cement
Dural Top Fast Set	Thin Top Supreme
Dural Top Gel	Duracal
High Power Fast Setting Concrete	

1.4.3 ASTM Testing Methods

According to AASHTO's National Transportation Product Evaluation Program (NTPEP), the following ASTM tests should be run on rapid-setting patching materials

(National Transportation Product Evaluation Program 2005). Table **1-2** lists the tests recommended for water-based materials and Table **1-3** lists the tests recommended for non-water-based materials. These tests are chosen because they are capable of determining the basic mechanical properties needed for preliminary material selection.

Table **1-2**: Testing for Water-Based Materials (National Transportation Product Evaluation Program 2005)

Test	**Specification**
Compression, Cylinders	ASTM C 39
Freeze/Thaw	ASTM C 666 and ASTM C 666 with salt water
Set Time	ASTM C 266 (Substituting ASTM C 191)
Bond Strength using Slant Shear	ASTM C 928
Thermal Expansion and Shrinkage	ASTM C 531 modified

Table **1-3**: Testing for Non-Water-Based Materials (National Transportation Product Evaluation Program 2005)

Test	**Specification**
Compression, Cylinders	ASTM C 39
Freeze/Thaw	ASTM C 666
Set Time	ASTM C 266 (Substituting ASTM C 191)
Bond Strength using Slant Shear	ASTM C 882
Thermal Expansion and Shrinkage	ASTM C 531 modified

Besides the research framework created by the NTPEP, not a great deal of research has been conducted in this area, and this underscores the need for this project. A similar study is currently being conducted by Oklahoma DOT in conjunction with the University of Oklahoma, but no results from the testing were available at the time of publication of this report.

Chapter 2

Testing Program A – Standard ASTM Testing

2.1 Patching Material Selected

For the first phase of testing, selected materials were tested using standard ASTM procedures. Surveys were given to various DOTs to determine what materials have been used and how successful their use has been. Unfortunately, there was a limited response from the DOTs. Beyond a recommendation from Indiana DOT to test Duracal, a specially formulated rapid-setting concrete, there were no other suggestions on what materials to test. PennDOT, however, indicated a special interest in several materials. Based on this feedback, the six materials listed in Table 2-1 were chosen. The following items were considered to arrive at this list:

- Materials already in use regularly by PennDOT (HP Fast Setting Concrete, Pavemend 15.0, Rapid Set with a latex modifier)
- Materials successfully used by other DOTs (Duracal)
- Representatives from each of the six applicable Bulletin 15 categories (still needed Polymer Modified Concrete and Polymer Concrete)
- Widespread range of manufacturers (chose Sikatop 122 Plus and T17 Polymer Concrete, which are from two different manufacturers)

Descriptions of the selected materials follow.

Table 2-1: Patching material to be subjected to ASTM Testing

Product Name	Company Name	Bulletin 15 Category
Rapid Set Concrete Mix (w/ latex modifier)	CTS Cement Mfg. Co.	Packaged Dry Cement
Pavemend 15.0	Ceratech, Inc.	Cementitious, Non-Metallic, Non-Staining
Duracal	U.S. Gypsum Co.	Magnesium Phosphate Cement
T17 Polymer Concrete	Transpo Industries Inc.	Polymer Concrete
Sikatop Plus 122	Sika Corporation	Polymer Modified
High Power Fast Setting Concrete	US Concrete Products	Special Cement

2.1.1 Rapid Set Concrete Mix (CTS Cement Manufacturing Co.) with Modifier A

Rapid Set Concrete Mix is a non-metallic mixture of hydraulic cement and aggregate. It sets within 45 minutes, and can obtain high early compressive strengths. It has a variety of applications, including bridge deck repair. Its intended use is for repair thicknesses ranging from 2 inches to 24 inches (5.1 cm to 61 cm). It is commonly mixed with "Modifier A" (which it was for this research), a latex modifier produced by Dow Chemical Company, in order to enhance its performance by increasing its strength and reducing is porosity.

2.1.2 Pavemend 15.0 (Ceratech, Inc.)

Pavemend 15.0 is a non-metallic, self-leveling repair mortar. It sets within a half hour and can obtain high early compressive strengths.

2.1.3 Duracal (U.S. Gypsum Company)

Duracal is listed as a magnesium phosphate cement. Magnesium phosphate is a compound that allows the concrete to set fast, have a high early strength, and bond well to the substrate surface. It also causes the concrete to have low permeability (Lafrenz 2007). Upon further inspection of the product, though, it was determined that it is primarily a plaster of paris and portland cement mix, which means that it should only be listed under the "Special Cement" category, and not under "Magnesium Phosphate Cement."

2.1.4 T17 Polymer Concrete (Transpo Industries Inc.)

T17 is a methyl methacrylate polymer concrete. A polymer concrete is a concrete where the binder is entirely composed of a synthetic polymer, in this case, methyl methacrylate. This polymer allows the concrete to gain strength, durability, and resistance to chloride penetration, while also reducing water permeability (Blaga 1985).

2.1.5 Sikatop Plus 122 (Sika Corporation)

Sikatop 122 Plus is a polymer-modified, cementitious mortar. A polymer-modified mortar is a mortar in which some of the binder (10-15%) is replaced with a synthetic polymer. This allows the mixture to exhibit some of the characteristics of the polymer (high strength and durability, for example), but at a lower cost than the polymer concrete, whose binder is entirely composed of expensive synthetic polymers (Blaga 1985).

2.1.6 High Power Fast Setting Concrete (U.S. Concrete Products)

HP Fast Setting Concrete is a specialized concrete mixture produced to obtain high early strength and rapid setting times.

2.2 Phase I Methodology: ASTM Testing

As detailed in Section 1.4.3, the National Transportation Product Evaluation Program has provided guidelines as to which ASTM tests should be run on each type of patching material. These tests are crucial because they determine important material properties that need to be ascertained when evaluating the value of the patching material. These material properties include compression strength over time (ASTM C 39), resistance to adverse freeze-thaw effects (ASTM C 666), time required to set (ASTM C 191), bond strength to substrate concrete (ASTM C 928/882), shrinkage percentage (ASTM C 531 M), and coefficient of thermal expansion (ASTM C 531 M). Descriptions of each of these tests follow.

2.2.1 Water-Based Materials

2.2.1.1 ASTM C 39 – Compressive Strength of Cylindrical Concrete Specimen

Apply a compressive load on a concrete cylinder at an increasing rate until the specimen fails (Figure 2-1). The compressive strength of the specimen is then found by dividing the maximum load seen by the cylinder by its cross-sectional area (ASTM 2006).

Figure 2-1: ASTM C 39

2.2.1.2 ASTM C 666 – Resistance of Concrete to Rapid Freezing and Thawing

Molded beam specimens submerged in water (Figure 2-2) are cycled between thawing [40°F (4.4°C)] and freezing [0°F (-17.8°C)] temperatures for "300 cycles or until the relative dynamic modulus of elasticity (a measurement of the solidity of the material's microstructure) reaches 60% of the initial modulus, whichever occurs first." This test is repeated using salt water (ASTM 2006).

Figure 2-2: ASTM C 666

2.2.1.3 ASTM C 266 – Time of Setting of Hydraulic-Cement Paste by Gillmore Needles

Cement and water are mixed together to form a paste. Then the initial and final time of setting is determined using two Gillmore needles of different sizes. Gillmore needles are weighted objects that have a specified diameter and are pressed into the paste using a mounting device to determine setting times. The initial Gillmore needle (0.250 lb [113.4 g], 0.084 inches [2.12 mm] diameter) is used to determine the initial time of setting by establishing when this needle can no longer make a large indentation in the specimen. Likewise, the final Gillmore needle (1.000 lb [453.6 g], 0.042 inches [1.06 mm] diameter) is used to determine the final time of setting (ASTM 2006).

2.2.1.4 ASTM C 191 – Time of Setting of Hydraulic Cement by Vicat Needle

In lieu of ASTM C 266, ASTM C 191 has been chosen to examine the time of setting of the various patching materials since the Gillmore test, in general, is being "phased out," while the Vicat test is becoming "the standard" (Significance of Tests and Properties of Concrete & Concrete-Making Materials 2006).

Mortars of the patching material are made and placed in a 1.57-inch (40-mm) high mold. Then, the initial and final setting time is determined by a Vicat needle, which is a weighted, 0.039-inch (1-mm) diameter needle that is mounted directly above the mortar, and is released, allowing it to drop into the specimen (Figure 2-3). The time when the needle only penetrates 0.98 inch (25 mm) into the mortar marks the time of initial setting, and the time when the needle cannot penetrate at all into the mortar marks the time of final setting (ASTM 2006).

Figure 2-3: ASTM C 191

2.2.1.5 Packaged Dry, Rapid-Hardening Cementitious Materials for Concrete Repairs – Section 8.5 for Slant Shear Test

A composite cylinder is composed of two equal volume sections, whose interface forms a 30-degree angle with vertical (Figure 2-4). The bottom half is base concrete and the other half is that of the patching material. A bonding system is not applied at the interface unless required by the manufacturer. Then, a compressive strength test (ASTM C 39) is run on the hybrid cylinder. The bond strength is determined by dividing the load at failure by the area of the interface between the two sections (ASTM 2006).

Figure 2-4: ASTM C 928 and ASTM C 882

2.2.1.6 ASTM C 531 Modified – Linear Shrinkage and Coefficient of Thermal Expansion of Chemical-Resistant Mortars, Grouts, Monolithic Surfacings, and Polymer Concretes

Specimens of the patching material (mortars) that have a cross-sectional area of 1 inch (2.54 cm) by 1 inch (2.54 cm) have nickel alloy studs on either end that are 10 inches (25.4 cm) apart. They are stored at a temperature of 73°F (23°C) for 1 week, and their length is measured on day 1, day 3, and day 7. They are then placed in an oven at 210°F (99°C) for 3 days (Figure 2-5) and then allowed to cool for 16 hours, after which the length is again measured. This procedure is repeated until the bars achieve a constant length at 73°F (23°C). The shrinkage can then be determined by dividing the change in length by the original length [(Lo-L)/Lo * 100%; where Lo = Original length, L=Final length after shrinkage] (ASTM 2006).

The specimens are heated again at 210°F (99°C), and then cooled at a temperature of 73°F (23°C) for 16 hours and measured. They are then heated again to 210°F (99°C) for 16 hours and removed one at a time and measured. The coefficient of thermal expansion can then be determined by dividing the length of the specimen at the elevated temperature by the length at the lower temperature and the temperature change [$L_E/(L_L*\Delta T)$; where L_E = Length at elevated temperature, L_L = Length at lower temperature, ΔT = Change in temperature] (ASTM 2006).

Figure 2-5: ASTM C 531 M (Specimens heated in oven)

2.2.1.7 Workability and Ease of Use

The ease or difficulty by which specimens for each material can be made is also an important consideration when determining the usefulness of the patching material. Therefore, each material is subjectively rated, incorporating factors such as working time, toxicity, ease of finishing, and ease of cleanup.

2.2.2 Non-Water-Based Material

2.2.2.1 ASTM C 882 – Bond Strength of Epoxy-Resin Systems Used with Concrete by Slant Shear

A composite cylinder is composed of two equal volume sections, whose interface forms a 30-degree angle with vertical (Figure 2-4). The bottom half is base concrete and the other half is that of the patching material. An epoxy bonding system is applied at the interface to join the two halves, if required by the manufacturer. Then, a compressive strength test (ASTM C 39) is run on the hybrid cylinder. The bond strength is determined by dividing the load at failure by the area of the interface between the two sections (ASTM 2006).

2.2.2.2 ASTM C 39, ASTM C 666, ASTM C 266, ASTM C 191, ASTM C 531 M, Workability and Ease of Use

See description in Section 2.2.1. Note that NTPEP does not require ASTM C 666 to be run with salt water for non-water-based materials (National Transportation Product Evaluation Program 2005).

2.3 ASTM Testing Results

The following is a compilation of the ASTM results. Note that the values given for each material are averages of results obtained from multiple test specimens to consolidate the data. Full tables of data are provided in Appendix A. Most data sets contained a small standard deviation, but some had a much larger standard deviation due to extreme outliers caused by experimental error such as specimen honeycombing. These extreme outliers were omitted from the calculation and are shown in bold text in the tables in Appendix A along with a description of the testing error that occurred. Table 2-2 through Table 2-8 contain results in tabular form. Figure 2-6 through Figure 2-13 contain the results in graphical form.

Table 2-2: Compression, Cylinders – ASTM C 39

Material	1-Hr. (psi)	3-Hr. (psi)	1-Day (psi)	7-Day (psi)
Duracal	1250	1960	3920	6440
HP	1170	1490	2860	4900
Pavemend	240	1960	3450	3760
Rapid Set	2620	4110	5540	6570
Sika	20	410	2950	4590
T17	600	1920	4240	4430

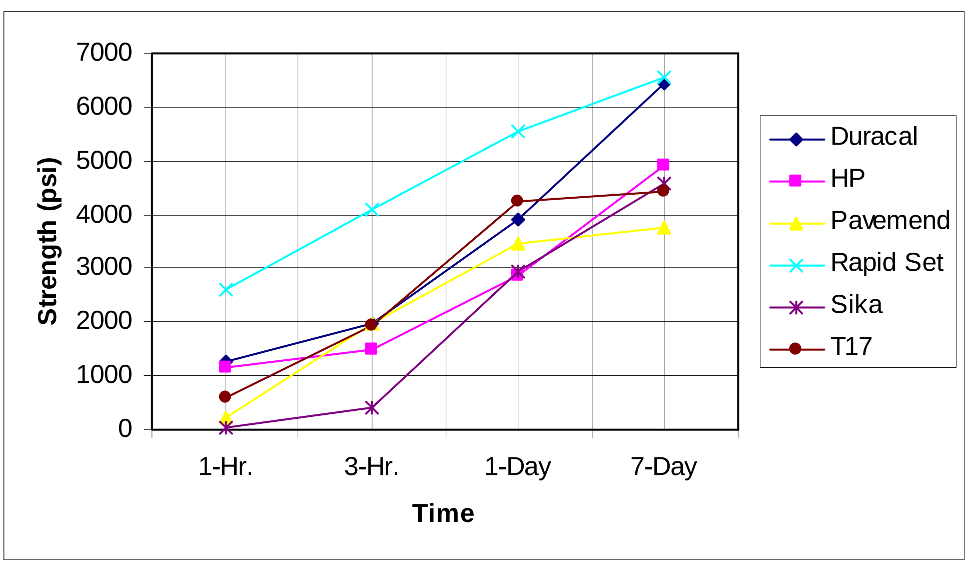

Figure 2-6: Compression, Cylinders – ASTM C 39

Table 2-3: Freeze-Thaw – ASTM C 666 (Regular Water)

Material	Durability Factor*	Comments
Duracal	41	Chipping and deterioration present
HP	44	Severe deterioration
Pavemend	74	Some flaking of outer layer
Rapid Set	98	Cracks and depressions present
Sika	99	Perfect condition
T17	N/A**	Slight deterioration of outer layer

* The "Durability Factor" is the measurement by which ASTM determines the amount of deterioration in a specimen. "100" would represent no deterioration and "0" would represent total deterioration.
** Measurements could not be taken on the T17 specimens due to its unusual material makeup. Visual inspection was the only means of testing.

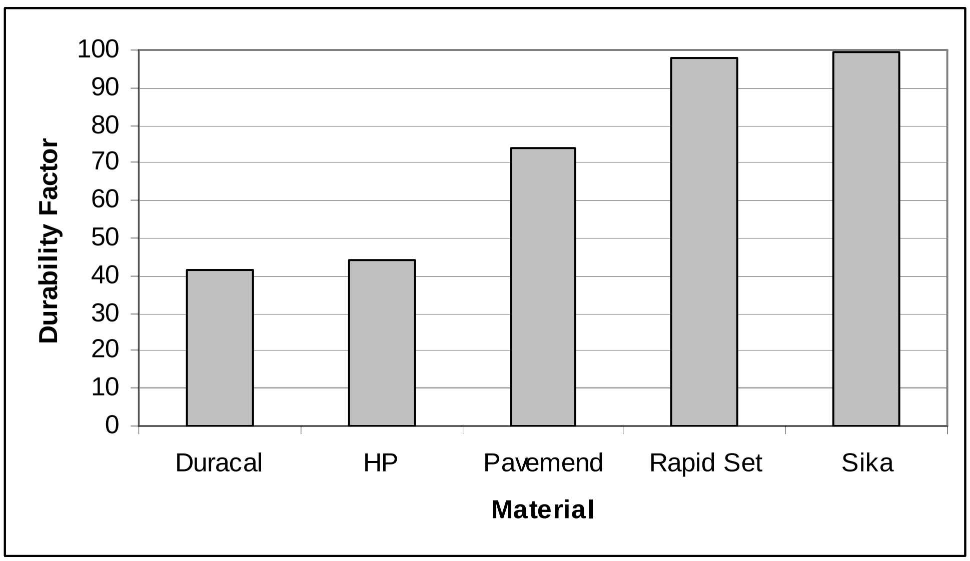

Figure 2-7: Freeze-Thaw – ASTM C 666 (Regular Water)

Table 2-4: Freeze-Thaw – ASTM C 666 (Salt Water)

Material	Durability Factor	Comments
Duracal	33	Scaling; Outer Layer Deteriorated
HP	26	Severe deterioration; Unrecognizable
Pavemend	118	Perfect Condition
Rapid Set	99	Depressions and scaling, but not severe

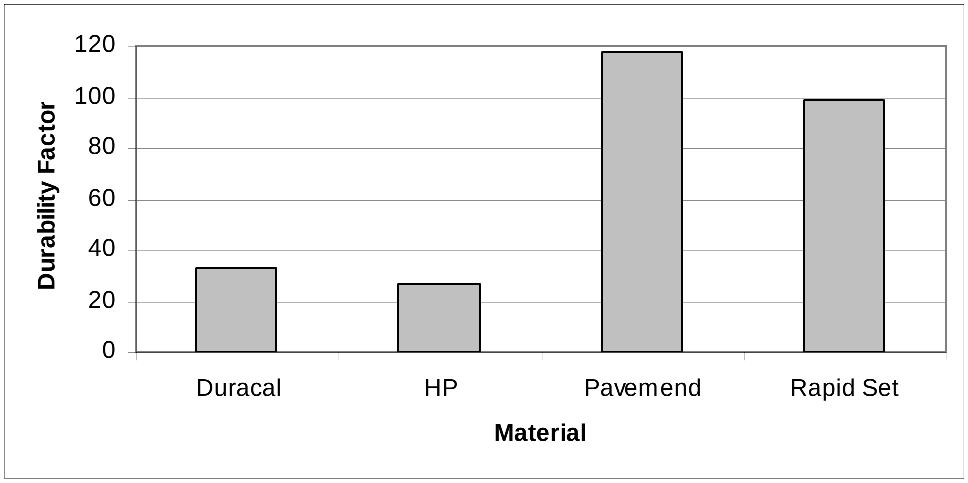

Figure 2-8: Freeze-Thaw – ASTM C 666 (Salt Water)

Table 2-5: Set Time – ASTM C 191 (Vicat Test)

Material	Initial Set Time (min)*	Final Set Time (min)**
Duracal	42	55
HP	5	8
Pavemend	8	11
Rapid Set	11	20
Sika	57	70
T17	25	27

* 0.039 inch (1 mm) diameter Vicat needle penetrates 0.98 inch (25 mm) into specimen.
** 0.039 inch (1 mm) diameter Vicat needle cannot penetrate specimen.

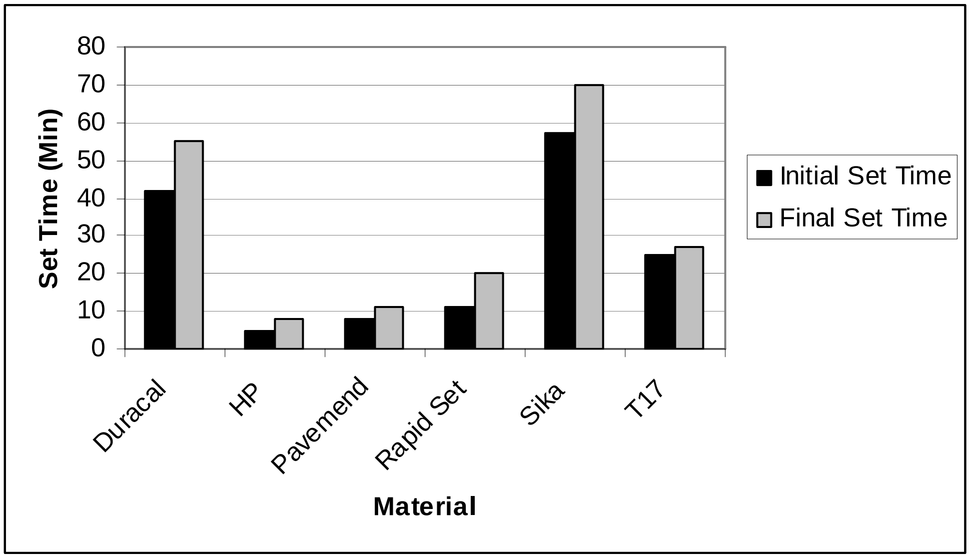

Figure 2-9: Set Time – ASTM C 191 (Vicat Test)

Table 2-6: Slant Shear Test – ASTM C 882/928

Material	1-Day (psi)	7-Day (psi)
Duracal	1040	1140
HP	130	450
Pavemend	660	480
Rapid Set	110	260
Sika	130	550
T17	170	680

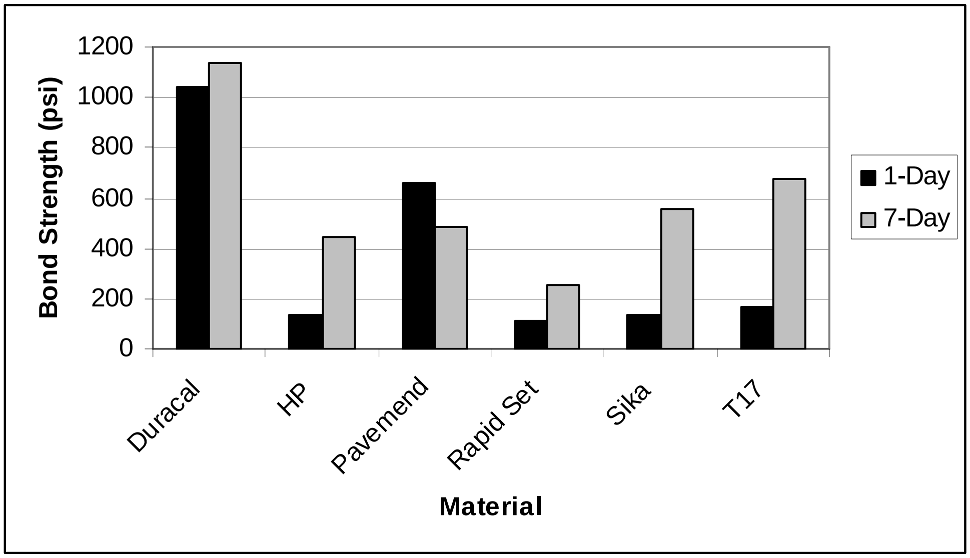

Figure 2-10: Slant Shear Test – ASTM C 882/928

Table 2-7: Thermal Expansion and Shrinkage Testing – ASTM C 531 M

Material	Shrinkage (%)	Coef. Of Therm. Exp. (1/°F)
Duracal	0.27	3.6×10^{-6}
HP	0.54	3.0×10^{-6}
Pavemend	0.20	4.5×10^{-6}
Rapid Set	0.29	4.5×10^{-6}
Sika	0.19	4.7×10^{-6}
T17	-0.21*	15×10^{-6}

* Exhibits expansive properties.

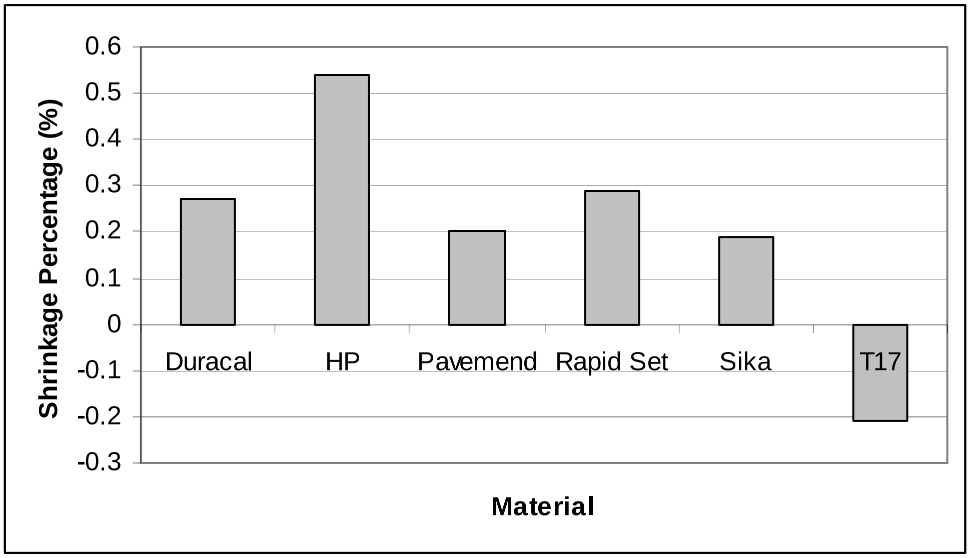

Figure 2-11: Shrinkage Testing – ASTM C 531 M

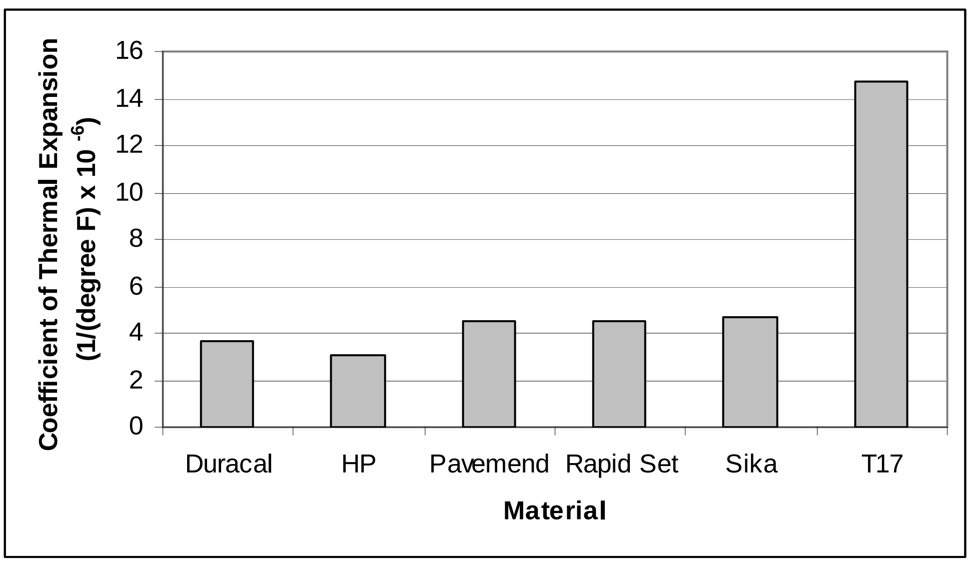

Figure 2-12: Thermal Expansion Testing – ASTM C 531 M

Table 2-8: Workability and Ease of Use (Scale of 1-10)

Material	Score	Comments
Duracal	7	Workable mixture with reasonable amount of working time
HP	2	Highly unworkable, even when water-to-cement ratio is higher than manufacturer recommends. Turns into dirt-like consistency just minutes after mixing. Extremely difficult to make specimens with – required much trial and error. Unable to finish surfaces properly. Difficult clean up as well due to very fast setting time.
Pavemend	10	Extremely easy to use – just mix, and then pour. Self-leveling, so finishing is not even required.
Rapid Set	6	Workable mixture, but fast setting time can make casting, finishing, and cleanup difficult.
Sika	8	Ample working time makes for easy casting.
T17	4	Mixture itself is easy to work with, but the fumes it produces are extremely strong. Also very flammable and produces waste that needs special precautions for disposal.

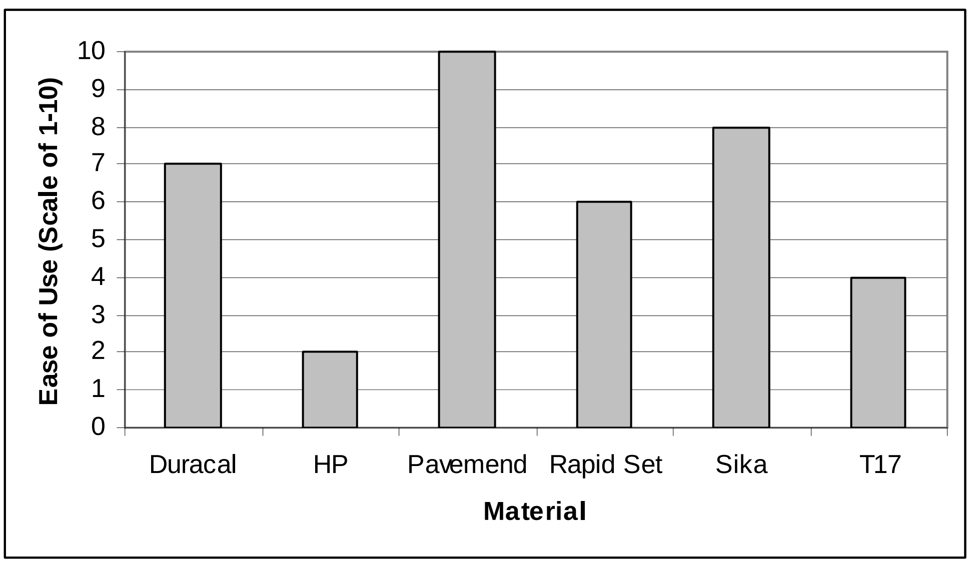

Figure 2-13: Workability and Ease of Use

Chapter 3

Testing Program B – Specialized Testing

3.1 Patching Material Selected

Based on the test results from Testing Program A, two materials were chosen for the next phase of testing: Pavemend 15.0 and Rapid Set Concrete Mix (with latex modifier). These materials obtained high early strengths (over 1,900 psi 3 hours after casting), set quickly (final setting in 20 minutes or less), had low shrinkage percentages (less than 0.3%), and resisted adverse freeze-thaw deterioration (durability factors greater than 70), while being easy to work with (Table 2-8).

The reasons for the recommendation of dismissal of the other four products vary. HP Fast Setting Concrete did not exhibit 3-hr strengths as high as the chosen two, while also severely deteriorating in freeze-thaw testing (durability factor less than 50) and exhibiting a high shrinkage percentage (0.54%). Most importantly, its difficulty of use (Table 2-8) would make it very challenging to use in the field. Sikatop 122 Plus performed well in every category of testing, except it took too long to set (over 1 hour until final set) and thus did not obtain high early strengths. With a 3-hr compressive strength of only 412 psi, it would not be able to stand up to traffic within 4 hours of casting. T17 Polymer Concrete was an unusual material with respect to workability as well as with test results (unable to test in freeze-thaw, expansive properties, initial setting time virtually equal to final setting time). Overall, it tested well in the tests that could be run, but was not moved forward to Phase II due to safety concerns. Its liquid component is both toxic and extremely flammable. This product could pose a threat to the maintenance crews as well as the public. Duracal tested reasonably well in most categories, but performed poorly in freeze-thaw testing (durability factor less than 50), which brings this product's long-term durability into question.

3.2 Phase II Methodology: Specialized Testing

The test planning phase was divided into two main focus areas, durability under traffic loading and durability in chloride environments. As discussed in Section 1.4.1, the main causes of bridge deck deterioration are corrosion in the reinforcement inhibited by chloride penetration, adverse freeze-thaw effects, and traffic loading. The effects of freeze-thaw have already been considered in the ASTM testing, therefore the specialized testing must address the other two major concerns. Hence, the following testing has been established to do just that.

- Durability under heavy traffic loading
    - Patch separation testing
        - A three-point bending test was used to evaluate the durability of the patched slab strips against patch separation under a given load/deflection and load-deflection curves were then plotted.

- Abrasion Testing
  - Durability of the patch under repetitive tire loading was evaluated using the MMLS3 (Mobile Model Load Simulator - 3rd scale), shown in Figure **3-1**.

Figure **3-1**: MMLS3

  - Resistance of the patch to abrasion was evaluated by means of ASTM C 418 – "Abrasion Resistance of Concrete by Sandblasting" (ASTM 2006).

- Durability in chloride environments
  - Ponding tests
    - Patched specimens for the chloride testing were cast with an electrical connection to the reinforcement and were evaluated in a cyclic salt-water ponding environment (1 week dry, 1 week surface submerged in 3% NaCl solution). Half-cell potential readings, in accordance with ASTM C876, were taken at 2-week intervals to track the probability (and location) of corrosion (ASTM 2006).

Specimens were cracked after 2 months to accelerate the corrosion process. After 3 months, the specimens were autopsied to visually inspect the quality of the patch and the encased reinforcement. Chloride penetration measurements were also taken at various locations in the patch and in the surrounding concrete.

For each patch material, a standard group of specimens were evaluated based on patch area and depth. Slab strips were cast of a base material of reinforced concrete with a typical field-prepped hole for fill of the patch material. Patch sizes are defined in Table **3-1**. The sizes of these patches were chosen for various reasons. For the depth, 4 inches and 8 inches were chosen for the shallow and deep patches, respectively, because the slabs to be tested were 8 inches deep according to PennDOT standards for a bridge deck spanning 8 ft, which was the longest length slab that could be used for the three-point bending test due to laboratory limitations. Therefore, 4 inches was half depth and 8 inches would be a full-depth patch. For patch area, the repetitive tire loading test controlled. The effective length on which the tires could run was 3 ft. Because of this, the largest dimension of the large patch could not exceed 3 ft. Also, since the slab could not be wider than 4 ft (laboratory limitations), and 1 ft of base material was desirable on each side of the slab, the width of the patch could not exceed 2 ft. Therefore, the dimension of the large patch was made to be 3 ft by 2 ft. In order to have two small patches run at the same time on the repetitive tire loading test, both patches had to fit within the 3-ft length limitation. Since having a 6-inch gap between the patches was desirable, the largest length the small patches could have was 15 inches. Then, in order to have square small patches, the width was made to be 15 inches as well.

Table 3-1: Patch Dimensions

	Patch Area	Patch Depth
1	Small Patch (15”x15”)	4” Deep (1 mat of rebar exposed)
2	Small Patch (15”x15”)	8” Deep (2 mats of rebar exposed)
3	Large Patch (3’ x 2’)	4” Deep (1 mat of rebar exposed)
4	Large Patch (3’ x 2’)	8” Deep (2 mats of rebar exposed)

Although not outlined specifically under the test plan, visual inspection and constructability were critical components of the testing program. Specifically, these included the following: ease of patch placement, workability of the patch material, pot life, and visual evaluation of shrinkage cracking and patch separation.

Table 3-2 lists the full matrix of test specimens that were tested for each of the two patch materials for a total of 14 specimens (four of these slab strips contained multiple patches, resulting in testing of a total of 18 patches). This number was established based on the fact that patches of all sizes should be tested in the three-point bending test to determine if a patch of any size is prone to separate from the substrate (four patches for each material – eight total on eight slabs). For the repetitive tire loading test and the corrosion test, the patch area was not of great importance, but the patch depth was. Therefore, only the small shallow and the small deep patches were examined in these tests (two patches for each material for each test – eight total on four slabs). For the ASTM sandblasting test, the size of the patch was not significant, so the large, shallow patch was chosen to give a large area to test without having to use a great deal of material (one patch for each material – two total on two slabs). See Figure 3-2, Figure 3-3, Figure 3-4, and Figure 3-5 for diagrams of each slab type.

Table 3-2: Patch Type Testing Matrix

Test	Patch Type
Patch Separation (4’ x 8’ slab)	Small shallow (See Fig. 3-2)
	Small deep (See Fig. 3-2)
	Large shallow (See Fig. 3-3)
	Large deep (See Fig. 3-3)
Repetitive Tire Load (4’ x 6’ slab)	Small shallow & Small deep* (See Fig. 3-4)
Sandblasting Test (4’ x 6’ slab)	Large shallow (See Fig. 3-5)
Chloride Durability (4’ x 6’ slab)	Small shallow & Small deep* (See Fig. 3-4)

*2 patches on one slab strip specimen

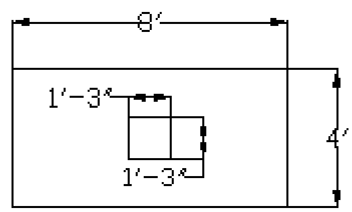

Figure 3-2: Large slab with small patch

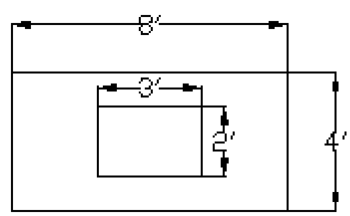

Figure 3-3: Large slab with large patch

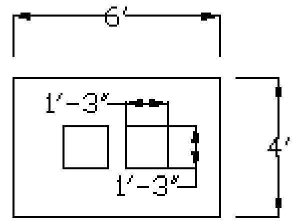

Figure 3-4: Small slab with (2) small patches

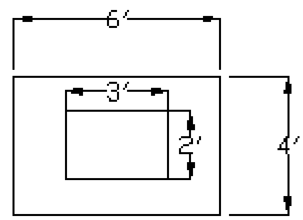

Figure 3-5: Small slab with large patch

3.2.1 Patch Placement

In order to test the material properly, it is first critical to prepare the holes to be patched in the same manner that would be done in the field. According to PennDOT, as demonstrated during a field view that occurred in October 2007, this task is performed in the following manner:

1. Mark the areas of deteriorated concrete on the bridge deck that are in need of replacement.
2. Saw cut around the perimeter of the marked areas, making sure that all of the perimeter angles are right angles (Figure 3-6).

Figure 3-6: Saw-Cut Test Slab

3. Jackhammer out the area within the saw-cut until solid substrate concrete is reached. For this testing, two different depths were considered: Half depth (Figure 3-7), which extends to 1 inch below the top mat of rebar (about 4 inches; according to PennDOT, this is a Type II patch), and full depth (Figure 3-8), which extends the entire way through the slab (8-inches deep in this case; according to PennDOT, this is a Type III patch).

Figure 3-7: Jackhammered Patch Area – Half Depth

Figure 3-8: Jackhammered Patch Area – Full Depth

4. Clean debris off of concrete and exposed rebar by either grinding or sandblasting, and then replace any rebar ties that may have been destroyed or damaged during jackhammering (Figure **3-9**).

Figure **3-9**: Cleaned Patching Hole

5. Refer to the following sections for the proper material placement procedures of Pavemend 15.0 and Rapid Set with the latex modifier.

3.2.1.1 Pavemend 15.0 – Patch Placement

Pavemend 15.0 is a rapid-setting, self-leveling repair mortar. It comes in prepackaged 5-gallon buckets with 45 lb of material. It can be used in temperatures between 30°F and 110°F, and one bucket yields approximately 0.42 ft^3. The manufacturer recommends that these steps be followed to ensure that the patch is placed correctly:

1. Ensure that the patching hole is dry and clean.
2. Using a paddle mixer with a drill capable of 300 rpm, loosen the material in the bucket.
3. Add 1 gallon of water to the bucket, and mix thoroughly until the material reaches 95°F, using a thermal gun to check the temperature (Figure 3-10).

Figure 3-10: Mixing Pavemend 15.0

4. Once the critical temperature is reached, quickly pour the material into the prepared hole. If desired, a dry trowel or straight edge may be used to finish, but material is self-leveling, so this is not necessarily required (Figure 3-11).

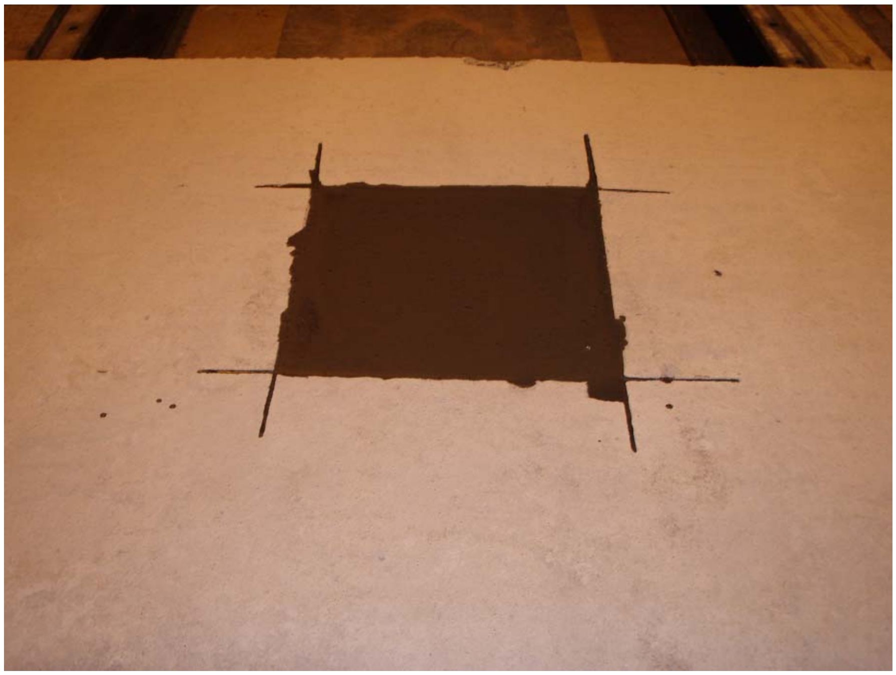

Figure 3-11: Pavemend 15.0 Patch

3.2.1.2 Rapid Set with Latex Modifier – Patch Placement

Rapid Set Concrete Mix is a mixture of hydraulic cement and aggregate. It is commonly mixed with "Modifier A," a latex modifier, to enhance its performance. Rapid Set comes in prepackaged 60-lb bags. It can be used in temperatures above 45°F, and one bag can yield 0.52 ft^3. The following steps should be followed to ensure that the patch is placed correctly:

1. Ensure that the patching hole is clean, and wet the hole to saturated surface dry conditions.
2. Wet, then drain the concrete mixer.
3. Add the water (0.45 gal per bag of material) and latex (0.45 gal per bag of material) to the mixer and turn on the mixer.
4. Add the concrete mix to the mixer, and mix for 1 to 3 minutes, whenever constant consistency is reached (Figure **3-12**).

Figure **3-12**: Mixing Rapid Set

5. Once mixing is complete, pour material into patching hole.

6. Pack material tighly into hole. This task is made easiest by the use of a vibrator (Figure **3-13**).

Figure **3-13**: Vibrating Rapid Set

7. Finish surface as soon as possible with dry trowel or straight edge.
8. Once material loses sheen, place wet burlap over the patch for 1 hour (Figure **3-14**).

Figure 3-14: Wet Curing Rapid Set

9. Remove burlap after 1 hour to reveal final product (Figure 3-15).

Figure 3-15: Rapid Set Patch

3.2.2 Three-Point Bending Test

3.2.2.1 Three-Point Bending Test Procedure

The purpose of the three-point bending test is to determine the performance of the patched slab under a given load and deflection. Although this test exhibits more extreme conditions on the patch than it is likely to experience in the field, it demonstrates the ability of the patch and slab to act as one continuous member, and gives an indication of the weakest location in the two-part patch/slab system. To test the slabs in this three-point bending test, the following steps are taken:

1. Patches are placed in 8-ft-by-4-ft slabs by using previously described procedures in Sections 3.2.1.1 and 3.2.1.2, and allowed to cure for 1 hour.
2. Slabs are then flipped over so that the patch is located on the bottom of the slab (Figure 3-16). This is done so that the patch will be in tension (worst-case scenario) when it is loaded.

Figure 3-16: Flipping Slap

3. Slabs are placed beneath the actuator where the load can be applied. Note that the span is 7-ft 6-inches long for the 8-ft slabs due to a 3-inch overhang on either side (Figure 3-17).

Figure 3-17: Slab Under Actuator

4. After the patch has reached 3-hour strength, the slab is loaded until failure (maximum load that slab can hold, as indicated by electronic actuator system), stopping every 5-kip increment to record the load and the deflection from the electronic system. Figure 3-18 is a schematic of the testing.

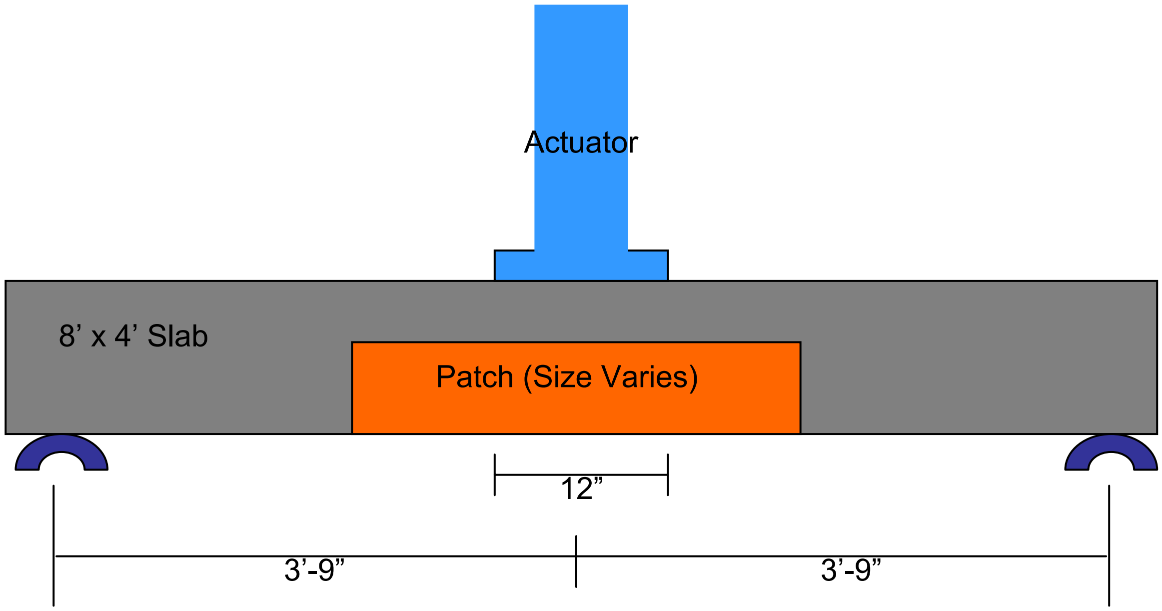

Figure 3-18: Three-Point Bending Test Schematic

3.2.2.2 Three-Point Bending Test Results

All eight slabs were tested in the manner described above. Refer to Table 3-2 for a list of the four different patch sizes of each material that were tested.

Both materials (Pavemend and Rapid Set) performed well under three-point loading. Neither material truly separated from the substrate concrete, even after the maximum load was reached and the specimen began deflecting heavily while losing the load. There was, however, slight cracking around the patch/substrate interface for all slabs, as demonstrated in Figure 3-19 and Figure 3-20. All slabs failed at loads greater than the load associated with the calculated nominal moment capacity, which was 37.3 kips (Figure 3-21). In fact, all slabs failed at loads greater than 50 kips, except the large, full-depth Pavemend slab, which failed at 41.4 kips. Also note that Rapid Set had slightly smaller deflections throughout testing, indicating that it is a stiffer material. Table 3-3 summarizes relevant test data and Figure 3-22 provides load-deflection plots for all eight tests. Appendix B contains test photos.

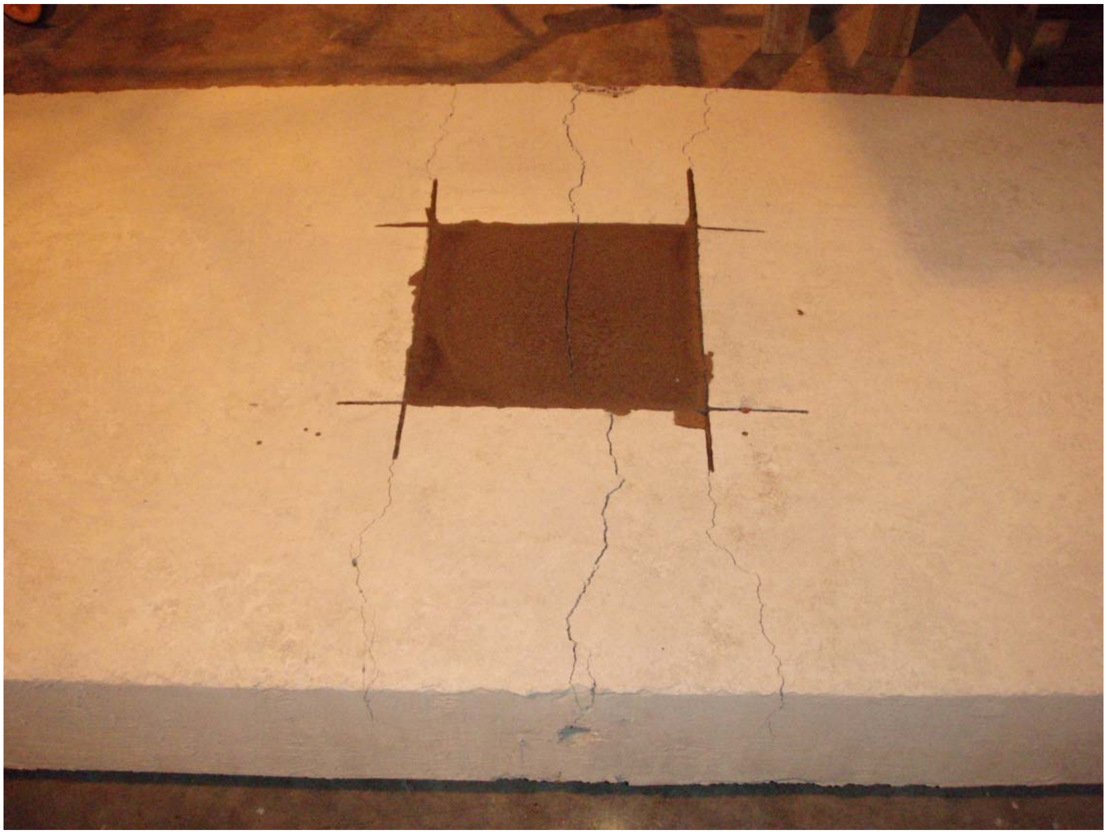

Figure 3-19: Cracking of Pavemend 15.0 Slab

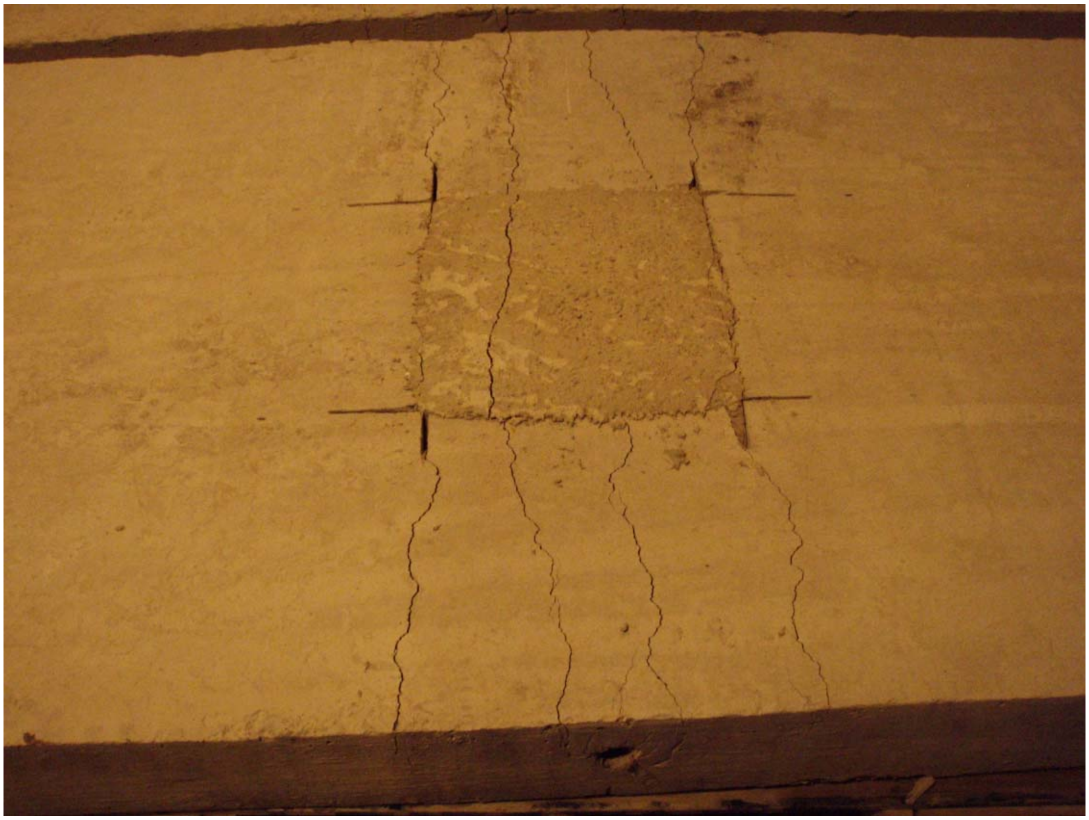

Figure 3-20: Cracking of Rapid Set Slab

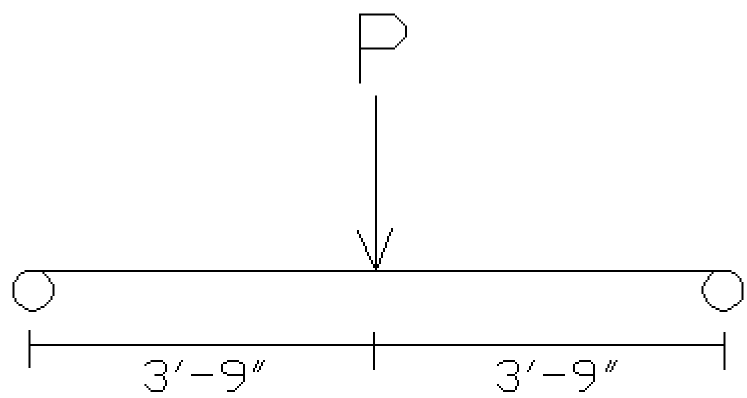

a = $(A_s f_y)/(0.85 f'_c b)$ = (7*0.44in^2*60ksi)/(0.85*5ksi*48") = 0.91"

M_n = $A_s f_y$*(d-a/2) = 7*0.44in^2*60ksi*(5"-0.91"/2) = 840.3k-in

M_n = PL/4 (Set M_n equal to the moment at midspan)

P = 4M_n/L = 4*840.3k-in/90" = **37.3 kips**

Note:
a = Depth of Whitney stress block (in)
A_s = Area of steel in tension = (7) # 6 bars
Area of #6 bar = 0.44in^2
f'_c = Strength of concrete = 5 ksi at time of testing
f_y = Yield strength of steel = 60 ksi
M_n = Nominal moment capacity of slab (k-in)
d = Depth from top compression fiber to centroid of steel in tension = 5 inches
P = Load applied (kips)
L = Length of span = 7 ft 6 inches = 90 inches

Figure 3-21: Three Point Loading Failure Calculation

Table 3-3: Three-Point Loading Test Data

Pavemend 15.0										
Small, Shallow			Large, Shallow			Small, Deep			Large, Deep	
Load(k)	Defl.(in)		Load(k)	Defl.(in)		Load(k)	Defl.(in)		Load(k)	Defl.(in)
0.0	0.00		0.0	0.00		0.0	0.00		0.0	0.00
5.0	0.09		5.0	0.11		5.0	0.09		5.0	0.11
10.0	0.18		10.0	0.22		10.0	0.17		10.0	0.21
15.0	0.25		15.0	0.32		15.0	0.25		15.0	0.31
20.0	0.34		20.0	0.41		20.0	0.34		20.0	0.41
25.0	0.43		25.0	0.51		25.0	0.44		25.0	0.51
30.0	0.52		30.0	0.61		30.0	0.54		30.0	0.63
35.0	0.61		35.0	0.77		35.0	0.63		35.0	0.74
40.0	0.71		40.0	0.82		40.0	0.73		40.0	0.94
45.0	0.88		45.0	1.08		45.0	1.13		41.4	1.03
50.0	1.38		50.0	1.83		50.0	1.43			
53.6	1.70		52.0	2.30		51.8	1.84			
Rapid Set										
Small, Shallow			Large, Shallow			Small, Deep			Large, Deep	
Load(k)	Defl.(in)		Load(k)	Defl.(in)		Load(k)	Defl.(in)		Load(k)	Defl.(in)
0.0	0.00		0.0	0.00		0.0	0.00		0.0	0.00
5.0	0.08		5.0	0.08		5.0	0.07		5.0	0.08
10.0	0.15		10.0	0.16		10.0	0.14		10.0	0.16
15.0	0.22		15.0	0.27		15.0	0.22		15.0	0.25
20.0	0.31		20.0	0.34		20.0	0.32		20.0	0.33
25.0	0.40		25.0	0.44		25.0	0.41		25.0	0.42
30.0	0.49		30.0	0.54		30.0	0.51		30.0	0.51
35.0	0.58		35.0	0.63		35.0	0.60		35.0	0.60
40.0	0.68		40.0	0.77		40.0	0.70		40.0	0.71
45.0	0.81		45.0	0.80		45.0	0.87		45.0	0.89
50.0	1.22		50.0	0.96		50.0	1.39		50.0	1.47
55.0	1.87		53.6	1.57		53.5	1.92		51.7	1.87

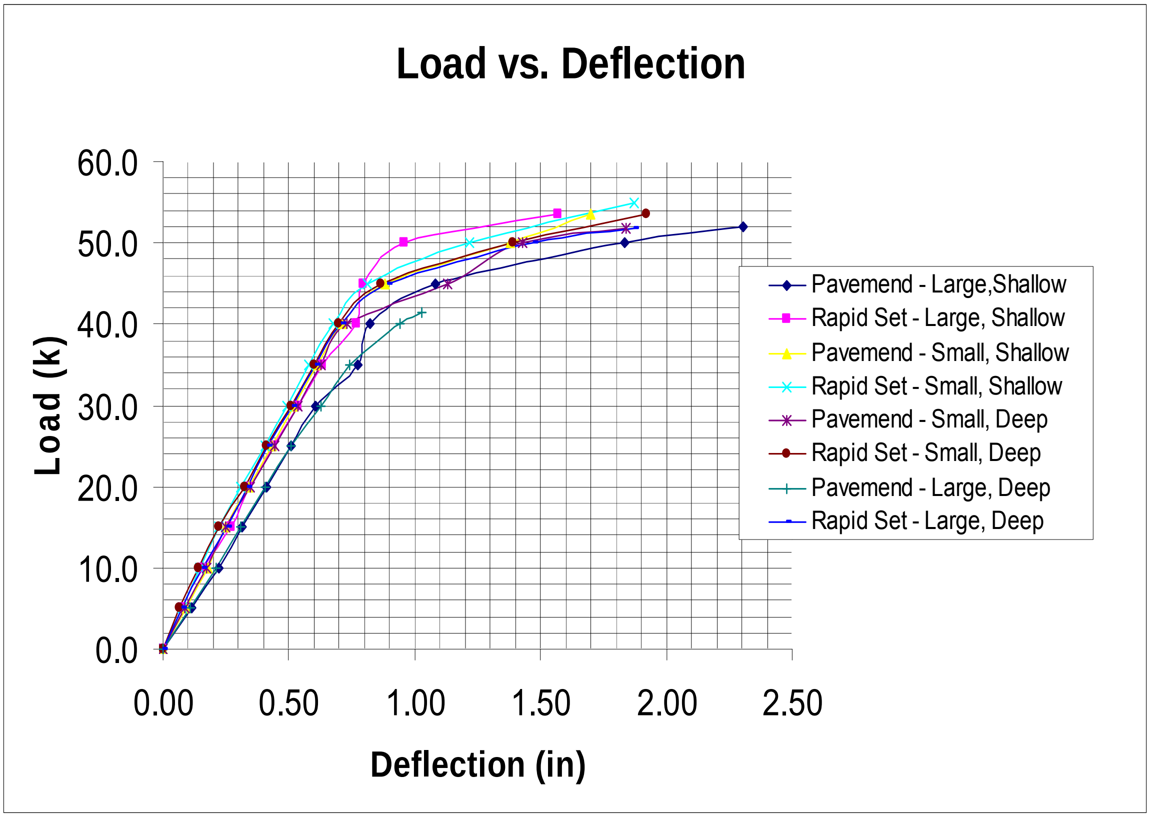

Note: The last three data points for "Rapid Set - Large, Shallow" were taken at the material's 1-day strength (equipment malfunction during initial day of testing).

Figure 3-22: Three Point Loading Load-Deflection Plots

3.2.3 Abrasion Resistance Testing – Repetitive Tire Load Simulation

3.2.3.1 Repetitive Tire Load Simulation Procedure

Durability of the patch under repetitive tire loading was evaluated using the MMLS3. This machine is designed to exert a wheel load with the same pressure on the slab as a vehicle driving over the bridge (100 psi). By testing slabs with various patch dimensions (See Table 3-2 for the list of tested patches), this test can determine the patch material's ability to resist wear and tear over the life of the patch. To test the slabs under repetitive tire load simulation, the following steps are taken:

1. Patches are placed in 6-ft-by-4-ft slabs by use of procedures described in Sections 3.2.1.1 and 3.2.1.2, and allowed to cure for 1 hour.
2. After 1-hour strength is reached, the slab is moved under the MMLS3, and the MMLS3 is calibrated to exert 100 psi of pressure (Figure 3-23).

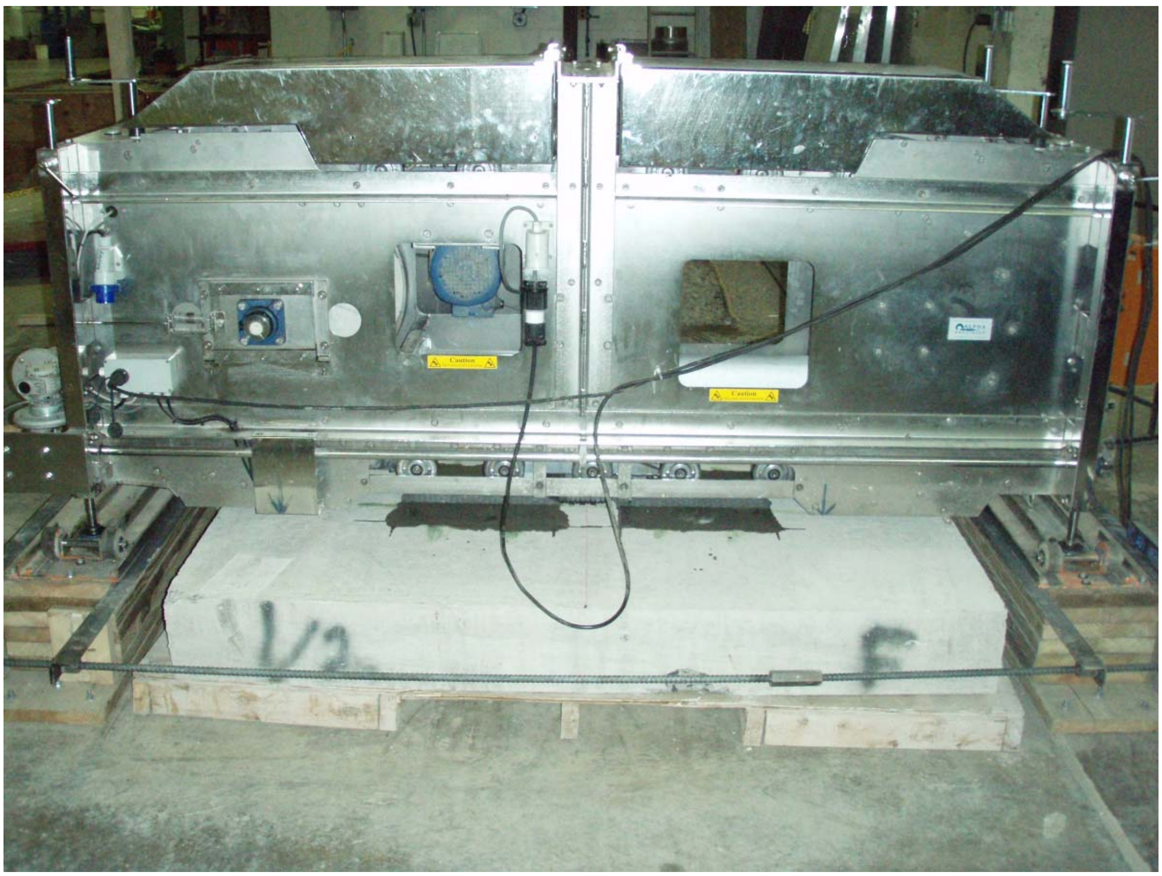

Figure 3-23: Specimen Loaded Under MMLS3

3. After the patching material has reached 3-hour strength, the MMLS3 is turned on and allowed to run for 200,000 cycles. This number of cycles was chosen upon the recommendation of the laboratory expert, Dr. Ghassan Chehab, who

determined that any specimen subjected to more than 200,000 cycles would not deteriorate much more than a specimen subjected to only 200,000 cycles. Therefore, 200,000 cycles is the maximum testing life for any experimentation in the lab (Chehab 2008). Figure 3-24 is a schematic of the testing.

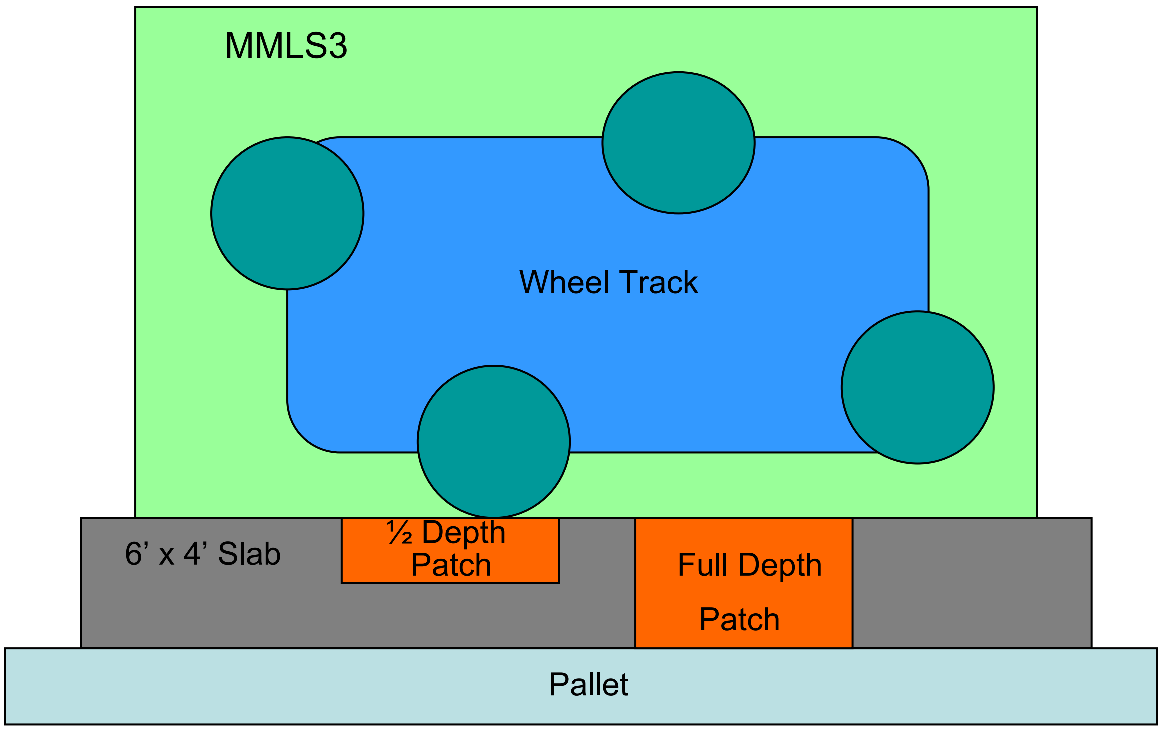

Figure 3-24: Repetitive Tire Loading Test Schematic

4. Once 200,000 cycles is reached, the specimen is removed from the test setup and is evaluated. This evaluation involves a general visual inspection in which cracks or wearing are noted and rut depths are to be measured.

3.2.3.2 Repetitive Tire Load Simulation Results

The results for the repetitive tire load simulation were very favorable for both materials. Any abrasive damage for Pavemend 15.0 was negligible after 200,000 cycles, as demonstrated by Figure 3-25, which shows the patches after the completion of this testing. There was also negligible damage to the Rapid Set patches, but interestingly there was a small amount of damage to the base material at the interface (Figure 3-26 and Figure 3-27). In spite of this, it is deemed that both have excellent resistance to abrasion after 3-hour strengths are achieved because only minor deterioration was observed. See Appendix B for more photographs of the tested patches.

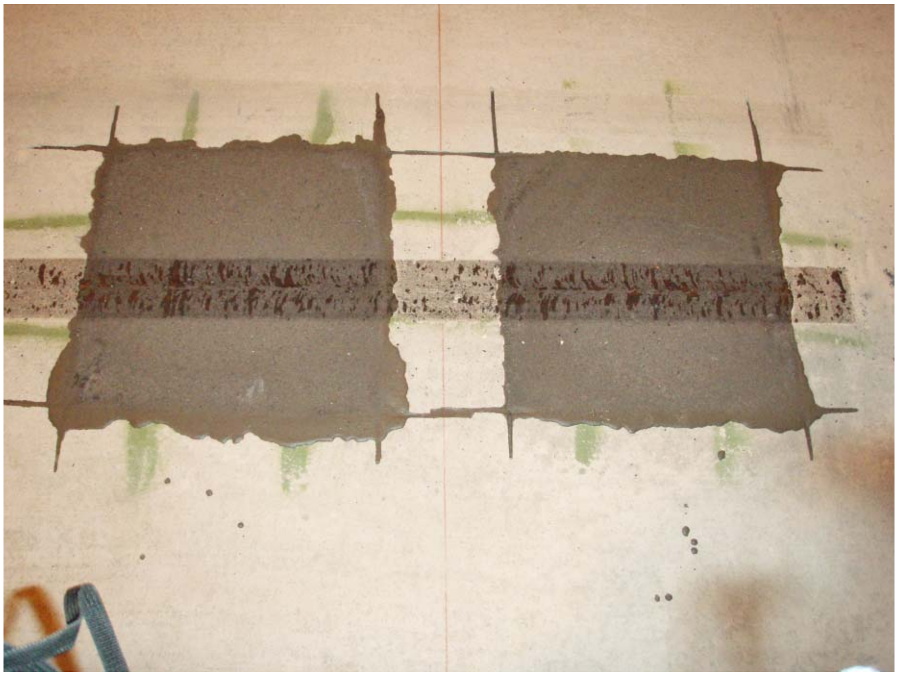

Figure 3-25: Repetitive Tire Loading – Pavemend 15.0 Patches

Figure 3-26: Repetitive Tire Loading – Rapid Set Patches

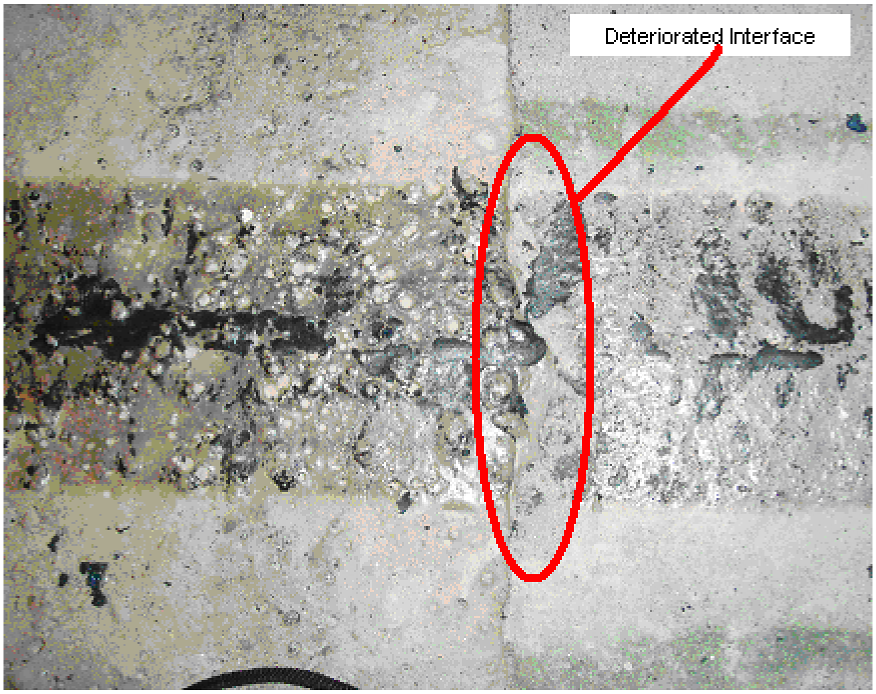

Figure 3-27: Repetitive Tire Loading – Rapid Set Patches – Deteriorated Interface

3.2.4 Abrasion Resistance Testing – Sandblasting Test

3.2.4.1 Sandblasting Test Procedure

Resistance of the patch to abrasion was also evaluated by means of ASTM C 418, "Abrasion Resistance of Concrete by Sandblasting." In this test, the slabs with a large, half-depth patch were subjected to sandblasting to determine the resistance to abrasion damage. To test the slabs in this fashion, the following steps are taken:

1. Patches are placed in 6-ft-by-4-ft slabs by use of procedures described in Sections 3.2.1.1 and 3.2.1.2 and allowed to obtain 3-hour strength.
2. Once 3-hour strength is reached, the sandblast nozzle is placed 3 inches above the surface of the specimen and the surface is blasted with sand (Grade 20 on 30) for 1 minute. Since this particular grade of sand was not available during testing, the test was run instead with grade 60 on 120 sand for an extended period of time, 90 seconds. A wooden box was used, as seen in Figure **3-28**, to both contain the sand particles and to ensure uniform blasting distances (3 inches) throughout.

Figure 3-28: Sandblasting Specimen – ASTM C 418

3. At completion of sandblasting, a mass of clay is weighed and pressed into the hole made by the blast. The hole is filled until it is flush with the surface and then the remaining mass of clay is weighed again to determine how much clay is in the cavity (Figure 3-29). This step is performed eight times for each of the three specimens (Pavemend 15.0 patch, Rapid Set patch, and base concrete [control]).

Figure 3-29: Sandblasted Hole Filled With Clay – ASTM C 418

4. The volume of the clay in the cavity is determined by using V = W / D, where V is the volume of the cavity, W is the weight of clay in the cavity, and D is the specific gravity of the clay (set equal to 2.0 by the manufacturer). (ASTM 2006)

3.2.4.2 Sandblasting Test Results

Table 3-4 and Figure 3-30 indicate that the volume of the sandblasted holes in the base concrete (0.43 in^3 [7 cm^3]) were roughly half the size of those made in the Pavemend patch (0.79 in^3 [13 cm^3]) but were approximately double the size of those made in the Rapid Set (0.18 in^3 [3 cm^3]). Therefore, from this testing it was deemed that Rapid Set is very abrasion resistant, four times moreso than Pavemend 15.0. One key factor in these results is that Pavemend is only a mortar and does not have the course aggregate that Rapid Set utilizes to resist abrasion.

Table 3-4: Abrasion Resistance of Concrete by Sandblasting – ASTM C 418

ASTM C 418 - Abrasion Resistance of Concrete by Sandblasting Note: 1g = 0.0022lbs; 1cm^3 = 0.061in^3							
Material	Test #	Mass of Clay before (g)	Mass of Clay after (g)	Amt. of Clay in Hole (g)	Spec. Gravity of Clay	Volume of Clay in Cavity (cm^3)	Avg. Volume of Cavity (cm^3)
Base Concrete	1	2337	2323	14	2.0	7	7
	2	2323	2310	13	2.0	6	
	3	2310	2296	14	2.0	7	
	4	2296	2283	13	2.0	6	
	5	2283	2270	13	2.0	7	
	6	2270	2255	15	2.0	7	
	7	2255	2242	13	2.0	7	
	8	2242	2229	13	2.0	7	
Pavemend 15.0	1	2229	2207	22	2.0	11	13
	2	2207	2183	24	2.0	12	
	3	2183	2158	25	2.0	12	
	4	2158	2129	29	2.0	14	
	5	2129	2097	32	2.0	16	
	6	2097	2069	28	2.0	14	
	7	2069	2047	22	2.0	11	
	8	2047	2018	29	2.0	15	
Rapid Set	1	2018	2011	7	2.0	3	3
	2	2011	2005	6	2.0	3	
	3	2005	1999	6	2.0	3	
	4	1999	1993	6	2.0	3	
	5	1993	1987	6	2.0	3	
	6	1987	1981	6	2.0	3	
	7	1981	1975	7	2.0	3	
	8	1975	1967	8	2.0	4	

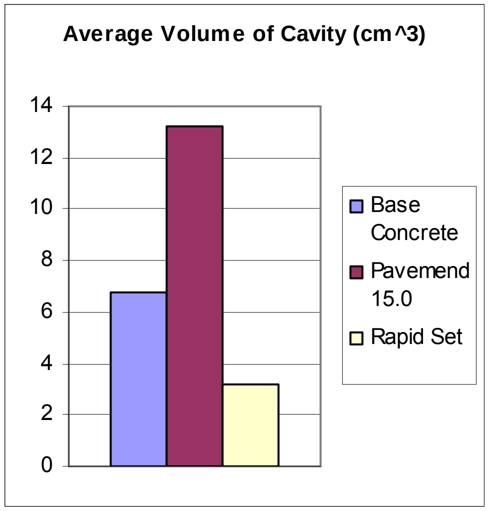

Figure 3-30: Abrasion Resistance of Concrete by Sandblasting – ASTM C 418

3.2.5 Corrosion Testing

3.2.5.1 Corrosion Testing Procedure

The ability of the patch to protect against corrosion of the reinforcement was evaluated by cyclically ponding saltwater on the specimens for 3 months and periodically taking half-cell potential measurements (ASTM C 876) and resistivity measurements, then autopsying the specimens to determine the depth of chloride penetration and the overall condition of the rebar. To corrosion test the slabs, the following steps are taken:

1. Patches are placed in 6-ft-by-4-ft slabs by use of procedures described in Sections 3.2.1.1 and 3.2.1.2 and allowed to reach 7-day strength.
2. Once the slabs have achieved 7-day strength, half-cell potential readings are taken in a grid-like pattern across the slab. The locations of these

measurements are indicated by green dots, as seen in Figure **3-31**. **T**hese spots were chosen to align with the intersection of the longitudinal and transverse reinforcement in the mats of rebar. It is possible to detect corrosion long before there are visual signs on the surface with a non-destructive technique called half-cell potential mapping. Since there is an electrical potential difference of up to 0.5 V between a corroding rebar and a passive rebar, monitoring potential differences across the structure can produce a contour map of equipotential lines and lead to inferences about the location and extent of corrosion. To take these readings, an electrical connection is made with the rebar, which is connected to a high-impedance voltmeter that is connected to a reference electrode (in this case, copper/copper sulfate). The reference electrode has a wet sponge at the bottom of it, and this sponge is placed in contact with the concrete at various locations to obtain readings through the specimen (Figure **3-32**). Resulting data may be influenced by a number of factors other than corrosion (concrete cover, concrete resistivity, etc.). Therefore, it is necessary to have more information than just the half-cell readings to fully understand the state of corrosion in the specimen (Bertolini 2004).

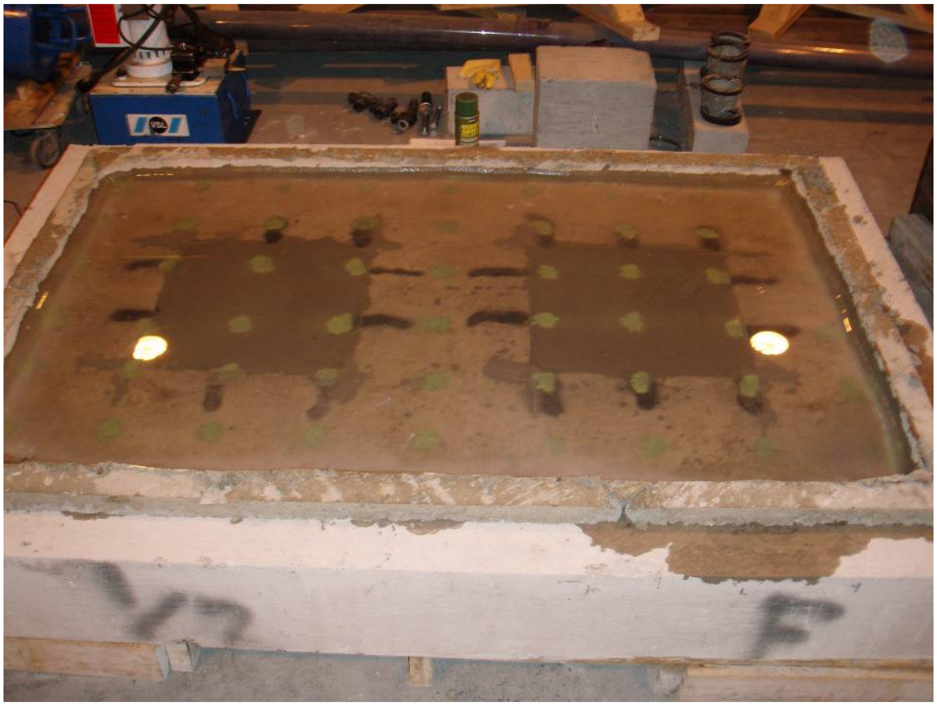

Figure 3-31: Set Locations of Half-Cell Potential Readings

Figure 3-32: Half-Cell Potential Readings

3. Measurements of the resistivity of the concrete are also taken along with the half-cell readings. These measurements are taken on both patches (half depth and full depth), at the patch/base concrete interface, and on the base concrete. Based on the fundamental principle of Ohm's Law (I=V/R), the current is reduced when the resistance is increased. As shown in Figure 1-1, the ionic current flows through the concrete. Therefore, the resistance provided by the concrete directly relates to the rate of corrosion. Resistivity measurements are used to quantitatively determine this resistance. This is accomplished by use of a Wenner Probe, which actually consists of four probes (Figure **3-33**). The outer two probes pass a current through the concrete, while the inner two measure the voltage difference. From this, it calculates the resistance, which helps determine how fast or slow the rate of corrosion can occur within the given concrete (Page 1990).

Figure 3-33: Resistivity Measurements

4. After these initial readings are taken, a 3% salt water solution is ponded on the specimens for 7 days, then the half-cell potential and resistivity measurements are taken again.

5. The specimen is allowed to stay dry for 1 week, then ponded for 1 week, and then measurements are taken again after the wet cycle. This wet-dry-measurement cycle continues for 2 months.

6. After 2 months, the specimen is cracked to speed up the corrosion process. This is accomplished by jacking up from the bottom of the slab until cracks are seen propogating 5 inches deep into the slab (just below the top mat of rebar). Figure 3-34 is a schematic of the jacking setup. Figure 3-35 and Figure 3-36 are photographs of the jacking setup and Figure 3-37 details the resulting crack pattern created on one of the slabs.

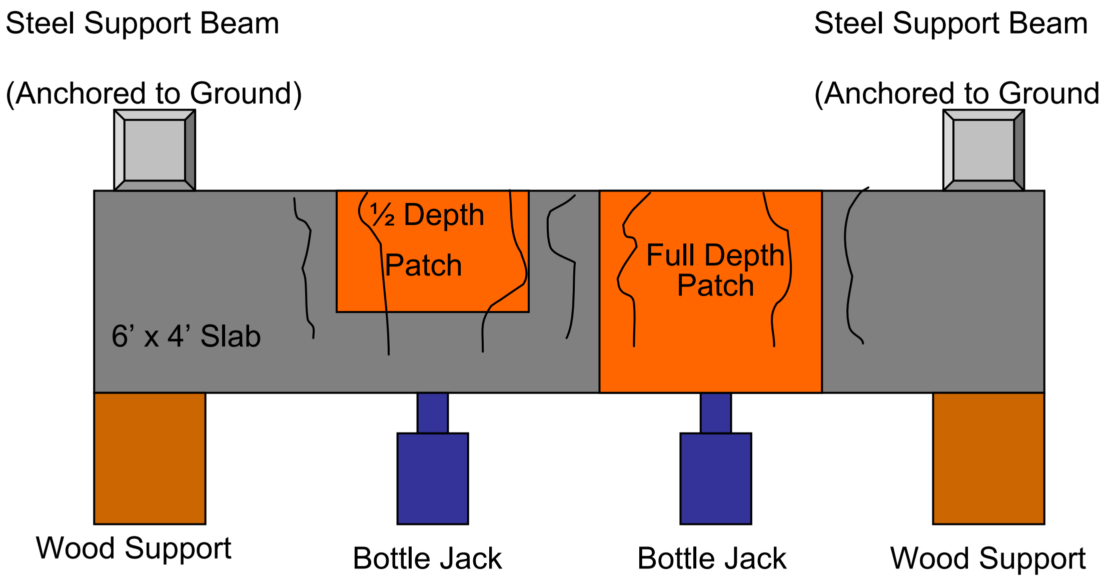

Figure 3-34: Jacking Setup Schematic

Figure 3-35: Cracking Corrosion Slab – Top View

Figure 3-36: Cracking Corrosion Slab – Side View

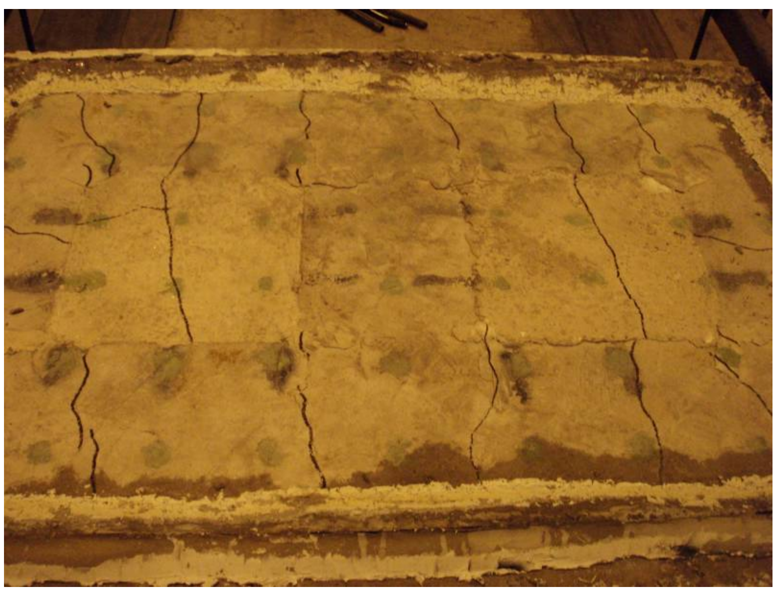

Figure 3-37: Cracking Created By Jacking Force

7. The specimen is then allowed to stay dry for 1 week, then ponded for 1 week (on the cracked side), and then measurements are taken again after the wet cycle. This wet-dry measurement cycle continues for 1 month.

8. After the final measurements are taken, the specimens are then cored. One core is taken in the middle of the half-depth patch, one is taken in the middle of the full-depth patch, and one is taken in the base concrete in the area between the two patches. Figure 3-38 is a diagram that shows the location of the half-cell potential readings, the resistivity measurements, and the cores.

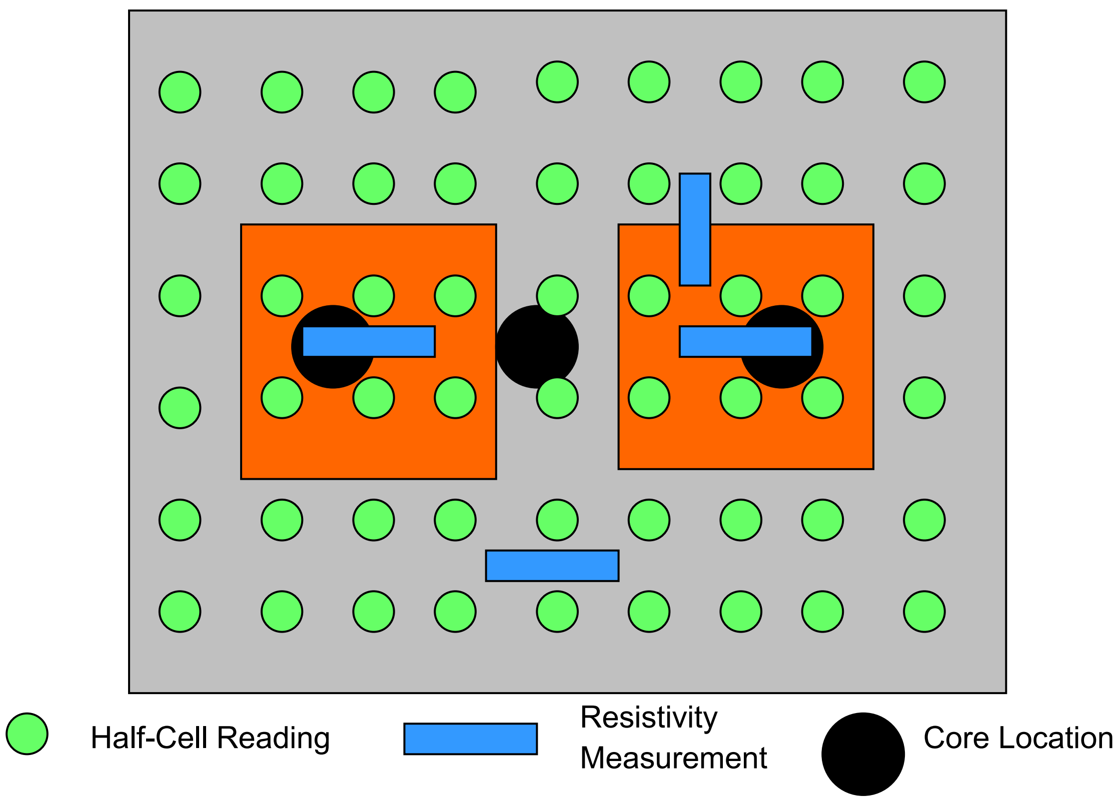

Figure 3-38: Corrosion Test Locations

9. These cores are then sprayed with silver nitrate, which will discolorize the areas that the chlorides have penetrated, thus revealing the extent of chloride penetration. Cylinders of each material (Pavemend 15.0, Rapid Set, and the base concrete) that have not been exposed to salt water will also be sprayed with silver nitrate to act as a control, and prove that chlorides are not a part of the material's constituents.
10. Finally, the top concrete cover is removed to expose the top mat of rebar, and for visual inspection of corrosion damage on the steel.

3.2.5.2 Corrosion Testing Results

To consolidate data for the half-cell potential readings, for each set of readings the average potential within the half-depth patch, the full-depth patch, and the base concrete was calculated. These tabulated values can be found in Table 3-5 along with the resistivity measurements in the half-depth patch, the full-depth patch, the base concrete, and at the patch/base concrete interface. Figure 3-35 is a graphical representation of the potentials over time, and Figure 3-36 is a graphical representation of the resistivities over time. For more extensive data on the half-cell readings, refer to Appendix B.

According to ASTM, there are three different categories for potential readings:

- 0 to -200 mV → >90% Probability of No Corrosion
- -200 to -350 mV → Uncertain Corrosion Activity
- More neg. than -350 mV → > 90% Probability of Corrosion

According to the resistivity meter manual, there are three different categories for resistivity measurements:

- Greater than 12 kΩcm → Corrosion Improbable
- 8 to 12 kΩcm → Corrosion Possible
- Less than 8 kΩcm → Corrosion Fairly Certain

Recall that slabs were cracked between the 5th and 6th cycle.

Table 3-5: Average Half-Cell Potential Readings and Resistivity Measurements

Pavemend 15.0								
	Initial	Cycle						
Average of:	0	1	2	3	4	5	6	7
Base Concrete Potential (mV)	-242	-336	-434	-358	-339	-336	-417	-405
1/2 Depth Patch Potential (mV)	-341	-469	-499	-433	-425	-416	-506	-477
Full Depth Patch Potential (mV)	-402	-421	-573	-465	-457	-444	-552	-527
Base Concrete Resistivity (kΩ-cm)	14	10	9	8	8	5	5	8
1/2 Depth Patch Resistivity (kΩ-cm)	4	2	2	2	3	2	3	2
Full Depth Patch Resistivity (kΩ-cm)	4	2	2	2	2	3	3	3
Interface Resistivity (kΩ-cm)	8	8	7	5	6	4	4	6
Rapid Set w/ Latex Modifier								
	Initial	Cycle						
Average of:	0	1	2	3	4	5	6	7
Base Concrete Potential (mV)	-144	-278	-266	-252	-289	-282	-313	-310
1/2 Depth Patch Potential (mV)	-233	-333	-297	-270	-288	-269	-322	-341
Full Depth Patch Potential (mV)	-234	-313	-308	-291	-337	-322	-367	-377
Base Concrete Resistivity (kΩ-cm)	17	13	16	8	8	5	8	6
1/2 Depth Patch Resistivity (kΩ-cm)	32	32	31	30	15	15	18	22
Full Depth Patch Resistivity (kΩ-cm)	32	32	31	13	12	12	15	18
Interface Resistivity (kΩ-cm)	29	32	30	14	12	8	9	12

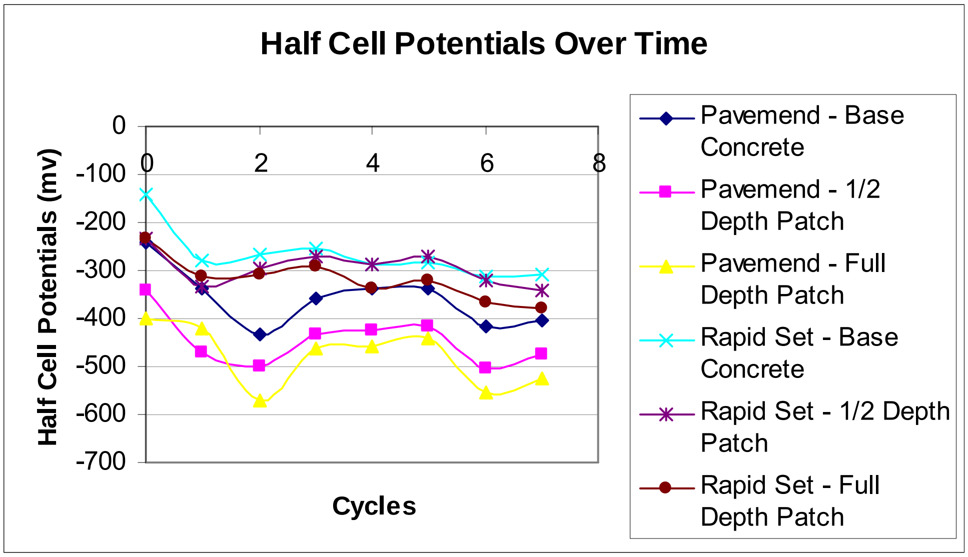

Figure 3-35: Half-Cell Potential Readings Over Time

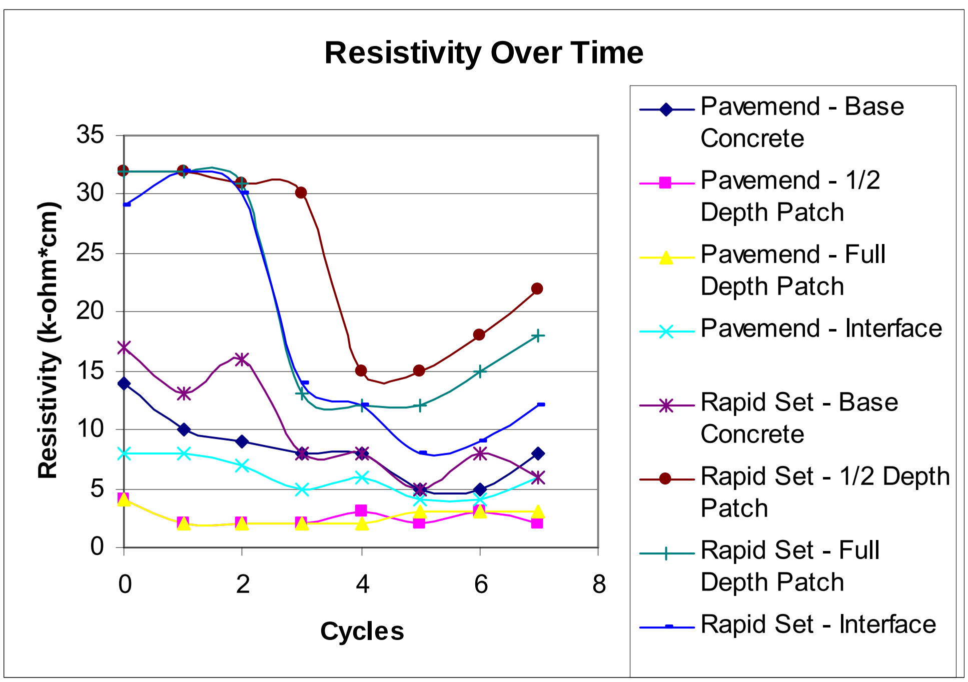

Figure 3-36: Resistivity Measurements Over Time

Figure 3-39 and Figure 3-40 contain the half-cell potential contour maps of Pavemend 15.0 and Rapid Set at the end of the 3-month wet-dry period (Cycle 7 readings). Note the "hot spots" over the patch areas, particularly over the Pavemend patches, where the potentials become much more negative due to corrosion activity.

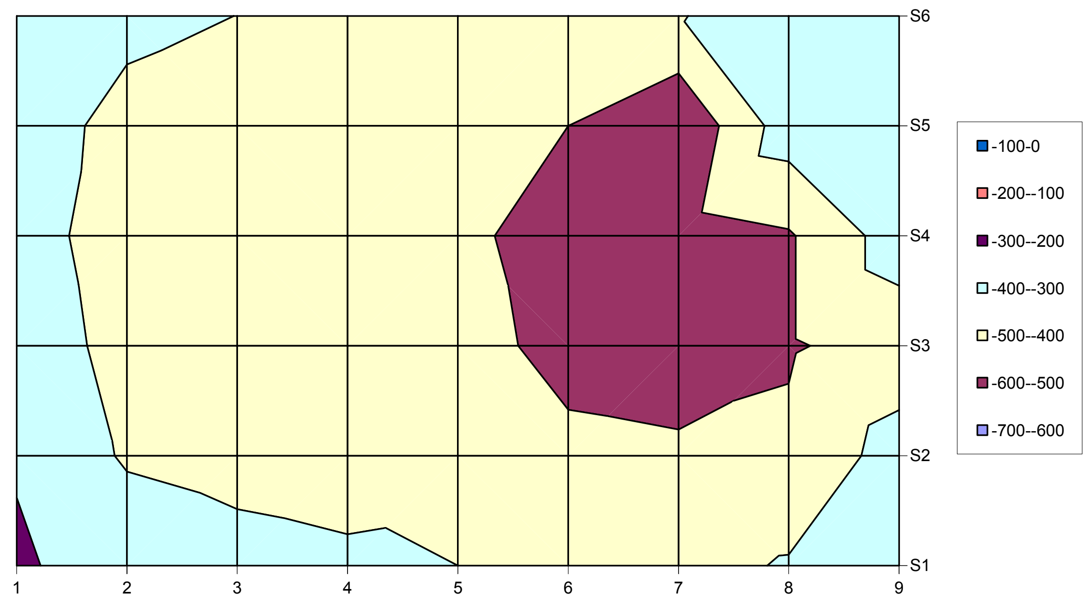

Figure 3-39: Pavemend 15.0 Half Cell Potential Contour Map – Final Readings

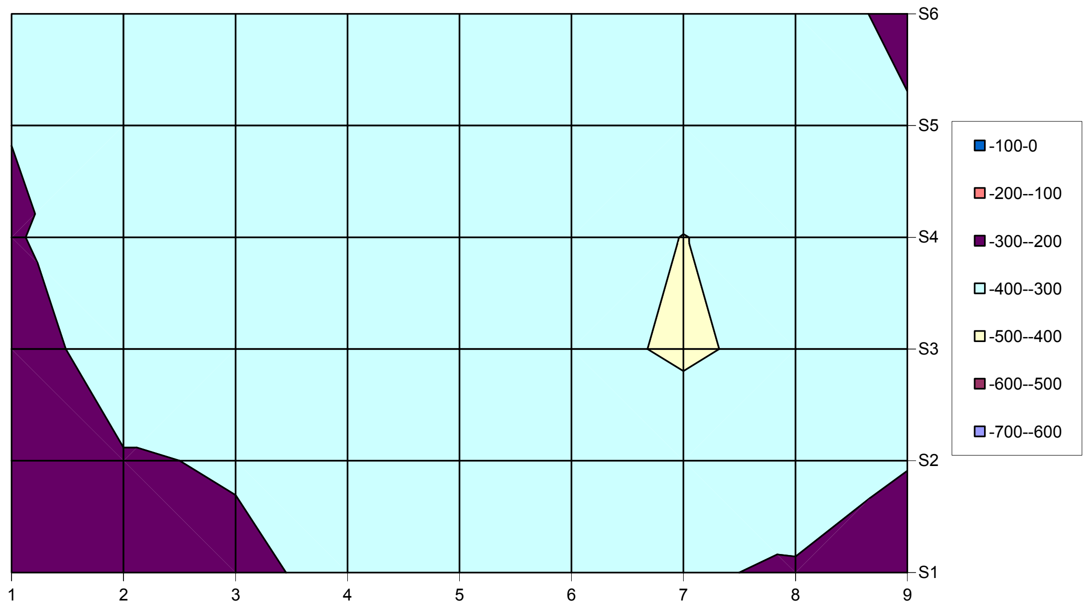

Figure 3-40: Rapid Set Half Cell Potential Contour Map – Final Readings

After the completion of the half-cell potential readings and the resistivity measurements, the ponding slabs were cored. Cores were removed from the half-depth patch, the full-depth patch, and the base concrete. By spraying silver nitrate ($AgNO_3$) on these cores, the depth of penetration could be determined by observing how much of the core became discolored, since $AgNO_3$ reacts with chlorides in the concrete to produce silver chloride (AgCl), which is a white precipitate (Meck 2003).

Figure 3-41 shows the results from this testing. Note that the chlorides completely penetrated through the Pavemend 15.0 samples, and less than 0.5 inch for the Rapid Set and base concrete samples. Figure 3-42 and Figure 3-43 are representative photographs of the Pavemend 15.0 and Rapid Set full-depth cores after exposure to silver nitrate. Note that the Pavemend sample has turned completely white, while the Rapid Set patch has remained largely unchanged except for a small band of white at the top, which was so small that it is not even visible in the picture (also because Rapid Set already has a whitish color due to the latex, so the difference in color between the AgCl precipitate and the material itself was very minor). The control group was composed of cylinders of each material that had not been exposed to salt water, to prove that chlorides are not a part of the material's chemical composition.

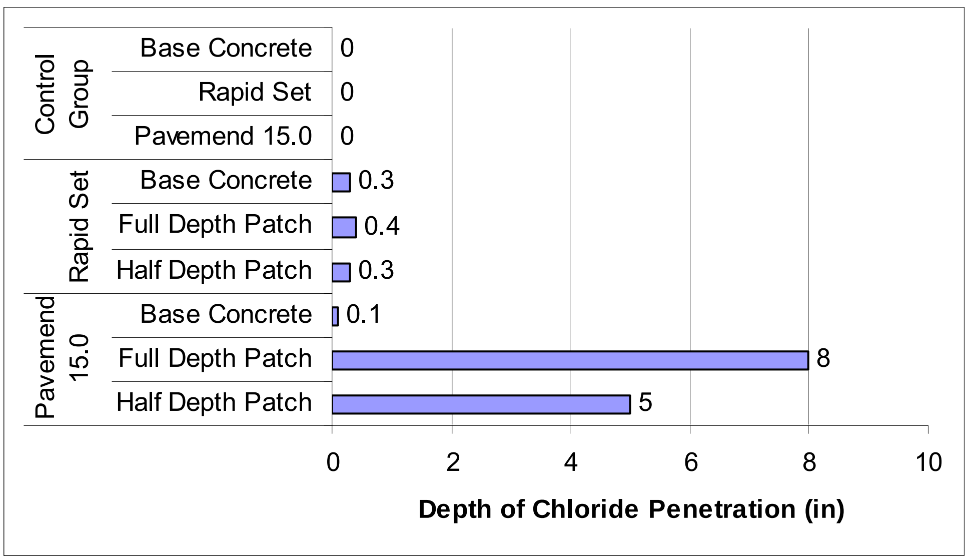

Figure 3-41: Chloride Penetration Test

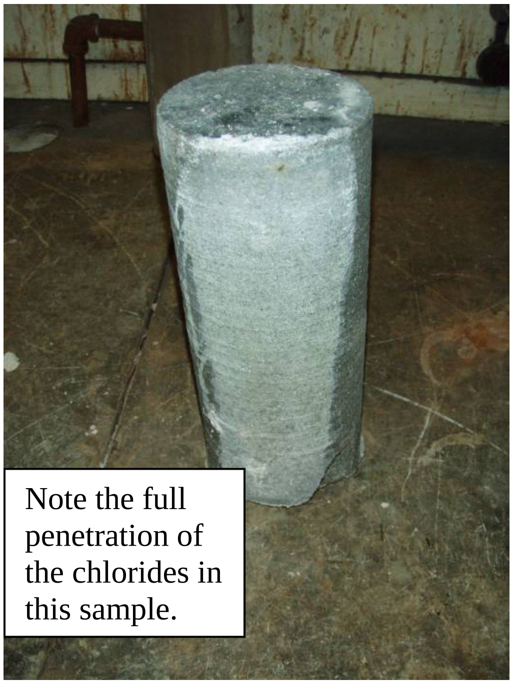

Figure **3-42**: Pavemend 15.0 Core After $AgNO_3$ Exposure

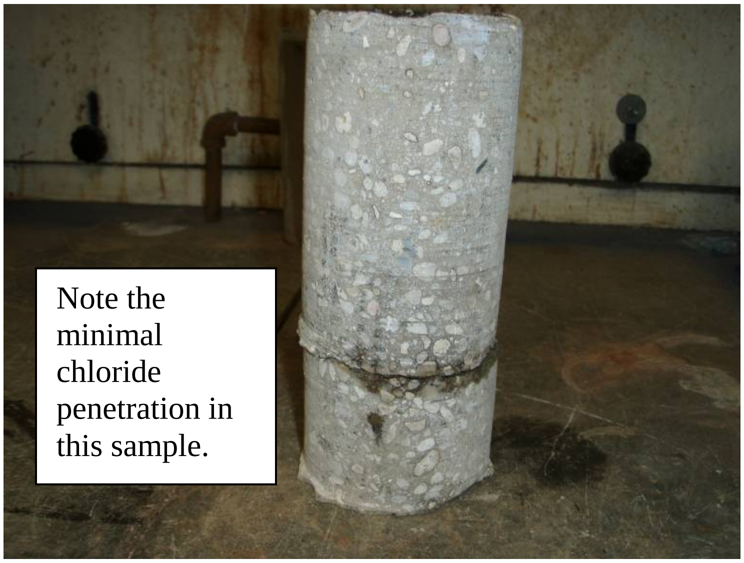

Figure **3-43**: Rapid Set Core After $AgNO_3$ Exposure

After coring the sample, the concrete cover on the center strip of the ponding slab (where the patches were located) was removed to reveal the extent of corrosion damage in the reinforcement. Refer to Figure 3-44. The Pavemend 15.0 slab had noticeably more rust on the reinforcement. This rust was only located in the areas where the patches were located. The Rapid Set slab, on the other hand, had much less corrosion taking place. There was no rust in areas outside of the patch, just like in the Pavemend slab, but inside the patch area there was only minor rusting, most likely from the exposure to the environment that the rebar received when the holes were originally jackhammered out.

Figure 3-44: Slabs After Autopsy (Rapid Set on Top, Pavemend on Bottom)

Refer to Figure 3-45 and Figure 3-46 to view the rust on the reinforcement within the Pavemend 15.0 slab. Note, on the second picture, the gap between the rusted areas. This non-rusted area corresponds to the strip of base concrete between the patch areas.

Figure 3-45: Pavemend 15.0 Corrosion Slab – Close-Up 1

Figure 3-46: Pavemend 15.0 Corrosion Slab – Close-Up 2

Refer to Figure 3-47 and Figure 3-48 to view the state of the reinforcement within the Rapid Set slab. From the first picture, it may be difficult to see that there is any rust on the reinforcement since the corrosion taking place within this slab was relatively minor, but by viewing the more extreme close-up in the second picture, it is noticeable that there is some rust on the rebar.

Figure 3-47: Rapid Set Corrosion Slab – Close-Up 1

Figure 3-48: Rapid Set Corrosion Slab – Close-Up 2

3.3 Specialized Testing Summary

Two patch materials (Pavemend 15.0 and Rapid Set) were chosen to move on for further testing after their favorable results in the ASTM testing. In this additional testing, the materials were evaluated to determine their durability under traffic loading and also in a corrosive environment.

In traffic loading testing, the patching materials were subjected to three experiments: three-point bending test, repetitive tire loading simulation, and sandblasting abrasion test. In the three-point bending test, both materials performed well, as both failed at higher loads (in general, >50 kips) than the calculated design load (37 kips), and neither material separated from the substrate concrete. However, Rapid Set did prove to be the stronger and stiffer material in this testing. In the repetitive tire loading simulation, both materials again performed well, as neither material showed significant deterioration after 200,000 loading cycles. In the sandblasting abrasion testing, Rapid Set proved to be the more abrasion-resistant material, as the cavities produced by sandblasting in the Rapid Set specimen (3 cm^3) were only a quarter of the size of the cavities produced in the Pavemend specimen (13 cm^3).

From the corrosion analysis, it has been determined that Rapid Set is far more corrosion resistant than Pavemend 15.0 due to the fact that its half-cell potential readings were not as negative (roughly -350 mV, as opposed to -500 mV for the final readings), its resistivity was much higher (20 kΩ-cm, as opposed to 3 kΩ-cm for the final readings), its chloride penetration measurements were much smaller (less than 0.5-inch penetration, as opposed to full-depth [8-inch] penetration), and it showed much less rust after autopsy.

Chapter 4

Summary and Conclusions

With deteriorating bridge decks in Pennsylvania, there is a need for a reliable, rapid-setting patch material. There are various products on the market today, and a number of these products are listed in *Bulletin 15*, a PennDOT publication that contains a comprehensive list of all materials that can be used in PennDOT projects. From this list, six materials (Duracal, HP Fast Setting Concrete, Pavemend 15.0, Rapid Set with a latex modifier, Sikatop Plus 122, and T17 Polymer Concrete) were chosen for analysis based on correspondence with PennDOT and neighboring DOTs. A series of ASTM tests were run on these products to determine their material properties and provide an indication as to which material would most likely make the best patch. From this ASTM testing, two materials emerged as superior to the others (Pavemend 15.0 and Rapid Set with a latex modifier). These two materials were then tested further in specialized testing to evaluate their durability under traffic loading and also in a corrosive environment. From this testing, the best patching material for variable conditions was chosen (Rapid Set with a latex modifier). Also, from the assessment of this study's testing plan, a recommended testing protocol was developed for PennDOT to examine patching materials that will be developed and available in the future.

As stated above, the objectives proposed in Section 1.2 have successfully been met by this research. They are as follows:

1. Determine the most suitable quick-setting patching material for patches of varying area and depth.
   - Throughout the testing, Rapid Set with the latex modifier has proven to be of superior quality, and an excellent patching material for patches of all sizes.
     - From ASTM tests, it was determined to:
       - Have the highest 3-hour compressive strength (over 4 ksi),
       - Have very high resistance to adverse freeze-thaw effects (durability factor close to 100 for both regular and salt water tests),
       - Set quickly (final set at 20 minutes),
       - Have low shrinkage (0.29%),
       - Have a coefficient of thermal expansion similar to that of the base concrete (4.5 x 10^{-6} / °F), and
       - Have good workability.
     - From specialized testing, it was determined to:
       - Form a strong bond with the base concrete, and to act as a continuous member with that concrete, even up to a failure load that was beyond the design load (there was no patch separation in the three-point bending test, where the slabs failed at a load above 50 kips [Nominal

Moment Capacity for the slabs occurred at only 37 kips]); and

- Resist abrasion better than the base concrete (from ASTM C 418 – Abrasion Resistance of Concrete by Sandblasting, where the cavity created in Rapid Set was half the size as that of the base concrete).

- It is important to note that while Rapid Set with the latex modifier proved superior over the other materials tested, Pavemend 15.0 also proved to be a quality material as well. While outperformed by Rapid Set in virtually every category, Pavemend 15.0 was not deemed deficient in any of these categories, and therefore would be an adequate product to use in most situations. The fact that it can be used in lower temperatures than Rapid Set (30°F, as opposed to 45°F for Rapid Set), actually makes it preferable for emergency winter repairs. Also, its ease of use (see Table 2-8) makes it an excellent candidate for smaller, half-depth patches. Because of its ease of use, a smaller crew could perform the necessary repairs, thus making it a more economical solution at times. Performing very large repairs with Pavemend 15.0 would not be advisable, though, for two reasons:
    - The three-point loading test with the large, full-depth Pavemend 15.0 patch failed at a load 20% lower than any other testing slab.

- When only one or two drills are available to mix Pavemend 15.0, as is often the case for many PennDOT crews, the time it takes to place the material can be extensive. For example, during three-point loading testing, it took 90 minutes to patch the large, full-depth hole with Pavemend 15.0, while it only took 30 minutes to place the same size patch using Rapid Set. This additional time causes unneeded, extended closure to traffic lanes on the bridge and goes against the purpose of using rapid-setting patching materials in the first place.

2. Determine the corrosion protection provided by the patch to the underlying reinforcement and verify that the patch does not increase corrosion rates in bars contained in the base material.

    - From the corrosion analysis, it was determined that Rapid Set provides more corrosion resistance to the reinforcement than Pavemend 15.0, with the following specific observations:
        - Rapid Set's half cell potential readings were not as negative (indicating that the reinforcement within Pavemend was more likely corroding) as Pavemend's (roughly -350 mV, as opposed to -500 mV for the final readings).
        - Rapid Set's resistivity was much higher than Pavemend's (20 kΩ-cm, as opposed to 3 kΩ-cm for the final readings).

- Rapid Set's chloride penetration measurements were much smaller than Pavemend's (less than 0.5-inch penetration, as opposed to full-depth [8-inch] penetration).
- Reinforcement within the Rapid Set slab showed much less rust after autopsy than the rebar within the Pavemend slab.

3. Develop a recommended testing protocol for evaluation of patching materials.
   - Based on the favorable results produced in this research, a standard testing protocol was developed from this plan.
     - It is first essential to determine the basic material properties (Table 4-1):

Table 4-1: ASTM Testing

Test	Keep or Omit	Comments
ASTM C 39	Keep	Compressive test at 1 hour, 3 hours, 1 day, and 7 days to determine strengths at various times.
ASTM C 666 in regular water	Keep	Determines resistance to adverse freeze-thaw effects.
ASTM C 666 in salt water	Omit	Not recommended to be run in addition to the regular water test. Results from these two tests proved to be extremely similar, and therefore it would be redundant to perform both.
ASTM C 531 Modified	Keep	Determines the shrinkage of the material and the coefficient of thermal expansion of the material.
ASTM C 191	Keep	Determines the setting time of the material.
ASTM C 882/928	Omit	Not recommended to be run due to the fact that this slant shear test (to determine bond strength of the material) proved to be highly variable and produced an unreliable set of data.

- After these basic tests are performed in order to determine if the material has suitable properties to be a patching material, more advanced testing can be run to prove the quality of that material (Table 4-2):

Table 4-2: Specialized Testing

Test	Keep or Omit	Comments
Three-Point Bending Test	Keep	Demonstrates the ability of the slab and patch to act as one continuous member, and gives an indication of the weakest location in the two-part system.
ASTM C 418	Keep	When run at 3-hour strength, determines the abrasion resistance of the material at the time when the bridge is reopened to traffic.
Repetitive Tire Load Simulation	Omit	Not included due to the fact that it requires special equipment that is not available for most researchers and did not provide significant information.
Corrosion Testing	Keep	Determines the ability of the patch to protect the reinforcement from corrosion.

For an overview of the recommended testing protocol, along with performance limits, please refer to Table 4-3 .

Table 4-3: Recommended Testing Protocol

Test	Performance Limit	Comments
ASTM C 39	3-hr strength > 1500 psi 7-day strength > 3500 psi	Tests run at 1 hr, 3 hr, 1 day, and 7 days
ASTM C 666 in regular water	Durability Factor > 60	
ASTM C 531 Modified	Shrinkage % < 0.5% 2×10^{-6}/°F < Coefficient of Thermal Expansion < 6×10^{-6}/°F	
ASTM C 191	Final Set Time < 90 min	
If results are favorable, move on to more advanced testing.		
Three-Point Bending Test	Minimal patch separation from substrate. Must fail at load greater than design load (37 kips).	Keep in accordance with test procedure in Section 3.2.2.1
ASTM C 418	Cavity size < 20cm^3	Keep in accordance with test procedure in Section 3.2.4.1
Corrosion Testing	No extreme corrosion present at time of specimen autopsy.	Keep in accordance with test procedure in Section 3.2.5.1, except only one patch (full depth) needs to be tested. Therefore, slab area may be reduced to half of indicated size.

References

American Concrete Institute (ACI). (1987). *Corrosion, Concrete, and Chlorides: Corrosion in Concrete: Causes and Restraints* (SP 102), American Concrete Institute, Michigan.

Bertolini, Luca, Bernhard Elsener, Pietro Pedeferri, Rob Polder. (2004). *Corrosion of Steel in Concrete: Prevention, Diagnosis, Repair,* Wiley-VCH Verlag GmbH & Co., Germany.

Blaga, A. and Beaudoin, J. J. (1985). "CBD-241 Polymer Modified Concrete." Canadian Building Digest.

Blaga, A. and Beaudoin, J. J. (1985). "CBD-242 Polymer Concrete." Canadian Building Digest.

Broomfield, John P. (2007). *Corrosion of Steel in Concrete: Understanding, Investigation, and Repair, 2nd Edition*, Taylor and Francis Group, New York.

Chehab, Ghasson (2008). Personal Communication. February 4, 2008, State College, Penn.

Cordon, William A. (1966). *Freezing and Thawing of Concrete*. American Concrete Institute, Detroit, Mich.

Farha, M.H., Hassan, Y., Halim, A. O. Abd El, Razaqpur, A. G., El-Desouky, A. and Mostafa, A. (2002). "Effects of New Deicing Alternatives on Airfield Asphalt Concrete Pavements." Final report to the 2002 Federal Aviation Administration Technology Transfer Conference.

Kirchner, Henry W. (2001) [Online] Available. "Using Deicers Correctly." http://www.saltinstitute.org/kirchner-1.html, January 17, 2006.

Lafrenz, Jim. [Online] Available. American Concrete Pavement Association Presentation. http://www.cement.ca/cement.nsf/eee9ec7bbd630126852566c40052107b/8e38d820a4c581c085256b800069ecef/$FILE/ATTPO7YB/Economical%20CPR%20for%20Airfield%20Pavement.pdf, April 5, 2007.

Meck, E. and Sirivivatnanon, V. (2003) [Online] Available. "Field Indicator of Chloride Penetration Depth."

http://www.sciencedirect.com/science?_ob=ArticleURL&_udi=B6TWG-47TWRK6-3&_user=209810&_rdoc=1&_fmt=&_orig=search&_sort=d&view=c&_acct=C000014439&_version=1&_urlVersion=0&_userid=209810&md5=b006a926d436a1b43f650c30970dbea2, February 28, 2008.

Mindess, Sidney, Young, J. Francis, and Darwin, David. (2003). *Concrete*. Prentice Hall, Upper Saddle River, N. J.

National Transportation Product Evaluation Program. (2005). [Online] Available. "Rapid Setting Patching Materials for Portland Cement Concrete: Work Plan." http://www.ntpep.org/ContentManagement/PageBody.asp?PAGE_ID=29, January 25, 2007.

Page, C.L., K.W.J. Treadaway, P.B. Bamforth. (1990). *Corrosion of Reinforcement in Concrete*, Elsevier Applied Science, New York.

Pennsylvania Department of Transportation. (2006). *Bulletin 15: Approved Construction Materials.*

Poulsen, Ervin and Leif Mejlbro. (2006). *Diffusion of Chloride in Concrete: Theory and Application,* Taylor and Francis, New York.

Richardson, Mark G. (2002). *Fundamentals of Durable Reinforced Concrete,* Spon Press, New York.

Russell, Henry G. (2004). NCHRP Synthesis 333, *Concrete Bridge Deck Performance: A Synthesis of Highway Practice*. Transportation Research Board, Washington, D.C.

Significance of Tests and Properties of Concrete & Concrete-Making Materials. (2006). Joseph F. Lamond and James H. Pielert, ed., ASTM International, Bridgeport, N.J.

2006 Annual Book of ASTM Standards. (2006). ASTM International, Baltimore, Mary.

Walker, Craig. (2000). [Online] Available. "Sulphate Attack on Concrete." http://www.civil.uwaterloo.ca/soudki/Classpresent/c-walker/index.htm, February 6, 2008.

Whitmore, David W. and J. Christopher Bell. (2005). [Online] Available. "Galvanic Corrosion Protection Systems for Concrete Bridges." http://www.gobridges.com/article.asp?id=258, February 6, 2008.

Appendix A

Testing Program A – Standard ASTM Testing

The following tables present all data from the ASTM testing described in Chapter 2. Summaries of these results are also listed in Chapter 2, where averages of these results were calculated. Extreme outliers were omitted from those calculations. These outliers are denoted in boldface type in the tables.

A.1 Compression Testing - ASTM C 39

Table **A-1** through Table **A-4** contain the ASTM C 39 results from the ASTM testing.

Table **A-1**: ASTM C 39 – 1 Hour Results

Material	Load (lbs)	Strength (psi)	Comments
Duracal	10150	810	Putty-like on top - 1 hr
Duracal	16290	1300	Putty-like on top - 1 hr 5 min
Duracal	20670	1640	Putty-like on top - 1 hr 10 min
HP	14630	1160	
HP	14390	1150	
HP	15110	1200	
Pavemend	3380	270	
Pavemend	2710	220	
Pavemend	3110	250	
Rapid Set	32550	2590	
Rapid Set	32520	2590	
Rapid Set	33520	2670	
Sika	300	20	Still Mud-like - 1 hr
Sika	1010	**80**	Set, but not much strength yet - 1 hr 30 min
Sika	2180	**170**	Set, but not much strength yet - 2 hrs
Sika	3930	**310**	Set, but not much strength yet - 2 hrs 30 min
T17	6580	520	
T17	9000	720	
T17	7080	560	

Table **A-2**: ASTM C 39 – 3 Hour Results

Material	Load (lbs)	Strength (psi)	Comments
Duracal	24850	1980	
Duracal	23880	1900	
Duracal	25260	2010	
HP	18570	1480	
HP	18600	1480	
HP	18900	1500	
Pavemend	20860	1660	
Pavemend	29770	2370	
Pavemend	23160	1840	
Rapid Set	52960	4210	
Rapid Set	48290	3840	
Rapid Set	53810	4280	
Sika	4550	360	
Sika	5580	440	
Sika	5420	430	
Sika	6840	**540**	4 hrs after casting
T17	29050	2310	
T17	21630	1720	
T17	21500	1710	

Table **A-3**: ASTM C 39 – 1 Day Results

Material	Load (lbs)	Strength (psi)	Comments
Duracal	48100	3830	
Duracal	49770	3960	
Duracal	50050	3980	
HP	34930	2780	
HP	21030	**1670**	Honeycombing
HP	38830	3090	
HP	33870	2700	
Pavemend	42680	3400	
Pavemend	46440	3700	
Pavemend	40920	3260	
Rapid Set	69520	5530	
Rapid Set	54150	**4310**	Honeycombing
Rapid Set	69820	5560	
Sika	37740	3000	
Sika	28520	**2270**	Honeycombing
Sika	36240	2880	
Sika	37320	2970	
T17	52540	4180	
T17	54620	4350	
T17	52810	4200	

Table A-4: ASTM C 39 – 7 Day Results

Material	Load (lbs)	Strength (psi)	Comments
Duracal	81080	6450	
Duracal	81080	6450	
Duracal	85660	6820	
Duracal	76090	6060	
HP	62590	4980	
HP	59960	4770	
HP	62250	4950	
Pavemend	48990	3900	
Pavemend	46130	3670	
Pavemend	46760	3720	
Rapid Set	82980	6600	
Rapid Set	82490	6560	
Rapid Set	82380	6560	
Sika	56870	4530	
Sika	58640	4670	
Sika	57700	4590	
T17	56450	4490	
T17	55570	4420	
T17	55110	4390	
T17	55600	4420	

A.2 Freeze-Thaw Testing – ASTM C 666

A.2.1 Freeze-Thaw Testing in Regular Water

Figure **A-1** shows the freeze-thaw specimens. Table **A-5** through Table **A-10** contain the ASTM C 666 (in regular water) results from the ASTM testing. Note that the "Fundamental Transverse Frequency" is the frequency of a wave that is propagated through the material. (The wave is caused by tapping the material with a hammer.) The "Relative Dynamic Modulus of Elasticity" is then determined by the following equation:

$RDME = FTF^2/FTF_0^2 * 100\%$, where RDME is the relative dynamic modulus of elasticity, FTF is the fundamental transverse frequency, and FTF_0 is the original fundamental transverse frequency. The durability factor is then calculated by the following equation: $DF = RDME_f * cyc/300$, where $RDME_f$ is the final relative dynamic modulus of elasticity and cyc is the number of cycles run on the specimen (ASTM 2006).

Figure **A-1**: Regular Water Freeze-Thaw Specimens

Table A-5: ASTM C 666 (Regular Water) - Duracal

Duracal 1				
# of Cycles	Fund. Tran. Freq. (kHz)	Rel. Dyn. Mod. Of Elasticity	Weight (g) (1g = 0.0022lbs)	Comments
0	1.610	100.0	5446.1	Ragged on Top Edge
33	1.468	83.1	5462.2	
66	1.381	73.6	5469.9	Chipping on top near edge
100	1.365	71.9	5462.1	Thin layer of top surface wore off
133	1.331	68.3	5457.3	Top Edges - More Ragged
166	1.301	65.3	5421.1	Deteriorating on Bottom
200	1.260	61.3	5394.5	More Deterioration - Esp. on Bottom
233	1.206	56.1	5380.0	Outside surface wearing off
208	1.247	60.0		INTERPOLATING
Durability Factor		42		

Duracal 2				
# of Cycles	Fund. Tran. Freq. (kHz)	Rel. Dyn. Mod. Of Elasticity	Weight (g) (1g = 0.0022lbs)	Comments
0	1.584	100.0	5413.4	Ragged on Top Edge
33	1.454	84.3	5423.4	
66	1.397	77.8	5430.7	Chipping on top near edge
100	1.346	72.2	5423.6	Thin layer of top surface wore off
133	1.303	67.7	5420.0	
166	1.266	63.9	5390.2	Deteriorating on Bottom
200	1.235	60.8	5351.6	More Deterioration - Esp. on Bottom
233	1.182	55.7	5323.1	Outside surface wearing off
205	1.227	60.0		INTERPOLATING
Durability Factor		41		

Duracal 3				
# of Cycles	Fund. Tran. Freq. (kHz)	Rel. Dyn. Mod. Of Elasticity	Weight (g) (1g = 0.0022lbs)	Comments
0	1.571	100.0	5287.5	
33	1.460	86.4	5295.4	
66	1.365	75.5	5296.0	Chipping on top near edge
100	1.345	73.3	5289.7	Thin layer of top surface wore off
133	1.297	68.2	5283.9	
166	1.255	63.8	5238.3	Deteriorating on Bottom
200	1.230	61.3	5186.4	More Deterioration - Esp. on Bottom
233	1.176	56.0	5152.7	Outside surface wearing off
208	1.217	60.0		INTERPOLATING
Durability Factor		42		

Table A-6: ASTM C 666 (Regular Water) - HP

HP 1				
# of Cycles	Fund. Tran. Freq. (kHz)	Rel. Dyn. Mod. Of Elasticity	Weight (g) (1g = 0.0022lbs)	Comments
0	1.550	100.0	5555.1	
33	1.550	100.0	5536.1	Chipping
66	1.517	95.8	5428.0	Top layer flaked off
100	1.490	92.4	5386.7	Further deterioration on top
133	1.302	70.6	5348.8	More deterioration
166	1.260	66.1	5320.1	
200	1.334	74.1	5286.5	
233	1.155	55.5	5237.2	Severe Deterioration on top and bot.
225	1.201	60.0		INTERPOLATING
Durability Factor		45		

HP 2				
# of Cycles	Fund. Tran. Freq. (kHz)	Rel. Dyn. Mod. Of Elasticity	Weight (g) (1g = 0.0022lbs)	Comments
0	1.596	100.0	5703.0	
33	1.559	95.4	5634.3	Chipping
66	1.565	96.2	5528.4	Top layer flaked off
100	1.541	93.2	5468.5	Further deterioration on top
133	1.397	76.6	5453.3	More deterioration
166	1.350	71.6	5430.2	
200	1.300	66.4	5382.8	
233	1.176	54.3	5338.0	Severe Deterioration on top and bot.
217	1.236	60.0		INTERPOLATING
Durability Factor		43		

Table **A-7**: ASTM C 666 (Regular Water) - Pavemend

Pavemend 1				
# of Cycles	Fund. Tran. Freq. (kHz)	Rel. Dyn. Mod. Of Elasticity	Weight (g) (1g = 0.0022lbs)	Comments
0	1.273	100.0	4933.0	
33	1.195	88.1	4934.0	
66	1.145	80.9	4936.6	
100	1.169	84.3	4925.3	
133	1.156	82.5	4923.6	Slight Flaking
166	1.160	83.0	4915.1	
200	1.151	81.8	4913.5	
233	1.123	77.8	4916.7	
266	1.097	74.3	4920.3	Edges Rounding
300	1.092	73.6	4920.8	Thin Outer Film Deteriorated; Otherwise OK
Durability Factor		74		
Pavemend 2				
# of Cycles	Fund. Tran. Freq. (kHz)	Rel. Dyn. Mod. Of Elasticity	Weight (g) (1g = 0.0022lbs)	Comments
0	1.245	100.0	4949.5	
33	1.166	87.7	4953.0	
66	1.101	78.2	4958.4	
100	1.142	84.1	4952.6	
133	1.118	80.6	4952.3	Slight Flaking
166	1.126	81.8	4945.1	
200	1.121	81.1	4945.2	
233	1.092	76.9	4948.9	
266	1.069	73.7	4955.4	Edges Rounding
300	1.069	73.7	4957.7	Thin Outer Film Deteriorated; Otherwise OK
Durability Factor		74		
Pavemend 3				
# of Cycles	Fund. Tran. Freq. (kHz)	Rel. Dyn. Mod. Of Elasticity	Weight (g) (1g = 0.0022lbs)	Comments
0	1.270	100.0	4994.7	
33	1.185	87.1	4997.5	
66	1.138	80.3	5005.4	
100	1.159	83.3	4997.5	
133	1.138	80.3	4998.6	Slight Flaking
166	1.147	81.6	4990.9	
200	1.136	80.0	4993.3	
233	1.118	77.5	4993.9	
266	1.102	75.3	5001.1	Edges Rounding
300	1.096	74.5	5005.1	Thin Outer Film Deteriorated; Otherwise OK
Durability Factor		75		

Table A-8: ASTM C 666 (Regular Water) - Rapid Set

Rapid Set 1				
# of Cycles	Fund. Tran. Freq. (kHz)	Rel. Dyn. Mod. Of Elasticity	Weight (g) (1g = 0.0022lbs)	Comments
0	1.521	100.0	5208.8	Ragged on top, minor honeycombing
33	1.500	97.3	5202.1	
66	1.507	98.2	5186.8	
100	1.515	99.2	5170.6	Aggregate at surface chipping
133	1.520	99.9	5156.9	Depressions in Specimen
166	1.509	98.4	5136.0	Small Cracks Developing
200	1.512	98.8	5123.0	Deeper Depressions
233	1.527	100.8	5098.4	Chipping Throughout
266	1.503	97.6	5081.9	Further Deterioration
300	1.520	99.9	5065.6	Chips and Depressions Throughout
Durability Factor		100		
Rapid Set 2				
# of Cycles	Fund. Tran. Freq. (kHz)	Rel. Dyn. Mod. Of Elasticity	Weight (g) (1g = 0.0022lbs)	Comments
0	1.491	100.0	5141.2	Ragged on top, minor honeycombing
33	1.478	98.3	5131.0	
66	1.468	96.9	5112.8	
100	1.479	98.4	5099.8	Aggregate at surface chipping
133	1.474	97.7	5092.1	Depressions in Specimen
166	1.463	96.3	5055.8	Deeper Depressions
200	1.458	95.6	5038.6	Deeper Depressions
233	1.452	94.8	5021.7	Chipping Throughout
266	1.430	92.0	5002.0	Further Deterioration
300	1.457	95.5	4979.2	Chips and Depressions Throughout
Durability Factor		96		
Rapid Set 3				
# of Cycles	Fund. Tran. Freq. (kHz)	Rel. Dyn. Mod. Of Elasticity	Weight (g) (1g = 0.0022lbs)	Comments
0	1.499	100.0	5154.7	Ragged on top, minor honeycombing
33	1.477	97.1	5144.3	
66	1.490	98.8	5130.5	
100	1.484	98.0	5119.9	Aggregate at surface chipping
133	1.491	98.9	5101.0	Depressions in Specimen
166	1.478	97.2	5076.4	Deeper Depressions
200	1.487	98.4	5058.7	Deeper Depressions
233	1.487	98.4	5040.2	Chipping Throughout
266	1.430	91.0	5002.0	Further Deterioration
300	1.482	97.7	5009.7	Chips and Depressions Throughout
Durability Factor		98		

Table A-9: ASTM C 666 (Regular Water) - Sika

Sika 1				
# of Cycles	Fund. Tran. Freq. (kHz)	Rel. Dyn. Mod. Of Elasticity	Weight (g) (1g = 0.0022lbs)	Comments
0	1.869	100.0	5783.5	
33	1.848	97.8	5787.6	
66	1.847	97.7	5788.9	
100	1.866	99.7	5786.0	
133	1.865	99.6	5786.7	
166	1.846	97.6	5787.6	
200	1.854	98.4	5788.3	
233	1.859	98.9	5788.9	
266	1.857	98.7	5790.2	
300	1.868	99.9	5788.2	Perfect condition
Durability Factor		100		

Sika 2				
# of Cycles	Fund. Tran. Freq. (kHz)	Rel. Dyn. Mod. Of Elasticity	Weight (g) (1g = 0.0022lbs)	Comments
0	1.857	100.0	5722.9	
33	1.829	97.0	5726.5	
66	1.832	97.3	5726.7	
100	1.838	98.0	5727.8	
133	1.848	99.0	5727.9	
166	1.835	97.6	5728.0	
200	1.833	97.4	5730.3	
233	1.841	98.3	5728.6	
266	1.836	97.8	5730.7	
300	1.851	99.4	5728.7	Perfect condition
Durability Factor		99		

Sika 3				
# of Cycles	Fund. Tran. Freq. (kHz)	Rel. Dyn. Mod. Of Elasticity	Weight (g) (1g = 0.0022lbs)	Comments
0	1.952	100.0	5824.7	
33	1.930	97.8	5824.4	
66	1.930	97.8	5825.4	
100	1.936	98.4	5827.6	
133	1.947	99.5	5827.0	
166	1.930	97.8	5827.8	
200	1.930	97.8	5829.2	
233	1.935	98.3	5828.9	
266	1.929	97.7	5829.9	
300	1.938	98.6	5829.8	Perfect condition
Durability Factor		99		

Table **A-10**: ASTM C 666 (Regular Water) – T17

T17 1				
# of Cycles	Fund. Tran. Freq. (kHz)	Rel. Dyn. Mod. Of Elasticity	Weight (g) (1g = 0.0022lbs)	Comments
0	N/A	N/A	5573.3	shaved on sides
33	N/A	N/A	5568.8	
66	N/A	N/A	5571.6	
100	N/A	N/A	5569.5	
133	N/A	N/A	5563.3	
166	N/A	N/A	5560.9	
200	N/A	N/A	5563.7	
233	N/A	N/A	5566.5	
266	N/A	N/A	5567.2	Deter. On Sides - Agg. Showing
300	N/A	N/A	5567.1	Slight Deter. of Outer Layer
Durability Factor		N/A		
T17 2				
# of Cycles	Fund. Tran. Freq. (kHz)	Rel. Dyn. Mod. Of Elasticity	Weight (g) (1g = 0.0022lbs)	Comments
0	N/A	N/A	5527.3	shaved on sides
33	N/A	N/A	5528.5	
66	N/A	N/A	5527.1	
100	N/A	N/A	5528.4	
133	N/A	N/A	5530.3	
166	N/A	N/A	5530.6	
200	N/A	N/A	5533.1	
233	N/A	N/A	5534.8	
266	N/A	N/A	5533.8	Deter. On Sides - Agg. Showing
300	N/A	N/A	5540.2	Slight Deter. of Outer Layer
Durability Factor		N/A		
T17 3				
# of Cycles	Fund. Tran. Freq. (kHz)	Rel. Dyn. Mod. Of Elasticity	Weight (g) (1g = 0.0022lbs)	Comments
0	N/A	N/A	5453.9	shaved on sides
33	N/A	N/A	5448.5	
66	N/A	N/A	5452.7	
100	N/A	N/A	5454.7	
133	N/A	N/A	5448.1	
166	N/A	N/A	5453.0	
200	N/A	N/A	5455.3	
233	N/A	N/A	5458.2	
266	N/A	N/A	5458.1	Deter. On Sides - Agg. Showing
300	N/A	N/A	5460.6	Slight Deter. of Outer Layer
Durability Factor		N/A		

A.2.2 Freeze-Thaw Testing in Salt Water

Figure **A-2** shows the specimens used in salt water freeze-thaw testing. Table **A-11** through Table **A-14** contain the ASTM C 666 (in salt water) results from the ASTM testing.

Figure **A-2**: Salt Water Freeze-Thaw Specimens

Table A-11: ASTM C 666 (Salt Water) - Duracal

Duracal 1				
# of Cycles	Fund. Tran. Freq. (kHz)	Rel. Dyn. Mod. Of Elasticity	Weight (g) (1g = 0.0022lbs)	Comments
0	1.608	100.0	5349.5	
33	1.502	87.3	5359.2	Outer Layer of paste deteriorated
66	1.448	81.1	5363.0	
100	1.387	74.4	5365.3	Aggregate Showing through
133	1.310	66.4	5360.8	Outer Layer - More deterioration
166	1.247	60.1	5368.7	Outer Layer - More deterioration
167	1.246	60.0		EXTRAPOLATING (Since value is very close to 60)
Durability Factor		33		

Duracal 2				
# of Cycles	Fund. Tran. Freq. (kHz)	Rel. Dyn. Mod. Of Elasticity	Weight (g) (1g = 0.0022lbs)	Comments
0	1.607	100.0	5420.7	
33	1.528	90.4	5434.2	Outer Layer of paste deteriorated
66	1.475	84.3	5442.8	
100	1.387	74.5	5445.2	Aggregate Showing through
133	1.305	66.0	5446.0	Outer Layer - More deterioration
166	1.248	60.3	5456.8	Outer Layer - More deterioration
168	1.245	60.0		EXTRAPOLATING (Since value is very close to 60)
Durability Factor		34		

Duracal 3				
# of Cycles	Fund. Tran. Freq. (kHz)	Rel. Dyn. Mod. Of Elasticity	Weight (g) (1g = 0.0022lbs)	
0	1.613	100.0	5337.1	
33	1.530	80.0	5335.9	Outer Layer of paste deteriorated
66	1.461	82.0	5338.6	
100	1.407	76.1	5336.5	Aggregate Showing through
133	1.290	64.0	5336.7	Outer Layer - More deterioration
166	1.244	59.5	5347.3	Outer Layer - More deterioration
162	1.249	60.0		INTERPOLATING
Durability Factor		32		

Table **A-12**: ASTM C 666 (Salt Water) - HP

HP 1				
# of Cycles	Fund. Tran. Freq. (kHz)	Rel. Dyn. Mod. Of Elasticity	Weight (g) (1g = 0.0022lbs)	Comments
0	1.736	100.0	5688.3	
33	1.680	93.7	5283.4	Deteriorated down to aggregate
66	1.670	92.5	5130.7	Further Deterioration
100	1.636	88.8	5001.5	
133	1.320	57.8	4713.1	Unrecognizable
131	1.345	60.0		INTERPOLATING
Durability Factor		26		

HP 2				
# of Cycles	Fund. Tran. Freq. (kHz)	Rel. Dyn. Mod. Of Elasticity	Weight (g) (1g = 0.0022lbs)	Comments
0	1.707	100.0	5609.8	
33	1.673	96.0	5235.7	Deteriorated down to aggregate
66	1.641	92.4	5045.7	Further Deterioration
100	1.627	90.9	4867.1	
133	1.313	59.2	4443.4	Unrecognizable
132	1.322	60.0		INTERPOLATING
Durability Factor		26		

HP 3				
# of Cycles	Fund. Tran. Freq. (kHz)	Rel. Dyn. Mod. Of Elasticity	Weight (g) (1g = 0.0022lbs)	Comments
0	1.739	100.0	5692.6	
33	1.709	96.6	5443.1	Deteriorated down to aggregate
66	1.673	92.6	5241.1	Further Deterioration
100	1.667	91.9	5104.2	
133	1.345	59.8	4713.1	Unrecognizable
133	1.347	60.0		INTERPOLATING
Durability Factor		27		

Table A-13: ASTM C 666 (Salt Water) - Pavemend

Pavemend 1				
# of Cycles	Fund. Tran. Freq. (kHz)	Rel. Dyn. Mod. Of Elasticity	Weight (g) (1g = 0.0022lbs)	Comments
0	1.161	100.0	4816.3	
33	1.177	102.8	4844.0	
66	1.207	108.1	4847.9	
100	1.220	110.4	4844.4	
133	1.230	112.2	4846.0	
166	1.230	112.2	4856.3	
200	1.258	117.4	4844.3	
233	1.246	115.2	4854.1	
266	1.252	116.3	4852.6	
300	1.264	118.5	4855.0	Perfect Condition
Durability Factor		119		
Pavemend 2				
# of Cycles	Fund. Tran. Freq. (kHz)	Rel. Dyn. Mod. Of Elasticity	Weight (g) (1g = 0.0022lbs))	Comments
0	1.171	100.0	4824.8	
33	1.170	99.8	4850.6	
66	1.195	104.1	4853.4	
100	1.215	107.7	4853.6	
133	1.221	108.7	4853.8	
166	1.237	111.6	4856.0	
200	1.260	115.8	4853.1	
233	1.252	114.3	4870.1	
266	1.259	115.6	4859.5	
300	1.273	118.2	4864.7	Perfect Condition
Durability Factor		118		
Pavemend 3				
# of Cycles	Fund. Tran. Freq. (kHz)	Rel. Dyn. Mod. Of Elasticity	Weight (g) (1g = 0.0022lbs)	Comments
0	1.166	100.0	4731.1	
33	1.170	100.7	4754.8	
66	1.196	105.2	4757.9	
100	1.216	108.8	4759.6	
133	1.220	109.5	4757.7	
166	1.235	112.2	4766.4	
200	1.260	116.8	4757.7	
233	1.245	114.0	4769.0	
266	1.262	15.9	4762.9	
300	1.260	116.8	4765.5	Perfect Condition
Durability Factor		117		

Table **A-14**: ASTM C 666 (Salt Water) - Rapid Set

Rapid Set 1				
# of Cycles	Fund. Tran. Freq. (kHz)	Rel. Dyn. Mod. Of Elasticity	Weight (g) (1g = 0.0022lbs)	Comments
0	1.670	100.0	5496.4	Top Edges Ragged
33	1.673	100.4	5502.3	
66	1.677	100.8	5504.6	
100	1.673	100.4	5501.3	
133	1.657	98.5	5487.9	Small Amount of Chipping
166	1.670	100.0	5480.8	Bottom corners cracked
200	1.638	96.2	5472.3	
233	1.642	96.7	5470.1	
266	1.670	100.0	5433.2	
300	1.663	99.2	5397.3	Depressions and Scaling, but not severe
Durability Factor		99		
Rapid Set 2				
# of Cycles	Fund. Tran. Freq. (kHz)	Rel. Dyn. Mod. Of Elasticity	Weight (g) (1g = 0.0022lbs)	Comments
0	1.651	100.0	5551.6	Top Edges Ragged
33	1.651	100.0	5559.7	
66	1.652	100.1	5559.3	
100	1.638	98.4	5541.7	
133	1.619	96.2	5508.4	Small Amount of Chipping
166	1.630	97.5	5458.5	Bottom Edge Deteriorated
200	1.590	92.8	5367.5	More Deterioration on Bottom
233	1.630	97.5	5301.0	More Deterioration on Bottom
266	1.672	102.6	5174.0	Bot. Corners severely deterior.
300	1.650	99.9	5095.9	Depressions and Scaling, but only severe on bottom
Durability Factor		100		
Rapid Set 3				
# of Cycles	Fund. Tran. Freq. (kHz)	Rel. Dyn. Mod. Of Elasticity	Weight (g) (1g = 0.0022lbs)	Comments
0	1.655	100.0	5441.1	Top Edges Ragged
33	1.665	101.2	5448.9	
66	1.670	101.8	5447.3	
100	1.662	100.9	5439.1	
133	1.639	98.1	5425.0	Small Amount of Chipping
166	1.655	100.0	5419.1	Some Chipping
200	1.632	97.2	5379.0	More Outer Layer Deterioration
233	1.645	98.8	5343.8	
266	1.672	102.1	5317.3	
300	1.644	98.7	5283.2	Depressions and Scaling, but not severe
Durability Factor		99		

A.3 Setting Time – ASTM C 191 (Vicat Test)

Table **A-15** contains the ASTM C 191 results from the ASTM testing.

Table **A-15**: ASTM C 191

Material	Initial Time of Setting	Final Time of Setting
Duracal	37	52
	47	59
	43	54
HP	6	8
	5	7
	5	9
Pavemend	8	12
	9	13
	7	15
Rapid Set	12	21
	10	21
	11	19
Sika	54	68
	57	69
	61	72
T17	25	26
	25	27
	26	28

A.4 Slant Shear Test – ASTM C 882/928

Table **A-16** and Table **A-17** contain the ASTM C 882/928 results from the ASTM testing.

Table **A-16**: ASTM C 882/928 – 1-Day

Material	Load (lbs)	Bond Strength (psi)	Comments
Duracal	12800	910	
	14650	1040	
	16790	1190	
HP	0	0	Debonded before comp. test
	0	0	Debonded before comp. test
	5670	400	
Pavemend	11000	780	Mortar wrapped around dummy specimen
	7020	500	Mortar wrapped around dummy specimen
	9900	700	Mortar wrapped around dummy specimen
Rapid Set	0	0	Debonded before comp. test
	3150	220	
	1620	110	
Sika	2200	160	
	1570	110	
	7690	**540**	Silicon helped bond specimen together
T17	2230	160	
	2460	170	
	5230	**370**	Silicon helped bond specimen together

Table A-17: ASTM C 882/928 – 7-Day

Material	Load (lbs)	Bond Strength (psi)	Comments
Duracal	15110	1070	
	16090	1140	
	17020	1200	
HP	0	0	Debonded before comp. test
	12750	900	
	6200	440	
Pavemend	7900	560	Mortar wrapped around dummy specimen
	6100	430	
	6530	460	Mortar wrapped around dummy specimen
Rapid Set	3210	230	
	5670	400	
	1980	140	
Sika	5020	360	
	12350	870	
	6090	430	
T17	9090	640	
	10220	720	
	9390	660	

A.5 Thermal Expansion and Shrinkage Testing – ASTM C 531 M

Table A-18 through Table A-23 contain the ASTM C 531 M results from the ASTM testing.

Table **A-18**: ASTM C 531 M - Duracal

Specimen #	1	2	3	4
Stud lengths 1 (in)	0.815	0.814	0.814	0.814
Stud lengths 2 (in)	0.814	0.8155	0.8125	0.813
Dist. b/w studs (in)	10.005	10.013	10.009	10.011
SHRINKAGE				
	Dist. b/w studs (in)			
Day 1	10.000	10.013	10.007	10.008
Day 3	9.999	10.009	10.003	10.006
Day 7	9.999	10.009	10.003	10.006
Day 11	9.987	9.998	9.993	9.996
Day 13	9.987	9.999	9.994	9.996
Day 17	9.987	9.999	9.994	9.997
Day 21	9.983	9.993	9.988	9.991
Day 23	9.983	9.995	9.990	9.994
Day 27	9.984	9.995	9.991	9.994
Day 31	9.981	9.991	9.986	9.989
Day 33	9.981	9.990	9.986	9.989
Day 37	9.980	9.991	9.987	9.989
Day 41	9.975	9.987	9.983	9.986
Day 43	9.979	9.989	9.985	9.988
Day 47	9.978	9.990	9.986	9.990
Day 51	9.975	9.987	9.982	9.985
Percent Shrinkage	0.30	0.26	0.27	0.26
COEF. OF THERMAL EXPANSION				
Length at 210°F (incl. studs)	11.611	11.623	11.616	11.620
Confirm 73°F Length – b/w studs (in)	9.975	9.987	9.983	9.986
Lin. Coef. Of T.E. (1/°F)	3.4E-06	3.5E-06	3.8E-06	3.8E-06

Table **A-19**: ASTM C 531 M - HP

Specimen #	1	2	3	4
Stud lengths 1 (in)	0.8155	0.815	0.816	0.814
Stud lengths 2 (in)	0.8155	0.817	0.8165	0.821
Dist. b/w studs (in)	10.005	9.987	9.982	9.971
SHRINKAGE				
	Dist. b/w studs (in)			
Day 1	9.999	9.986	9.976	9.964
Day 3	9.996	9.977	9.976	9.956
Day 7	9.997	9.978	9.976	9.958
Day 11	9.966	9.945	9.944	9.927
Day 13	9.968	9.946	9.947	9.929
Day 17	9.968	9.947	9.947	9.930
Day 21	9.961	9.939	9.938	9.922
Day 23	9.963	9.941	9.941	9.924
Day 27	9.963	9.942	9.943	9.925
Day 31	9.958	9.937	9.937	9.919
Day 33	9.957	9.936	9.936	9.919
Day 37	9.958	9.937	9.937	9.920
Day 41	9.954	9.932	9.933	9.915
Day 43	9.955	9.934	9.935	9.917
Day 47	9.956	9.936	9.935	9.918
Day 51	9.953	9.932	9.931	9.915
Percent Shrinkage	0.52	0.55	0.51	0.56
COEF. OF THERMAL EXPANSION				
Length at 210°F (incl. studs)	11.590	11.569	11.571	11.556
Confirm 73°F Length – b/w studs (in)	9.953	9.932	9.932	9.915
Lin. Coef. Of T.E. (1/°F)	3.1E-06	2.7E-06	3.4E-06	2.9E-06

Table **A-20**: ASTM C 531 M - Pavemend

Specimen #	1	2	3	4
Stud lengths 1 (in)	0.812	0.812	0.812	0.8125
Stud lengths 2 (in)	0.8155	0.811	0.8155	0.8075
Dist. b/w studs (in)	9.983	10.009	10.008	10.008
SHRINKAGE				
	Dist. b/w studs (in)			
Day 1	9.979	10.013	10.025	10.005
Day 3	9.978	10.012	10.024	10.004
Day 7	9.976	10.009	10.021	10.001
Day 11	9.965	9.999	10.004	9.989
Day 13	9.966	9.999	10.002	9.989
Day 17	9.966	10.000	10.002	9.990
Day 21	9.965	9.997	9.988	9.988
Day 23	9.964	9.996	9.986	9.986
Day 27	9.964	9.997	9.987	9.987
Day 31	9.963	9.995	9.983	9.985
Day 33	9.963	9.996	9.983	9.986
Day 37	9.965	9.997	9.984	9.987
Day 41	9.963	9.995	9.983	9.986
Percent Shrinkage	0.20	0.14	0.25	0.22
COEF. OF THERMAL EXPANSION				
Length at 210°F (incl. studs)	11.599	11.626	11.619	11.614
Confirm 73°F Length – b/w studs (in)	9.964	9.996	9.984	9.987
Lin. Coef. Of T.E. (1/°F)	4.5E-06	4.4E-06	4.6E-06	4.5E-06

Table A-21: ASTM C 531 M - Rapid Set

Specimen #	1	2	3	4
Stud lengths 1 (in)	0.8165	0.813	0.815	0.8115
Stud lengths 2 (in)	0.8145	0.8135	0.8175	0.8155
Dist. b/w studs (in)	9.994	9.996	10.005	10.01
SHRINKAGE				
	Dist. b/w studs (in)			
Day 1	9.994	9.995	10.005	10.013
Day 3	9.990	9.995	10.002	10.010
Day 7	9.990	9.995	10.004	10.011
Day 11	9.977	9.983	9.991	9.999
Day 13	9.979	9.984	9.992	9.999
Day 17	9.980	9.984	9.992	10.000
Day 21	9.970	9.975	9.983	9.990
Day 23	9.973	9.977	9.985	9.992
Day 27	9.972	9.978	9.986	9.993
Day 31	9.966	9.972	9.979	9.986
Day 33	9.966	9.971	9.979	9.986
Day 37	9.968	9.971	9.979	9.987
Day 41	9.964	9.968	9.975	9.983
Day 43	9.962	9.969	9.976	9.984
Day 47	9.964	9.970	9.977	9.985
Day 51	9.962	9.968	9.975	9.983
Percent Shrinkage	0.32	0.28	0.30	0.27
COEF. OF THERMAL EXPANSION				
Length at 210°F (incl. studs)	11.601	11.603	11.615	11.617
Confirm 73°F Length – b/w studs (in)	9.962	9.968	9.975	9.983
Lin. Coef. Of T.E. (1/°F)	4.8E-06	4.7E-06	4.4E-06	4.3E-06

Table A-22: ASTM C 531 M - Sika

Specimen #	1	2	3	4
Stud lengths 1 (in)	0.8145	0.8125	0.814	0.8135
Stud lengths 2 (in)	0.8175	0.813	0.813	0.816
Dist. b/w studs (in)	9.987	9.997	10.022	9.981
SHRINKAGE				
	Dist. b/w studs (in)			
Day 1	9.983	9.996	10.020	9.981
Day 3	9.978	9.992	10.015	10.002
Day 7	9.978	9.991	10.014	9.975
Day 11	9.969	9.983	10.006	9.966
Day 13	9.970	9.984	10.007	9.967
Day 17	9.972	9.986	10.008	9.969
Day 21	9.968	9.982	10.004	9.965
Day 23	9.970	9.983	10.006	9.967
Day 27	9.972	9.985	10.008	9.969
Day 31	9.968	9.982	10.005	9.965
Day 33	9.969	9.982	10.005	9.967
Day 37	9.970	9.983	10.006	9.967
Day 41	9.966	9.979	10.002	9.963
Day 43	9.969	9.982	10.005	9.965
Day 47	9.971	9.984	10.007	9.967
Day 51	9.967	9.980	10.003	9.963
Percent Shrinkage	0.20	0.17	0.19	0.18
COEF. OF THERMAL EXPANSION				
Length at 210°F (incl. studs)	11.607	11.614	11.638	11.601
Confirm 73°F Length – b/w studs (in)	9.967	9.980	10.003	9.964
Lin. Coef. Of T.E. (1/°F)	4.9E-06	4.6E-06	4.7E-06	4.6E-06

Table A-23: ASTM C 531 M – T17

Specimen #	1	2	4
Stud lengths 1 (in)	0.814	0.814	0.812
Stud lengths 2 (in)	0.814	0.815	0.8155
Dist. b/w studs (in)	9.994	9.982	9.995
SHRINKAGE			
	Dist. b/w studs (in)		
Day 1	10.042	10.027	10.043
Day 3	10.041	10.026	10.042
Day 7	10.044	10.029	10.030
Day 11	10.027	10.008	10.025
Day 13	10.027	10.008	10.025
Day 17	10.027	10.008	10.025
Day 21	10.025	10.005	10.021
Day 23	10.025	10.006	10.022
Day 27	10.026	10.007	10.022
Day 31	10.023	10.004	10.020
Day 33	10.023	10.004	10.020
Day 37	10.022	10.003	10.019
Day 41	10.020	10.001	10.016
Day 43	10.020	10.001	10.017
Day 47	10.021	10.003	10.018
Day 51	10.018	10.000	10.016
Percent Shrinkage	-0.24	-0.18	-0.21
COEF. OF THERMAL EXPANSION			
Length at 210°F (incl. studs)	11.666	11.652	11.667
Confirm 73°F Length – b/w studs (in)	10.018	10.000	10.016
Lin. Coef. Of T.E. (1/°F)	1.4E-05	1.5E-05	1.5E-05

Appendix B

Testing Program B – Specialized Testing

B.1 Three-Point Bending Test Photographs

Refer to Figure **B-1** through Figure **B-8** to see photographs of each of the patches after failure from the three-point bending test.

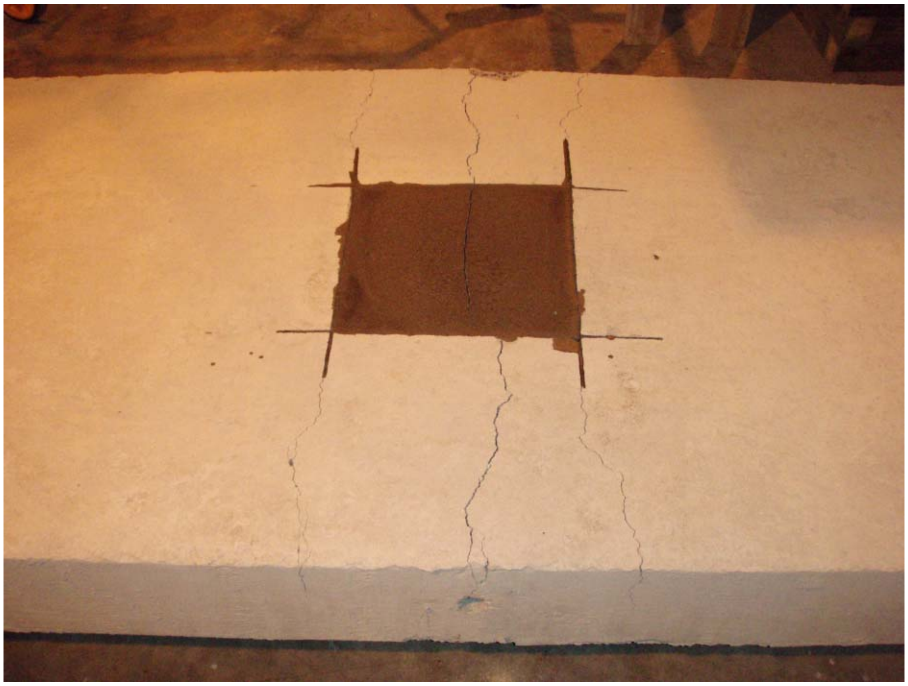

Figure **B-1**: Three-Point Loading – Pavemend 15.0 – Small, Shallow

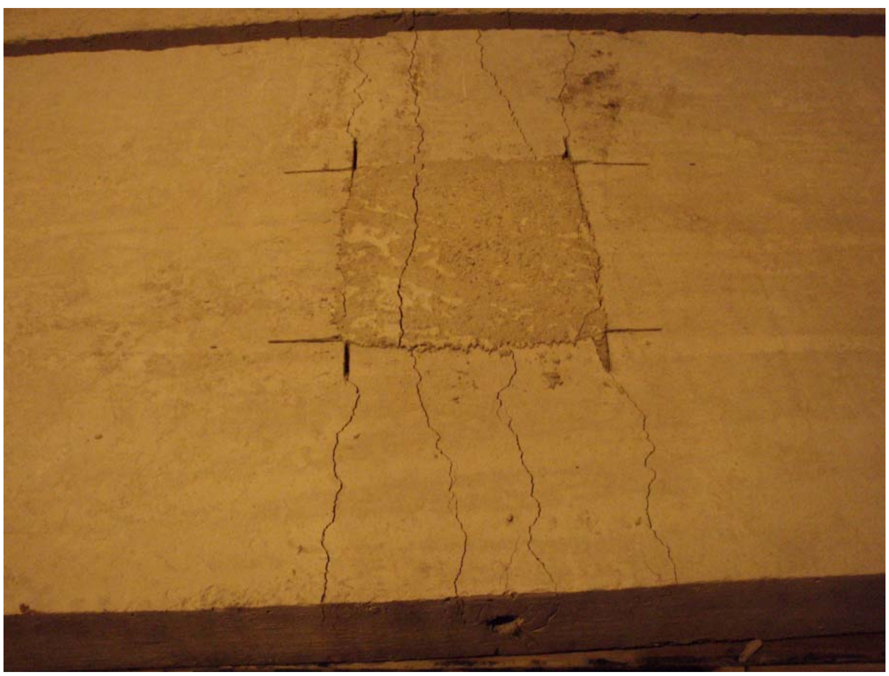

Figure **B-2**: Three-Point Loading – Rapid Set – Small, Shallow

Figure **B-3**: Three-Point Loading – Pavemend 15.0 – Large, Shallow

Figure **B-4**: Three-Point Loading – Rapid Set – Large, Shallow

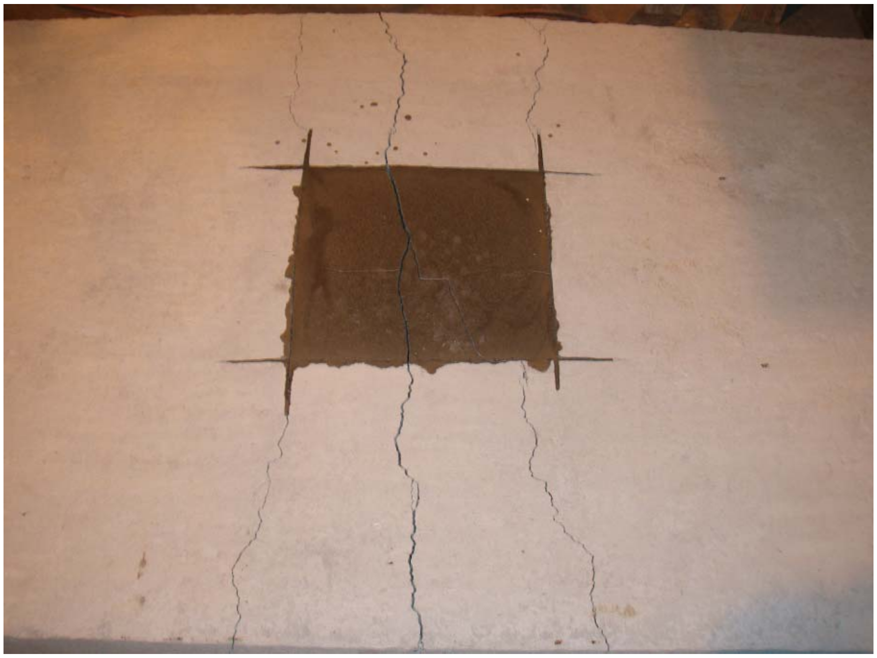

Figure **B-5**: Three-Point Loading – Pavemend 15.0 – Small, Deep

Figure **B-6**: Three-Point Loading – Rapid Set – Small, Deep

Figure B-7: Three-Point Loading – Pavemend 15.0 –Large, Deep

Figure B-8: Three-Point Loading – Rapid Set – Large, Deep

B.2 Repetitive Tire Load Simulation Photographs

Refer to Figure B-9, Figure B-10, and Figure B-11 to see photographs of the Pavemend 15.0 patches after 200,000 repetitive tire loads have been run on them.

Figure B-9: Pavemend 15.0 Patch after Tire Load Simulation – Close-up 1

Figure B-10: Pavemend 15.0 Patch after Tire Load Simulation – Close-up 2

Figure B-11: Pavemend 15.0 Patch after Tire Load Simulation – Close-up 3

Refer to Figure B-12, Figure B-13, and Figure B-14 to see photographs of the Rapid Set patches after 200,000 repetitive tire loads have been run on them.

Figure B-12: Rapid Set Patch after Tire Load Simulation – Close-up 1

Figure B-13: Rapid Set Patch after Tire Load Simulation – Close-up 2

Figure B-14: Rapid Set Patch after Tire Load Simulation – Close-up 3

B.3 Corrosion Testing

Refer to Table B-1 through Table B-8 for the half cell readings of the Pavemend 15.0 and Rapid Set ponding slabs. Note that the darkened boxes in the tables represent the location of the patches, with the half depth patch on the left and the full depth patch on the right.

Table **B-1**: Half Cell Potential Readings – Initial

Pavemend								
-168	-185	-182	-181	-202	-209	-224	-202	-194
-202	-249	-219	-230	-246	-301	-314	-285	-237
-204	-320	-357	-322	-263	-406	-426	-388	-260
-110	-330	-378	-337	-282	-402	-410	-377	-236
-224	-329	-339	-333	-271	-335	-335	-337	-200
-187	-223	-237	-247	-243	-250	-250	-234	-191
Rapid Set								
-66	-154	-141	-172	-176	-176	-174	-153	-140
-125	-110	-158	-165	-183	-143	-143	-160	-156
-144	-206	-247	-208	-174	-231	-253	-244	-167
-150	-251	-249	-236	-170	-219	-228	-230	-167
-142	-142	-134	-159	-165	-122	-133	-133	-154
-66	-103	-133	-153	-143	-125	-120	-123	-110

Table **B-2**: Half Cell Potential Readings – Cycle 1

Pavemend								
-267	-289	-296	-308	-301	-297	-303	-304	-293
-292	-376	-314	-421	-351	-368	-356	-361	-310
-330	-421	-479	-486	-392	-425	-429	-408	-317
-328	-445	-492	-490	-413	-426	-431	-405	-315
-318	-451	-463	-484	-376	-288	-280	-370	-295
-275	-323	-357	-366	-341	-315	-311	-304	-287
Rapid Set								
-290	-291	-282	-287	-288	-288	-276	-257	-241
-314	-323	-297	-295	-308	-343	-301	-294	-257
-326	-369	-331	-304	-300	-335	-327	-323	-270
-320	-338	-307	-349	-282	-293	-293	-307	-258
-304	-321	-288	-270	-258	-253	-240	-258	-240
-301	-273	-260	-257	-245	-234	-225	-228	-227

Table **B-3**: Half Cell Potential Readings – Cycle 2

Pavemend								
-292	-297	-320	-340	-377	-449	-448	-462	-452
-297	-385	-426	-454	-455	-403	-434	-537	-481
-423	-450	-495	-520	-500	-577	-583	-568	-480
-331	-482	-511	-538	-514	-570	-583	-555	-448
-332	-470	-505	-529	-496	-547	-545	-529	-414
-311	-373	-428	-458	-472	-480	-488	-451	-394
Rapid Set								
-247	-253	-251	-260	-267	-279	-276	-269	-269
-259	-279	-263	-267	-287	-331	-310	-305	-277
-264	-318	-288	-278	-288	-329	-321	-322	-284
-268	-338	-288	-273	-273	-274	-291	-309	-276
-288	-286	-257	-248	-245	-255	-249	-267	-273
-247	-247	-242	-237	-237	-237	-242	-255	-273

Table **B-4**: Half Cell Potential Readings – Cycle 3

Pavemend								
-280	-290	-298	-306	-316	-327	-357	-381	-346
-293	-334	-378	-400	-370	-404	-430	-402	-380
-306	-374	-436	-446	-414	-476	-482	-452	-363
-312	-418	-448	-474	-415	-473	-458	-446	-358
-302	-406	-444	-455	-390	-422	-419	-394	-340
-286	-307	-340	-355	-350	-348	-355	-346	-332
Rapid Set								
-232	-240	-238	-242	-250	-262	-261	-258	-265
-242	-266	-248	-249	-266	-302	-292	-290	-270
-246	-292	-262	-256	-264	-303	-297	-304	-280
-254	-303	-260	-246	-250	-274	-268	-298	-289
-240	-254	-234	-221	-229	-237	-238	-269	-290
-232	-227	-220	-222	-222	-223	-232	-265	-292

Table **B-5**: Half Cell Potential Readings – Cycle 4

Pavemend								
-276	-285	-291	-292	-295	-304	-308	-318	-307
-283	-343	-364	-377	-344	-394	-408	-371	-320
-297	-392	-424	-441	-388	-459	-471	-451	-332
-312	-408	-433	-453	-398	-461	-466	-432	-329
-303	-382	-423	-448	-371	-400	-411	-388	-312
-287	-304	-332	-336	-328	-330	-332	-321	-304
Rapid Set								
-244	-254	-257	-269	-284	-306	-312	-321	-328
-253	-273	-265	-272	-298	-336	-326	-330	-332
-255	-298	-281	-283	-302	-340	-335	-338	-329
-259	-308	-279	-277	-294	-328	-333	-347	-339
-248	-266	-255	-260	-272	-300	-318	-338	-345
-244	-244	-244	-249	-261	-280	-302	-328	-347

Table **B-6**: Half Cell Potential Readings – Cycle 5

Pavemend								
-281	-290	-319	-324	-325	-324	-324	-326	-310
-288	-326	-361	-367	-355	-378	-382	-365	-322
-292	-377	-420	-427	-388	-440	-460	-420	-327
-288	-394	-428	-450	-398	-451	-463	-427	-320
-290	-365	-413	-433	-374	-392	-404	-367	-306
-274	-305	-322	-326	-316	-310	-317	-322	-292
Rapid Set								
-240	-247	-252	-265	-281	-297	-304	-305	-306
-245	-256	-255	-264	-284	-318	-311	-313	-306
-246	-272	-265	-267	-285	-317	-320	-327	-320
-248	-282	-263	-264	-275	-311	-321	-336	-376
-241	-253	-247	-250	-265	-291	-320	-330	-348
-234	-235	-238	-245	-257	-278	-306	-332	-355

Table **B-7**: Half Cell Potential Readings – Cycle 6

Pavemend								
-317	-350	-375	-396	-417	-437	-445	-415	-385
-320	-407	-435	-466	-443	-498	-510	-480	-377
-334	-472	-518	-529	-487	-558	-565	-545	-380
-339	-477	-510	-531	-494	-560	-562	-524	-373
-341	-460	-492	-510	-466	-519	-518	-473	-345
-329	-374	-397	-433	-417	-418	-417	-383	-340
Rapid Set								
-245	-273	-255	-310	-319	-326	-328	-309	-289
-266	-288	-306	-228	-302	-347	-336	-340	-302
-281	-326	-229	-338	-322	-361	-376	-367	-326
-308	-364	-351	-326	-320	-357	-376	-365	-326
-312	-341	-353	-329	-315	-324	-338	-342	-317
-312	-327	-366	-334	-312	-307	-326	-322	-306

Table B-8: Half Cell Potential Readings – Cycle 7

Pavemend								
-292	-329	-362	-380	-400	-425	-437	-391	-343
-305	-412	-436	-450	-438	-482	-490	-481	-358
-322	-444	-485	-487	-470	-525	-532	-510	-459
-345	-461	-484	-500	-479	-542	-541	-510	-351
-337	-439	-468	-488	-444	-500	-589	-347	-318
-324	-369	-401	-436	-418	-416	-403	-369	-307
Rapid Set								
-244	-283	-291	-311	-312	-311	-306	-294	-270
-259	-296	-304	-328	-329	-343	-331	-336	-303
-272	-330	-330	-330	-330	-364	-417	-364	-307
-291	-363	-369	-325	-315	-352	-402	-364	-313
-302	-334	-344	-322	-310	-322	-332	-337	-304
-305	-324	-343	-322	-306	-306	-319	-317	-291

Refer to Figure B-15 through Figure B-30 for contour maps of the half cell potentials listed in the tables above.

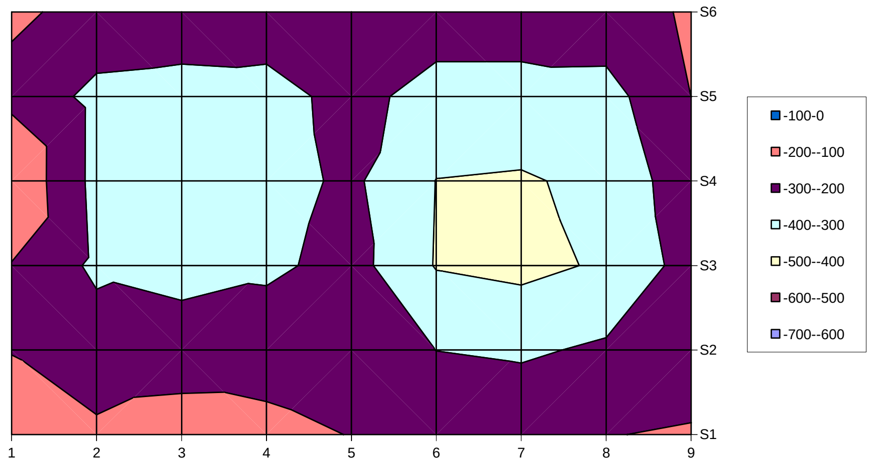

Figure **B-15**: Pavemend 15.0 Half Cell Potential Readings – Initial

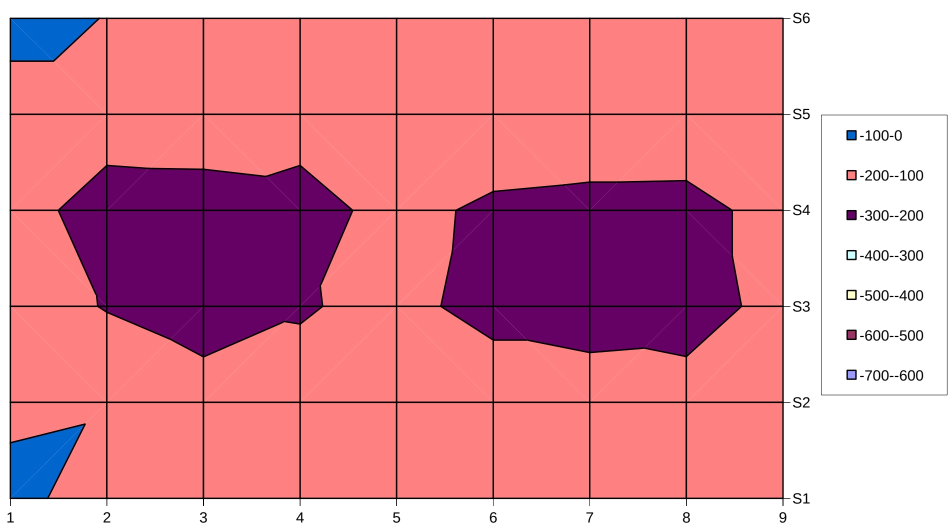

Figure **B-16**: Rapid Set Half Cell Potential Readings – Initial

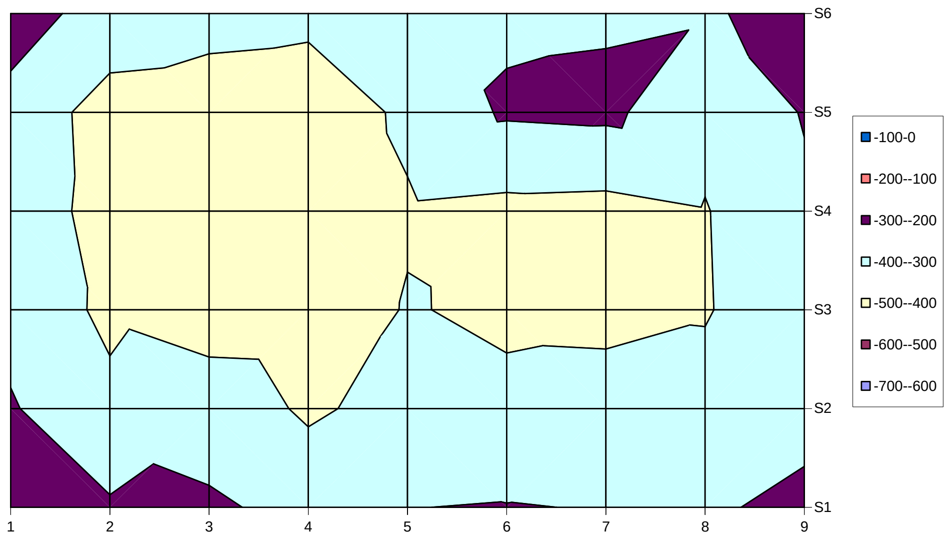

Figure **B-17**: Pavemend 15.0 Half Cell Potential Readings – Cycle 1

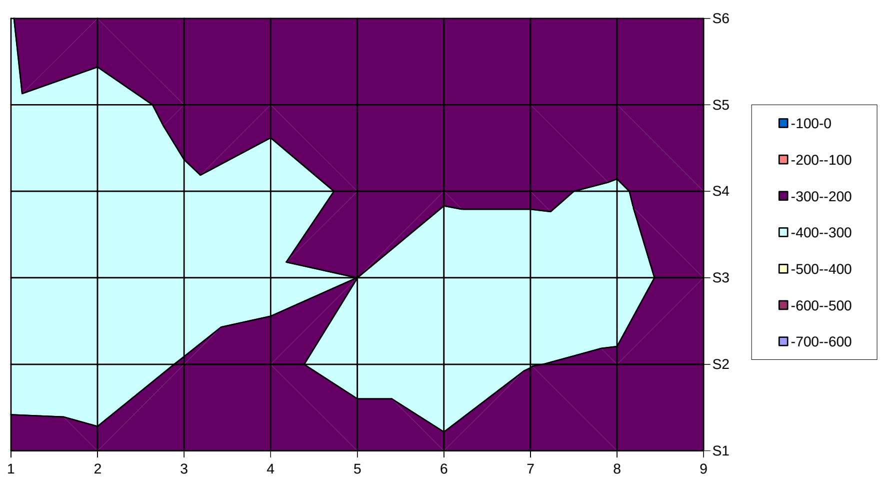

Figure **B-18**: Rapid Set Half Cell Potential Readings – Cycle 1

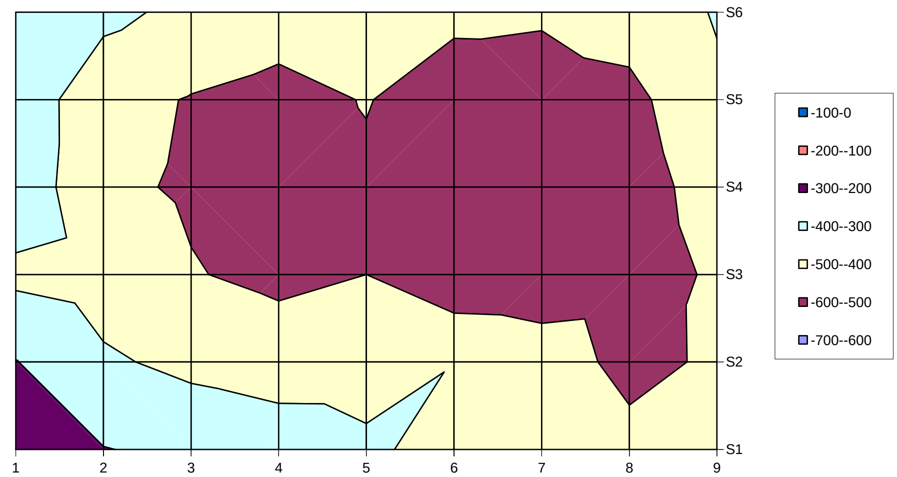

Figure **B-19**: Pavemend 15.0 Half Cell Potential Readings – Cycle 2

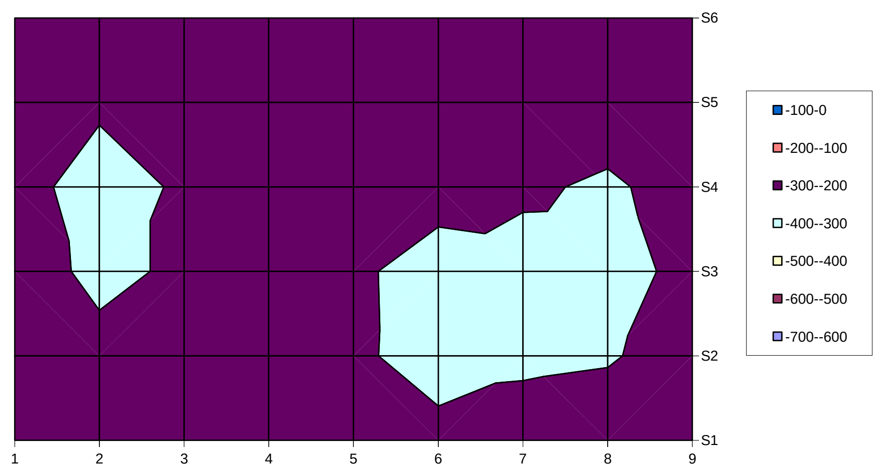

Figure **B-20**: Rapid Set Half Cell Potential Readings – Cycle 2

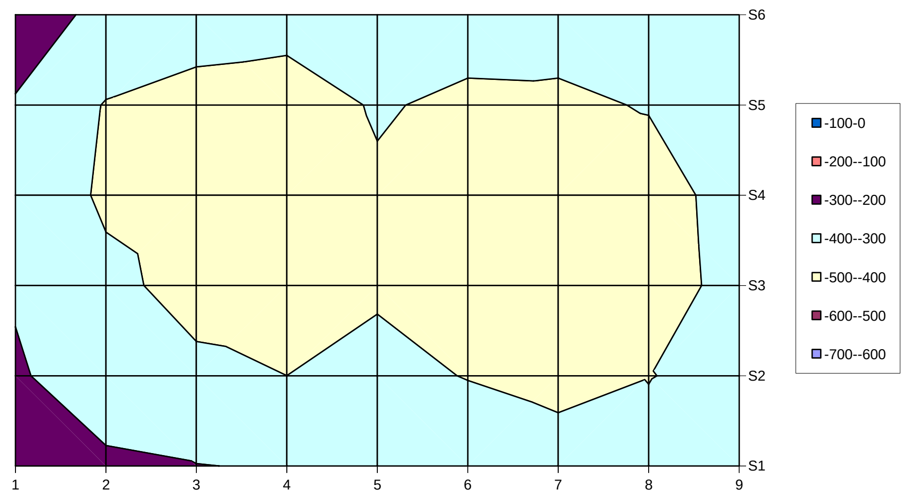

Figure **B-21**: Pavemend 15.0 Half Cell Potential Readings – Cycle 3

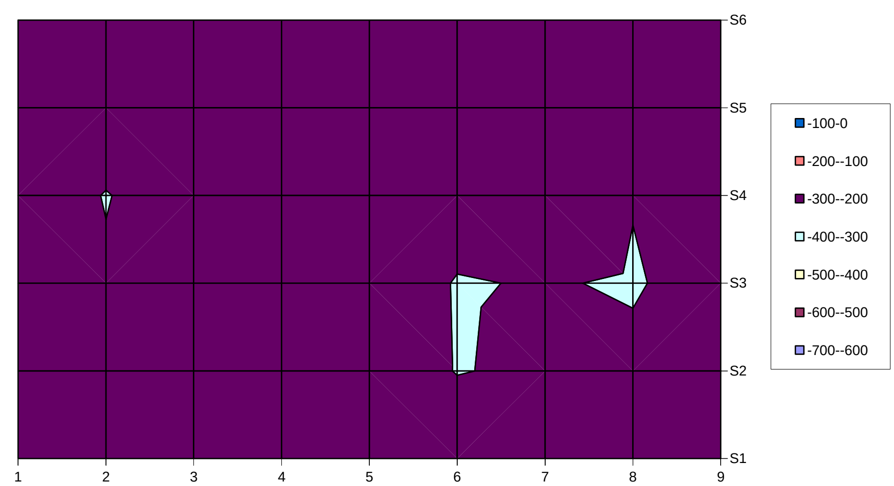

Figure **B-22**: Rapid Set Half Cell Potential Readings – Cycle 3

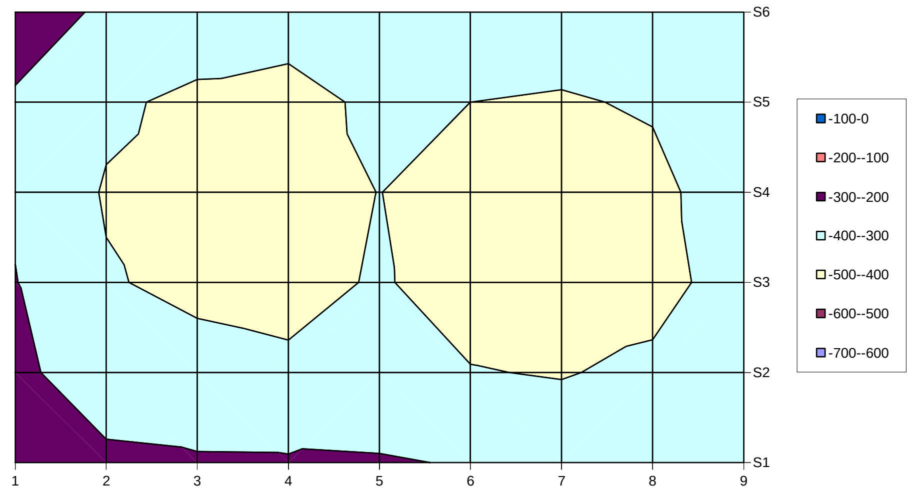

Figure **B-23**: Pavemend 15.0 Half Cell Potential Readings – Cycle 4

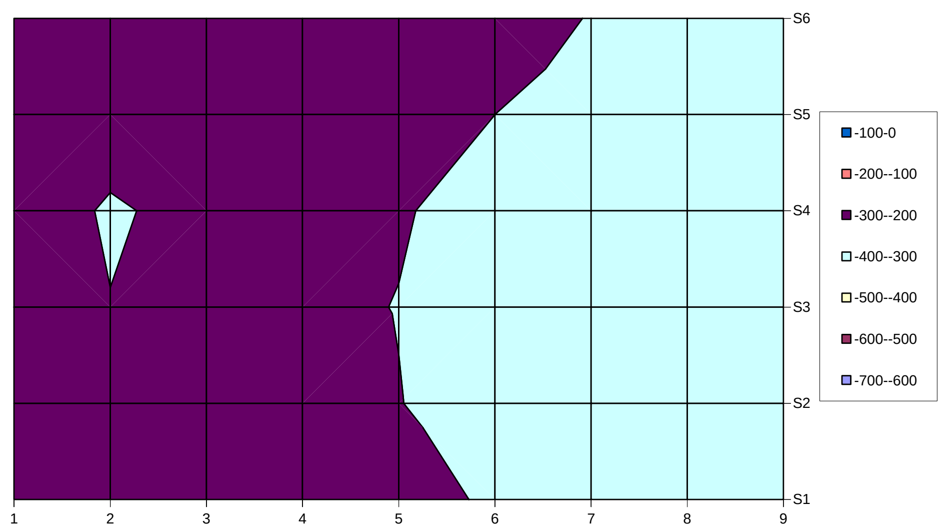

Figure **B-24**: Rapid Set Half Cell Potential Readings – Cycle 4

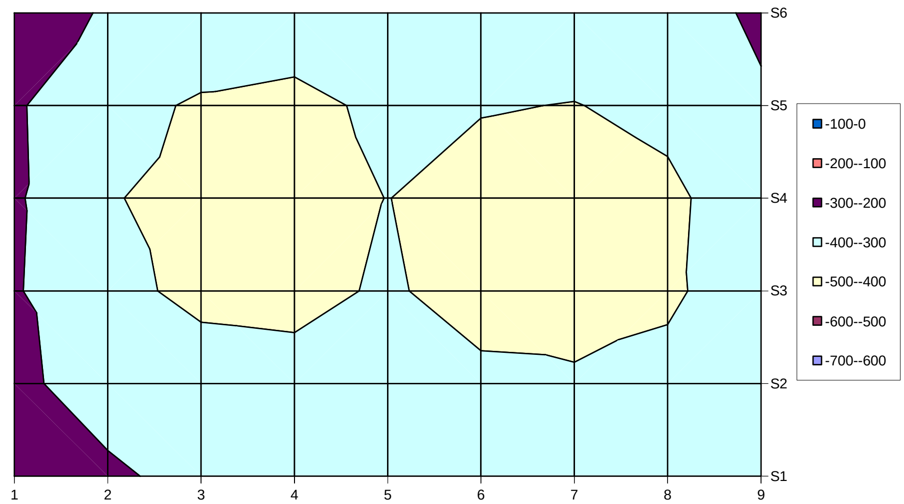

Figure **B-25**: Pavemend 15.0 Half Cell Potential Readings – Cycle 5

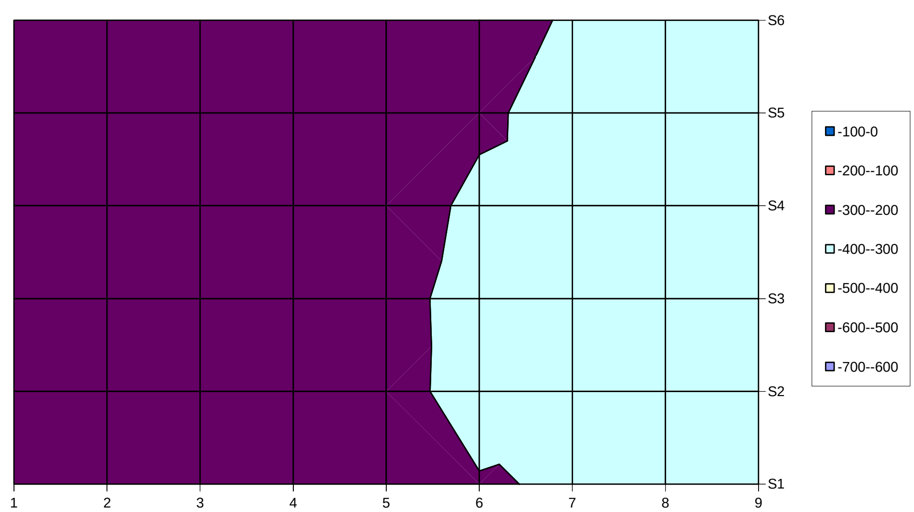

Figure **B-26**: Rapid Set Half Cell Potential Readings – Cycle 5

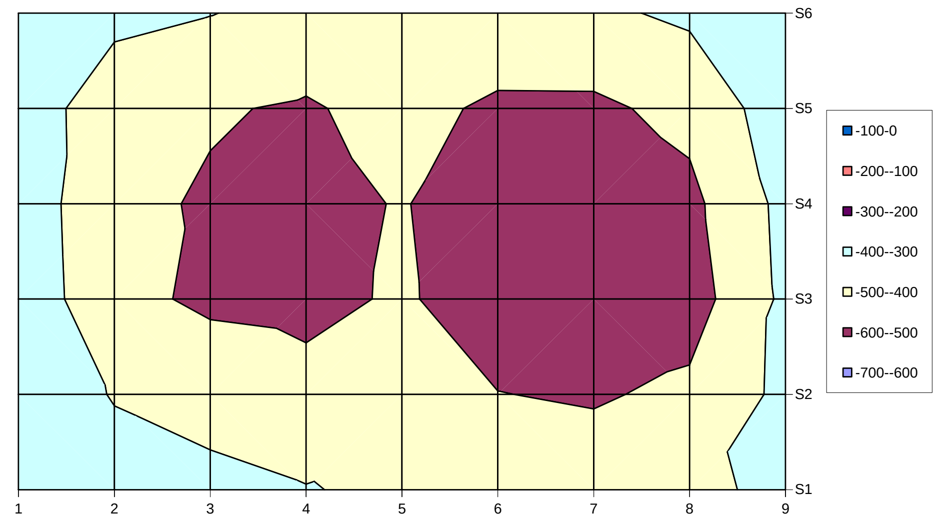

Figure **B-27**: Pavemend 15.0 Half Cell Potential Readings – Cycle 6

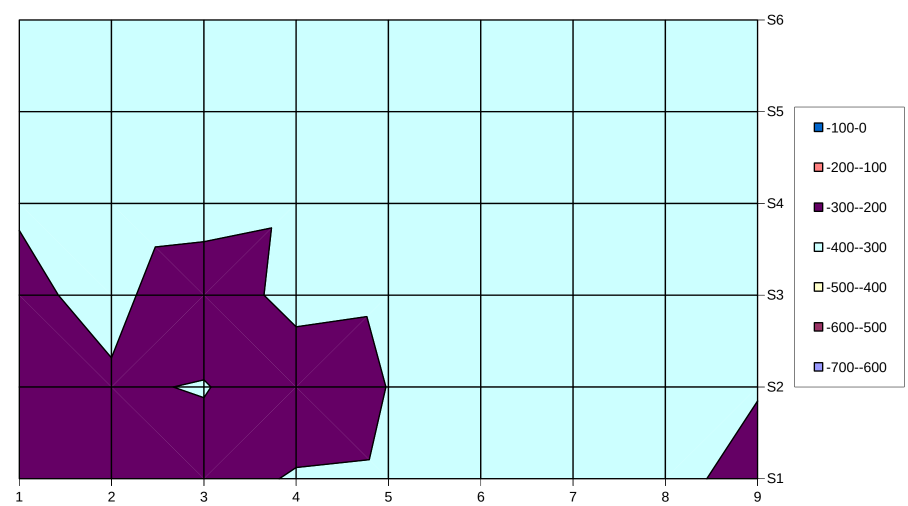

Figure **B-28**: Rapid Set Half Cell Potential Readings – Cycle 6

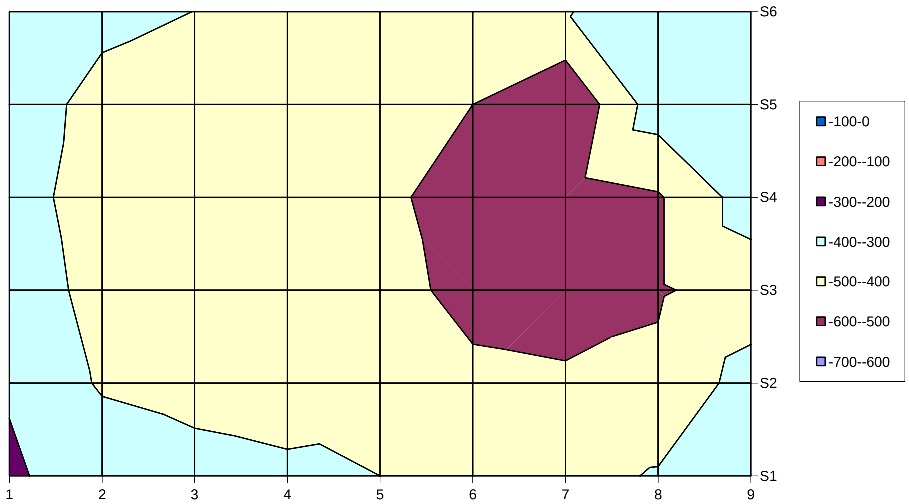

Figure **B-29**: Pavemend 15.0 Half Cell Potential Readings – Cycle 7

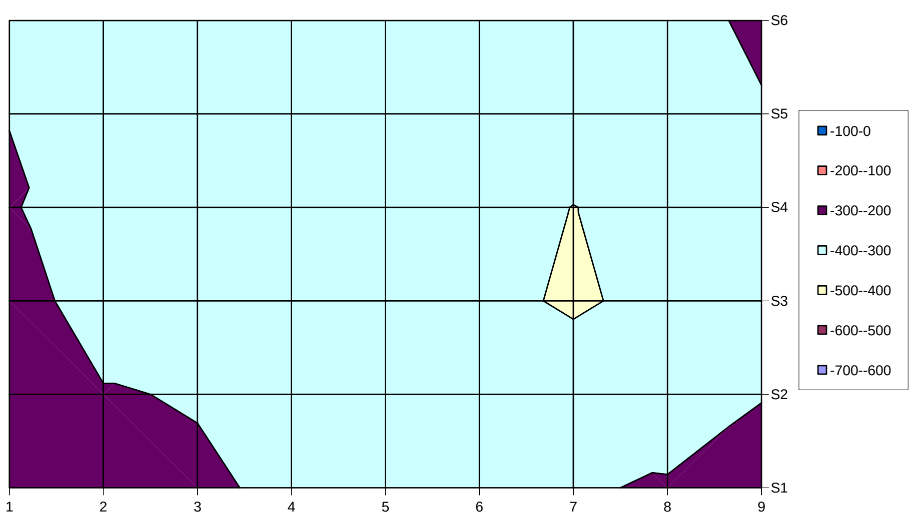

Figure **B-30**: Rapid Set Half Cell Potential Readings – Cycle 7